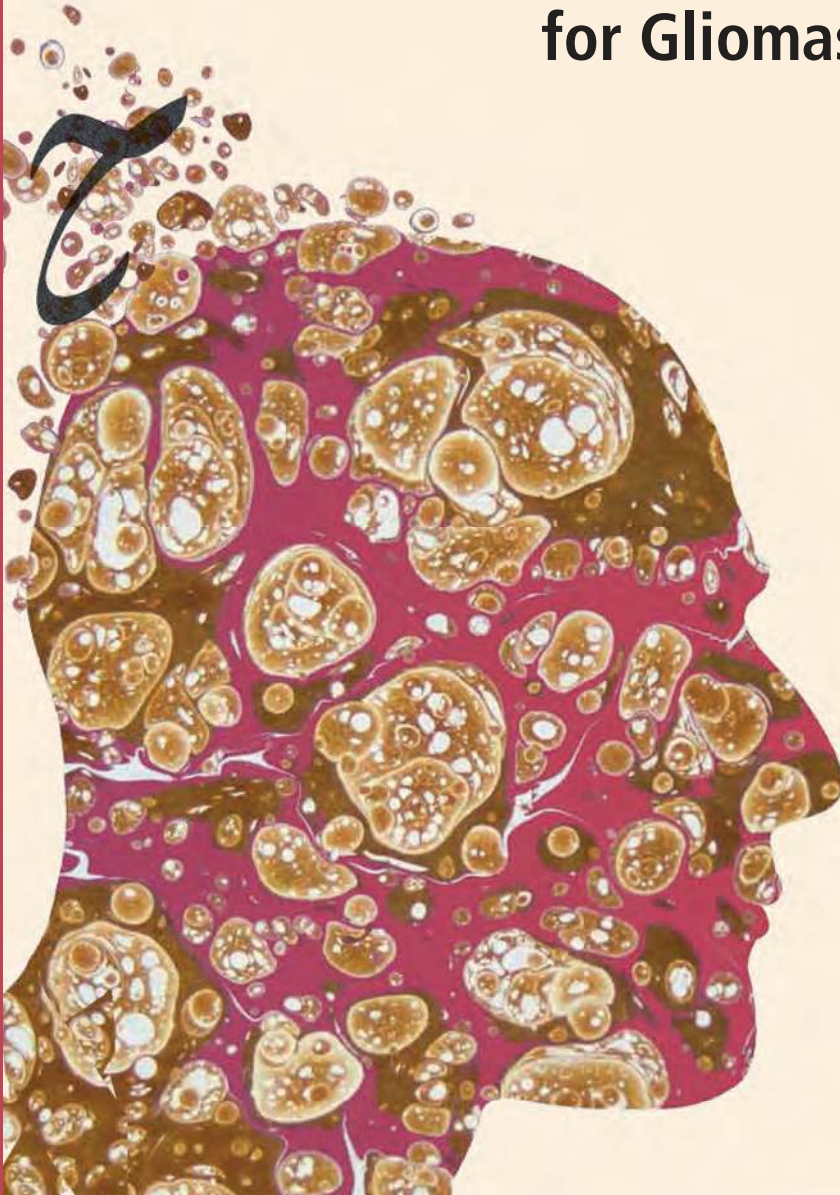Lale Erdem–Eraslan

Identification of Predictive Response Markers and Novel Treatment Targets for Gliomas

Identification of Predictive Response Markers and Novel Treatment Targets for Gliomas

Lale Erdem-Eraslan

Identification of Predictive Response Markers and Novel Treatment Targets for Gliomas

Identificatie van therapierespons voorspellende markers en nieuwe therapeutische doelwitten voor gliomen

Proefschrift

ter verkrijging van de graad van doctor aan de

Erasmus Universiteit Rotterdam op gezag van de
Rector magnificus

Prof.dr. H.A.P. Pols

en volgens besluit van het College voor Promoties.

De openbare verdediging zal plaatsvinden op

dinsdag 15 maart 2015 om 15:30 uur
door
Lale Erdem

geboren te Rotterdam

Erasmus University Rotterdam

TABLE OF CONTENTS

GENERAL INTRODUCTION

Gliomas are the most common type of primary brain tumors in adults (incidence 5.97 per 100.000 in the US (1)), and often have a dismal prognosis (2, 3). Based on their histo-pathological features, gliomas can be subdivided into oligodendrocytic (OD), astrocytic (A) and mixed oligoastrocytic tumors (MOA). They are further subcategorized into various malignancy grades according to the WHO2007 criteria. Oligodendrocytic and mixed oligoastrocytic tumors are separated into low-grade (II) and anaplastic tumors (III). Astrocytic tumors are further separated into pilocytic astrocytomas (PAs) (I), low-grade tumors (II), anaplastic tumors (III) and glioblastoma multiforme (GBM, grade IV) (4). GBMs are the most common and can either arise *de novo* (primary) or from previously diagnosed lower grade astrocytomas (secondary) (5). The patients' prognosis is related to the type and grade of the tumor. For example, patients with a glioblastoma have a median survival of approximately one year, whereas patients with grade II OD have a more favorable prognosis with a median survival of 11.5 years (6). Apart from pilocytic astrocytoma, all glioma subtypes will eventually lead to death (6).

Current treatment options depend on the histological diagnosis in combination with clinical features (age, Karnofsky performance score (KPS)) and include surgical resection, radiotherapy and chemotherapy. The extent of resection is positively correlated with prolonged progression-free survival, improved seizure control and reduced risk of malignant transformation (7, 8). However, a complete resection of gliomas cannot be performed because individual glioma cells infiltrate the parenchyma of the brain (9). Especially in or nearby eloquent areas, resection is often stopped before complete resection is achieved to prevent postoperative neurologic deficits (10). The extent of tumor resection is therefore highly dependent on tumor location.

Treatment options for glioma patients
Radiotherapy is the recommended treatment for tumors that are at higher risk for malignant transformation, though this treatment is associated with significant side effects (11). The optimal dose and timing of RT has been investigated in many trials for LGG (12-14). No significant overall survival (OS) benefit was found in patients receiving low (45 Gy in 5 weeks or 50.4 Gy/28 fractions) versus high (59.4 Gy in 6.6 weeks or 64.8 Gy/36 fractions) dose of RT (13, 14). Likewise, early versus late RT showed an improvement in progression-free survival (PFS), but not in OS (12).

A combination of Procarbazine, CCNU (lomustine) and vincristine (PCV) or temozolomide (TMZ) are the choices for chemotherapy in patients with low grade or anaplastic gliomas. Part of PCV chemotherapy is administered intravenously and is associated with significant hematopoietic toxicity. TMZ on the other hand is easier to administer and better tolerated. In RTOG9802, a significant improvement in OS after adjuvant PCV

chemotherapy was observed in high-risk LGG patients (15). In recurrent LGGs, TMZ has also shown to improve outcome (16-18). Similar improvements in PFS and OS after adjuvant PCV were obtained in anaplastic oligodendrogliomas and oligoastrocytomas (19-21). Whether PCV or TMZ gives similar survival benefit for patients is currently being investigated.

TMZ has also shown improved outcome in newly diagnosed glioblastomas (22, 23). Especially those patients containing a methylated *MGMT* promoter benefited from TMZ (23-25).

Novel treatment modalities
Unfortunately, despite these aggressive treatments, all gliomas eventually recur and therefore new treatment modalities are required. One of the recent drugs that have been tested is bevacizumab, a monoclonal antibody directed against the vascular endothelial growth factor (*VEGF*). An improvement of PFS was observed in patients with newly diagnosed GBMs (26, 27). Unfortunately, no improvement of OS was noted in newly diagnosed GBMs (26, 27). The effect of bevacizumab on OS in recurrent GBMs is still under investigation (28).

Cilengitide is an αvβ3 and αvβ5 integrin inhibitor, which showed modest results in recurrent GBM patients (29, 30). In newly diagnosed GBM however, no additional benefit with cilengitide was observed (31, 32).

Another approach to treat gliomas involves using the immune system to clear the tumor. Examples of these include peptide-based vaccines like rindopepimut, a peptide-based vaccine targeting *EGFR*vIII (33, 34). Dendritic cell vaccines are also currently being investigated (35).

Molecular classification of gliomas

In gliomas, selection of treatment options is at least partly determined by histological classification of the tumor. However, a limitation of histological diagnosis and grading includes interobserver variability, which can lead to misdiagnosis of gliomas. For example, patients diagnosed with a PA will need less aggressive treatment regimens than patients with grade II-IV gliomas. More accurate methods are required to overcome the limitation in the histopathological diagnosis of gliomas and provide a more effective and personalized treatment. Molecular subtyping of gliomas can be used to improve diagnosis, provide more accurate prognostic information and develop targeted therapies. Gliomas can be classified by their gene expression profile, DNA methylation profile or by their genetic changes.

Gene-expression based molecular classification of gliomas have shown a reasonable concordance between studies. Phillips et al. have identified three subtypes (proneural, mesenchymal and proliferative) in high-grade gliomas using supervised clustering (36).

Verhaak et al. identified four subtypes in GBMs: classical, neural, proneural and mesen-chymal (37). Li et al. performed gene expression in all histological subtypes and identi-fied two main groups as GBM-rich (mesenchymal) and OD-rich (proneural) separable into six subtypes by unsupervised clustering (38). Similarly, Gravendeel et al. identified six intrinsic glioma subtypes when clustering all histological subtypes of glioma (39). Several of these studies have shown that subtypes differ from histological classification of gliomas and that they are correlated to patient prognosis.

With the genome-wide methylation profiling of gliomas, two major glioma subtypes can be identified; CpG island methylator phenotype (CIMP)- and CIMP+ tumors (40-42). Patients with a CIMP+ phenotype have a longer survival than CIMP- tumors. Several groups have identified additional subtypes (40, 43).

Gliomas can also be classified on their genetic changes. For example, grade I pilocytic astrocytomas often have mutations or structural rearrangements in the *BRAF* gene (44, 45). Grade II/III As and secondary GBMs frequently harbor mutations in the *IDH1/IDH2*, *TP53* and *ATRX* genes (46-52). Primary GBMs are characterized by genetic aberrations in the three pathways (RTK, TP53 and RB) and frequently involve *EGFR* amplification, *PTEN* deletion, *TERT* gene promoter mutations; mutations in the *IDH1* gene are infrequent in primary GBMs (53-59) Among oligodendrocytic tumors, the majority of grade II and anaplastic ODs exhibit combined loss of heterozygosity (LOH) of chromosome arms 1p and 19q and mutations in the genes *IDH1/2, CIC, FUBP1* and *TERT* promoter (49, 59-62).

In a recent paper of Aldape et al., integrated data from multiple platforms identified three subtypes of low-grade gliomas that were concordant with *IDH*, 1p19q, and *TP53* status. Low-grade gliomas with an *IDH* mutation and 1p19q co-deletion had the best clinical outcome. Patients with a low-grade glioma with mutations in *IDH* and without 1p19q co-deletion consisted of mutations in *TP53* and *ATRX*. Low-grade gliomas without mutations in *IDH* had a clinical outcome more similar to primary GBMs. Analyzing low-grade gliomas based on *IDH*, *TP53* and 1p19q status may allow classification of patients into distinct glioma subtypes with different clinical outcomes, making use of other platforms unnecessary (63).

Tumor biomarkers

Tumor biomarkers are molecular characteristics of the tumor that can aid diagnosis, provide prognostic information for the patient or predict response to a given treatment. (64). More recently, biomarkers are used to select subgroups of patients in targeted therapy or personalized medicine trials. (65). *EGFR*vIII expression for example is used as an inclusion criterium marker to investigate the effect of rindopepimut (a vaccine for *EGFR*vIII) in newly diagnosed and recurrent GBMs. The biomarkers that have shown clini-cal relevance in gliomas will be described in more detail and include 1p19q deletions, mutations in *IDH1/2, EGFR*, *BRAF* and *MGMT* promoter methylation.

Co-deletion of 1p19q

Co-deletion of chromosome arms 1p and 19q due to an unbalanced translocation of 19p to 1q is a hallmark of pure ODs (66). Patients with 1p19q loss have a more favorable prognosis and are sensitive to alkylating agents such as PCV chemotherapy (19, 21). The high percentage of this genetic change suggested the presence of tumor suppressor genes on the remaining arms.

Recent exome sequencing studies indeed have identified mutations in two tumor suppressor genes, the *CIC* gene, on chromosome 19q and the *FUBP1* gene on chromosome 1p (60-62). Their additional role on the outcome of patients with 1p19q loss is still under investigation.

IDH1/IDH2

Somatic mutations in the *IDH1* gene were initially identified in 2008 by one of the first whole exome sequencing efforts (53). Similar genetic changes in the homologous *IDH2* enzyme were identified soon after (67). The *IDH1* and *IDH2* genes encode for proteins with identical metabolic activity but are localized in different subcellular compartments, cytoplasm/peroxisomes and mitochondria respectively. Wildtype *IDH1* and *IDH2* convert isocitrate into α-ketoglutarate and generate NADPH from NADP in this process. Both *IDH1* and *2* mutations are localized around the highly conserved codons 132 and 140/172, respectively, amino acids that are involved in substrate binding (68). *IDH1* and *IDH2* mutations are often (but not always) mutually exclusive and always heterozygous. Mutant *IDH1* or *2* have an altered substrate specificity; the protein binds to α-ketoglutarate and uses it as a substrate to produce the oncometabolite D-2-hydroxyglutarate (D-2-HG) (69). D-2-HG production from α-ketoglutarate by mutant *IDH* inhibits α-KG–dependent enzymes such as *TET2*. The *TET* family of dioxygenases (*TET1, TET2,* and *TET3*) catalyzes the hydroxylation of 5-methylcytosine in DNA; the first step in the demethylation of DNA. D-2-HG inhibits the formation of 5-hydroxymethylcytosine levels and so reduces DNA-demethylation. Indeed, in gliomas the CIMP-phenotype is highly associated with *IDH1* mutations (70, 71). The competitive inhibition of a-ketoglutarate dependent on hydroxygenases ultimately results in a block in cellular differentiation, which is one of the hallmarks of cancer.

IDH1 and *IDH2* mutations are frequently found in grade II/III gliomas, in secondary GBMs and in other neoplasms, AML (acute myeloid leukemia), chondrosarcomas and intrahepatic cholangiocarcinomas (72, 73). *IDH1* mutations precede *TP53* mutations and 1p19q co-deletion, which represent astrocytic and oligodendroglial differentiation markers respectively (46, 47, 62, 74).

In gliomas, *IDH*-mutations serve as prognostic markers: *IDH*-mutated tumors have a more favorable prognosis than *IDH*-wildtype tumors (74-76). *IDH*-mutations may also be predictive for response to PCV in anaplastic oligodendrogliomas and for surgical resec-

tion: only in mutant *IDH1* gliomas an additional survival benefit associated with maximal surgical resection was found (77, 78).

EGFR

Strictly speaking, *EGFR* is neither a predictive nor prognostic biomarker that is used in the clinic. However, as *EGFR* is one of the most common genetic changes in primary GBMs (and as such aids the diagnosis of pGBMs), it is an active target for treatment and several clinical trials currently use the genetic changes in the *EGFR* locus as inclusion criterium.

EGFR gene amplification and activating mutations occur frequently in primary GBMs, and rarely in lower grade gliomas (54, 79). After amplification, additional genetic changes occur in the *EGFR* locus of which *EGFR*vIII is the most frequent activating mutant form in which the ligand-binding domain (exons 2-7) is deleted (53, 80). Missense mutations also have been identified in exons encoding the extracellular *EGFR* domains (81). All mutation types result in a constitutively activated RAS-RAF-MAPK, PI3K-AKT-mTOR and JAK-STAT pathway (82, 83).

In some studies, *EGFR* amplification or mutation was indicative for a worse long-term survival in GBM patients (84). Other studies however have failed to demonstrate an effect on survival (85). *EGFR* amplification or mutation may also predict response to tyrosine kinase inhibitors or serve as a target for immunotherapy (86, 87). *EGFR* targeted therapies, such as monoclonal antibodies or tyrosine kinase inhibitors have been explored in patients with newly diagnosed or recurrent GBM, but did not reach significant results in phase II trials (88-90). *EGFR* is also frequently mutated in other cancer types including pulmonary adenocarcinomas and breast cancer (91). The mutations found in these cancer types are different from GBMs, but both result in an activated *EGFR* pathway.

BRAF

BRAF belongs to the RAF serine threonine kinases family and is involved in directing cell growth via the MAPK and ERK pathways (92, 93). Duplications of this gene are frequently found in pilocytic astrocytomas and rarely in other grades of astrocytic tumors (93, 94). The tandem duplication often (but not always) produces a fusion gene of the genes *KIAA1549* and *BRAF*, such that the 5' end of the *KIAA1549* is fused to the 3' end of *BRAF* (95). Most common fusion variants are *KIAA1549:BRAF* exon 16-exon 9 followed by *KIAA1549:BRAF* 15-9 (92, 96). The presence of the *KIAA1549:BRAF* gene fusion is significantly associated with a better prognosis and can be used to distinguish prognostically favorable pilocytic astrocytomas from grade II astrocytomas (48).

MGMT

The *O-6*-methylguanine DNA methyltransferase *(MGMT)* gene on chromosome 10q26 encodes for a DNA repair enzyme that repairs damage induced by DNA alkylating agents (such as temozolomide) (97). The CpG island of the *MGMT* promoter is frequently methylated in gliomas. Methylation of the CpG island in the promoter region leads to altered chromatin structure and reduced binding of transcription factors resulting in silencing of the *MGMT* gene (98). Therefore, tumor cells with an unmethylated *MGMT* promoter are resistant to alkylating agents, while those having silenced *MGMT* are more chemosensitive (23-25). *MGMT* promoter hypermethylation therefore serves as a predictive marker for response to temozolomide in newly diagnosed glioblastomas (23).

Additionally *MGMT* promoter hypermethylation has been associated with a more favorable prognosis in grade III gliomas (41, 76). There are several assays (MS-MLPA, MS-PCR) to measure *MGMT* promoter methylation. These assays interrogate different sets of CpG sites and have shown different outcome (23-25, 99-101). It is therefore important to select CpG sites that have sufficient predictive power when conducting an analysis. *MGMT*-STP27, identified using logistic regression, determines the *MGMT* promoter methylation status for use as a predictive response marker to TMZ (102). This model includes probes cg12434587 and cg12981133 and covers CpG sites within the *DMR1* and *DMR2* regions (99). *DMR1* and *DMR2* are two regions that lie within the *MGMT* promoter and play an important role in the transcriptional control of *MGMT* (102). CpG sites within *DMR1* and *DMR2* have shown good classification properties and prognostic value, making these regions a good target for methylation testing (99).

Scope of this thesis

Although several prognostic and predictive biomarkers have been identified, there is still considerable need to improve on these. For example, there are patients with *MGMT*-methylated promoters who perform poorly. Therefore, in chapters 1-3 of this thesis, we describe additional predictive biomarkers in two randomized clinical trials.

Although these predictive markers may help patients select treatment, the prognosis for glioma patients remains poor. Therefore, novel treatment modalities require to be developed. In this thesis, we have analyzed the functional effects of different mutations in *EGFR* (chapter 4) and of genes mutated at a low frequency in ODs (chapter 5). *EGFR* mutations are frequently detected in many types of cancer with different cancer types having distinct genetic mutations. If distinct *EGFR* mutations have different functional differences, they may lead to the development of mutation specific targeted therapies. Less attention has been paid to the role of genes mutated at low frequency in ODs with 1p19q co-deletion. If these infrequent mutations play a role in tumorigenesis and progression, they may offer new therapeutic options for the treatment of ODs.

In summary, this thesis describes several methods to identify predictive markers in gliomas and the functional consequences of different mutations in *EGFR* and infrequent gene mutations in ODs.

REFERENCES

1. Ostrom QT, Gittleman H, Liao P, Rouse C, Chen Y, Dowling J, et al. CBTRUS statistical report: primary brain and central nervous system tumors diagnosed in the United States in 2007-2011. Neuro-oncology. 2014;16 Suppl 4:iv1-63.

2. Bromberg JE, van den Bent MJ. Oligodendrogliomas: molecular biology and treatment. Oncologist. 2009;14(2):155-63.

3. Coons SW, Johnson PC, Scheithauer BW, Yates AJ, Pearl DK. Improving diagnostic accuracy and interobserver concordance in the classification and grading of primary gliomas. Cancer. 1997;79(7):1381-93.

4. Louis DN, Ohgaki H, Wiestler OD, Cavenee WK, Burger PC, Jouvet A, et al. The 2007 WHO classification of tumours of the central nervous system. Acta Neuropathol. 2007;114(2):97-109.

5. Olar A, Aldape KD. Using the molecular classification of glioblastoma to inform personalized treatment. J Pathol. 2014;232(2):165-77.

6. Ohgaki H, Kleihues P. Population-based studies on incidence, survival rates, and genetic alterations in astrocytic and oligodendroglial gliomas. J Neuropathol Exp Neurol. 2005;64(6):479-89.

7. Turkoglu E, Gurer B, Sanli AM, Dolgun H, Gurses L, Oral NA, et al. Clinical outcome of surgically treated low-grade gliomas: a retrospective analysis of a single institute. Clin Neurol Neurosurg. 2013;115(12):2508-13.

8. Smith JS, Chang EF, Lamborn KR, Chang SM, Prados MD, Cha S, et al. Role of extent of resection in the long-term outcome of low-grade hemispheric gliomas. J Clin Oncol. 2008;26(8):1338-45.

9. Kelly PJ. Stereotactic resection and its limitations in glial neoplasms. Stereotact Funct Neurosurg. 1992;59(1-4):84-91.

10. Lowenstein PR, Castro MG. Pushing the limits of glioma resection using electrophysiologic brain mapping. J Clin Oncol. 2012;30(20):2437-40.

11. Mrugala MM. Advances and challenges in the treatment of glioblastoma: a clinician's perspective. Discov Med. 2013;15(83):221-30.

12. van den Bent MJ, Afra D, de Witte O, Ben Hassel M, Schraub S, Hoang-Xuan K, et al. Long-term efficacy of early versus delayed radiotherapy for low-grade astrocytoma and oligodendroglioma in adults: the EORTC 22845 randomised trial. Lancet. 2005;366(9490):985-90.

13. Karim AB, Maat B, Hatlevoll R, Menten J, Rutten EH, Thomas DG, et al. A randomized trial on dose-response in radiation therapy of low-grade cerebral glioma: European Organization for Research and Treatment of Cancer (EORTC) Study 22844. Int J Radiat Oncol Biol Phys. 1996;36(3):549-56.

14. Shaw E, Arusell R, Scheithauer B, O'Fallon J, O'Neill B, Dinapoli R, et al. Prospective randomized trial of low- versus high-dose radiation therapy in adults with supratentorial low-grade glioma: initial report of a North Central Cancer Treatment Group/Radiation Therapy Oncology Group/Eastern Cooperative Oncology Group study. J Clin Oncol. 2002;20(9):2267-76.

15. van den Bent MJ. Practice changing mature results of RTOG study 9802: another positive PCV trial makes adjuvant chemotherapy part of standard of care in low-grade glioma. Neuro Oncol. 2014;16(12):1570-4.

16. Hoang-Xuan K, Capelle L, Kujas M, Taillibert S, Duffau H, Lejeune J, et al. Temozolomide as initial treatment for adults with low-grade oligodendrogliomas or oligoastrocytomas and correlation with chromosome 1p deletions. J Clin Oncol. 2004;22(15):3133-8.

17. Pace A, Vidiri A, Galie E, Carosi M, Telera S, Cianciulli AM, et al. Temozolomide chemotherapy for progressive low-grade glioma: clinical benefits and radiological response. Ann Oncol. 2003;14(12):1722-6.

18. Quinn JA, Reardon DA, Friedman AH, Rich JN, Sampson JH, Provenzale JM, et al. Phase II trial of temozolomide in patients with progressive low-grade glioma. J Clin Oncol. 2003;21(4):646-51.

19. van den Bent MJ, Brandes AA, Taphoorn MJ, Kros JM, Kouwenhoven MC, Delattre JY, et al. Adjuvant procarbazine, lomustine, and vincristine chemotherapy in newly diagnosed anaplastic oligodendroglioma: long-term follow-up of EORTC brain tumor group study 26951. J Clin Oncol. 2013;31(3):344-50.

20. Giannini C, Burger PC, Berkey BA, Cairncross JG, Jenkins RB, Mehta M, et al. Anaplastic oligodendroglial tumors: refining the correlation among histopathology, 1p19q deletion and clinical outcome in Intergroup Radiation Therapy Oncology Group Trial 9402. Brain Pathol. 2008;18(3):360-9.

21. Cairncross G, Wang M, Shaw E, Jenkins R, Brachman D, Buckner J, et al. Phase III trial of chemoradiotherapy for anaplastic oligodendroglioma: long-term results of RTOG 9402. J Clin Oncol. 2013;31(3):337-43.

22. Stupp R, Mason WP, van den Bent MJ, Weller M, Fisher B, Taphoorn MJ, et al. Radiotherapy plus concomitant and adjuvant temozolomide for glioblastoma. N Engl J Med. 2005;352(10):987-96.

23. Hegi ME, Diserens AC, Gorlia T, Hamou MF, de Tribolet N, Weller M, et al. *MGMT* gene silencing and benefit from temozolomide in glioblastoma. N Engl J Med. 2005;352(10):997-1003.

24. Malmstrom A, Gronberg BH, Marosi C, Stupp R, Frappaz D, Schultz H, et al. Temozolomide versus standard 6-week radiotherapy versus hypofractionated radiotherapy in patients older than 60 years with glioblastoma: the Nordic randomised, phase 3 trial. Lancet Oncol. 2012;13(9):916-26.

25. Wick W, Platten M, Meisner C, Felsberg J, Tabatabai G, Simon M, et al. Temozolomide chemotherapy alone versus radiotherapy alone for malignant astrocytoma in the elderly: the NOA-08 randomised, phase 3 trial. Lancet Oncol. 2012;13(7):707-15.

26. Chinot OL, Wick W, Mason W, Henriksson R, Saran F, Nishikawa R, et al. Bevacizumab plus radiotherapy-temozolomide for newly diagnosed glioblastoma. N Engl J Med. 2014;370(8):709-22.

27. Gilbert MR, Dignam JJ, Armstrong TS, Wefel JS, Blumenthal DT, Vogelbaum MA, et al. A randomized trial of bevacizumab for newly diagnosed glioblastoma. N Engl J Med. 2014;370(8):699-708.

28. Taal W. OHM, Walenkamp A.M.E., Beerepoot L.V., Hanse M., Buter J., Honkoop A., Boerman D., F, de Vos F.Y.F.L., Jansen R.L., van den Berkmortel F.W.P.J., Brandsma D, Kros J.M., Bromberg J.E., van Heuvel I., Smits M., van der Holt B., Vernhout R., van Den Bent M.J. A randomized phase II study of bevacizumab versus bevacizumab plus lomustine versus lomustine single agent in recurrent glioblastoma: The Dutch BELOB study. J Clin Oncol 2013;31((suppl; abstr 2001)).

29. Reardon DA, Fink KL, Mikkelsen T, Cloughesy TF, O'Neill A, Plotkin S, et al. Randomized phase II study of cilengitide, an integrin-targeting arginine-glycine- aspartic acid peptide, in recurrent glioblastoma multiforme. J Clin Oncol. 2008;26(34):5610-7.

30. Stupp R, Hegi ME, Neyns B, Goldbrunner R, Schlegel U, Clement PM, et al. Phase I/IIa study of cilengitide and temozolomide with concomitant radiotherapy followed by cilengitide and temozolomide maintenance therapy in patients with newly diagnosed glioblastoma. J Clin Oncol. 2010;28(16):2712-8.

31. Stupp R, Hegi ME, Gorlia T, Erridge SC, Perry J, Hong YK, et al. Cilengitide combined with standard treatment for patients with newly diagnosed glioblastoma with methylated *MGMT* promoter (CENTRIC EORTC 26071-22072 study): a multicentre, randomised, open-label, phase 3 trial. Lancet Oncol. 2014;15(10):1100-8.

32. Nabors LB, Fink KL, Mikkelsen T, Grujicic D, Tarnawski R, Nam do H, et al. Two cilengitide regimens in combination with standard treatment for patients with newly diagnosed glioblastoma and unmethylated *MGMT* gene promoter: results of the open- label, controlled, randomized phase II CORE study. Neuro Oncol. 2015;17(5):708-17.

33. Thomas AA, Fisher JL, Ernstoff MS, Fadul CE. Vaccine-based immunotherapy for glioblastoma. CNS Oncol. 2013;2(4):331-49.

34. Sampson JH, Heimberger AB, Archer GE, Aldape KD, Friedman AH, Friedman HS, et al. Immuno-logic escape after prolonged progression-free survival with epidermal growth factor receptor variant III peptide vaccination in patients with newly diagnosed glioblastoma. J Clin Oncol. 2010;28(31):4722-9.

35. Mitchell DA, Batich KA, Gunn MD, Huang MN, Sanchez-Perez L, Nair SK, et al. Tetanus tox-oid and CCL3 improve dendritic cell vaccines in mice and glioblastoma patients. Nature. 2015;519(7543):366-9.

36. Phillips HS, Kharbanda S, Chen R, Forrest WF, Soriano RH, Wu TD, et al. Molecular subclasses of high-grade glioma predict prognosis, delineate a pattern of disease progression, and resemble stages in neurogenesis. Cancer Cell. 2006;9(3):157-73.

37. Verhaak RG, Hoadley KA, Purdom E, Wang V, Qi Y, Wilkerson MD, et al. Integrated genomic analysis identifies clinically relevant subtypes of glioblastoma characterized by abnormalities in PDGFRA, *IDH1*, *EGFR*, and NF1. Cancer Cell. 2010;17(1):98-110.

38. Li A, Walling J, Ahn S, Kotliarov Y, Su Q, Quezado M, et al. Unsupervised analysis of transcriptomic profiles reveals six glioma subtypes. Cancer Res. 2009;69(5):2091-9.

39. Gravendeel LA, Kouwenhoven MC, Gevaert O, de Rooi JJ, Stubbs AP, Duijm JE, et al. Intrinsic gene expression profiles of gliomas are a better predictor of survival than histology. Cancer Res. 2009;69(23):9065-72.

40. Noushmehr H, Weisenberger DJ, Diefes K, Phillips HS, Pujara K, Berman BP, et al. Identification of a CpG island methylator phenotype that defines a distinct subgroup of glioma. Cancer Cell. 2010;17(5):510-22.

41. van den Bent MJ, Gravendeel LA, Gorlia T, Kros JM, Lapre L, Wesseling P, et al. A hypermethylated phenotype is a better predictor of survival than *MGMT* methylation in anaplastic oligodendroglial brain tumors: a report from EORTC study 26951. Clin Cancer Res. 2011;17(22):7148-55.

42. Christensen BC, Smith AA, Zheng S, Koestler DC, Houseman EA, Marsit CJ, et al. DNA methylation, isocitrate dehydrogenase mutation, and survival in glioma. J Natl Cancer Inst. 2011;103(2):143-53.

43. Kloosterhof NK, de Rooi JJ, Kros M, Eilers PH, Sillevis Smitt PA, van den Bent MJ, et al. Molecular subtypes of glioma identified by genome-wide methylation profiling. Genes, chromosomes & cancer. 2013;52(7):665-74.

44. Collins VP, Jones DT, Giannini C. Pilocytic astrocytoma: pathology, molecular mechanisms and markers. Acta Neuropathol. 2015.

45. Jones DT, Hutter B, Jager N, Korshunov A, Kool M, Warnatz HJ, et al. Recurrent somatic alterations of FGFR1 and NTRK2 in pilocytic astrocytoma. Nat Genet. 2013;45(8):927-32.

46. Watanabe T, Nobusawa S, Kleihues P, Ohgaki H. *IDH1* mutations are early events in the develop-ment of astrocytomas and oligodendrogliomas. Am J Pathol. 2009;174(4):1149-53.

47. Mellai M, Piazzi A, Caldera V, Monzeglio O, Cassoni P, Valente G, et al. *IDH1* and *IDH2* mutations, im-munohistochemistry and associations in a series of brain tumors. J Neurooncol. 2011;105(2):345-57.

48. Korshunov A, Meyer J, Capper D, Christians A, Remke M, Witt H, et al. Combined molecular analysis of BRAF and *IDH1* distinguishes pilocytic astrocytoma from diffuse astrocytoma. Acta Neuropathol. 2009;118(3):401-5.

49. Jiao Y, Killela PJ, Reitman ZJ, Rasheed AB, Heaphy CM, de Wilde RF, et al. Frequent ATRX, CIC, FUBP1 and *IDH1* mutations refine the classification of malignant gliomas. Oncotarget. 2012;3(7):709-22.

50. Kannan K, Inagaki A, Silber J, Gorovets D, Zhang J, Kastenhuber ER, et al. Whole-exome sequencing identifies ATRX mutation as a key molecular determinant in lower-grade glioma. Oncotarget. 2012;3(10):1194-203.

51. Liu XY, Gerges N, Korshunov A, Sabha N, Khuong-Quang DA, Fontebasso AM, et al. Frequent ATRX mutations and loss of expression in adult diffuse astrocytic tumors carrying *IDH1/IDH2* and TP53 mutations. Acta Neuropathol. 2012;124(5):615-25.

52. Aldape K, Zadeh G, Mansouri S, Reifenberger G, von Deimling A. Glioblastoma: pathology, molecular mechanisms and markers. Acta Neuropathol. 2015;129(6):829-48.

53. Parsons DW, Jones S, Zhang X, Lin JC, Leary RJ, Angenendt P, et al. An integrated genomic analysis of human glioblastoma multiforme. Science. 2008;321(5897):1807-12.

54. Cancer Genome Atlas Research N. Comprehensive genomic characterization defines human glioblastoma genes and core pathways. Nature. 2008;455(7216):1061-8.

55. Parker BC, Annala MJ, Cogdell DE, Granberg KJ, Sun Y, Ji P, et al. The tumorigenic FGFR3-TACC3 gene fusion escapes miR-99a regulation in glioblastoma. J Clin Invest. 2013;123(2):855-65.

56. Morris LG, Kaufman AM, Gong Y, Ramaswami D, Walsh LA, Turcan S, et al. Recurrent somatic mutation of FAT1 in multiple human cancers leads to aberrant Wnt activation. Nat Genet. 2013;45(3):253-61.

57. Singh D, Chan JM, Zoppoli P, Niola F, Sullivan R, Castano A, et al. Transforming fusions of FGFR and TACC genes in human glioblastoma. Science. 2012;337(6099):1231-5.

58. Brennan CW, Verhaak RG, McKenna A, Campos B, Noushmehr H, Salama SR, et al. The somatic genomic landscape of glioblastoma. Cell. 2013;155(2):462-77.

59. Killela PJ, Reitman ZJ, Jiao Y, Bettegowda C, Agrawal N, Diaz LA, Jr., et al. TERT promoter mutations occur frequently in gliomas and a subset of tumors derived from cells with low rates of self-renewal. Proc Natl Acad Sci U S A. 2013;110(15):6021-6.

60. Bettegowda C, Agrawal N, Jiao Y, Sausen M, Wood LD, Hruban RH, et al. Mutations in CIC and FUBP1 contribute to human oligodendroglioma. Science. 2011;333(6048):1453-5.

61. Sahm F, Koelsche C, Meyer J, Pusch S, Lindenberg K, Mueller W, et al. CIC and FUBP1 mutations in oligodendrogliomas, oligoastrocytomas and astrocytomas. Acta Neuropathol. 2012;123(6):853-60.

62. Yip S, Butterfield YS, Morozova O, Chittaranjan S, Blough MD, An J, et al. Concurrent CIC mutations, *IDH* mutations, and 1p/19q loss distinguish oligodendrogliomas from other cancers. J Pathol. 2012;226(1):7-16.

63. Cancer Genome Atlas Research N, Brat DJ, Verhaak RG, Aldape KD, Yung WK, Salama SR, et al. Comprehensive, Integrative Genomic Analysis of Diffuse Lower-Grade Gliomas. N Engl J Med. 2015;372(26):2481-98.

64. Freidlin B, Sun Z, Gray R, Korn EL. Phase III clinical trials that integrate treatment and biomarker evaluation. J Clin Oncol. 2013;31(25):3158-61.

65. Freidlin B, McShane LM, Korn EL. Randomized clinical trials with biomarkers: design issues. J Natl Cancer Inst. 2010;102(3):152-60.

66. Jenkins RB, Blair H, Ballman KV, Giannini C, Arusell RM, Law M, et al. A t(1;19)(q10;p10) mediates the combined deletions of 1p and 19q and predicts a better prognosis of patients with oligodendroglioma. Cancer Res. 2006;66(20):9852-61.

67. Ducray F, Marie Y, Sanson M. *IDH1* and *IDH2* mutations in gliomas. N Engl J Med. 2009;360(21):2248-9; author reply 9.

68. Kloosterhof NK, Bralten LB, Dubbink HJ, French PJ, van den Bent MJ. Isocitrate dehydrogenase-1 mutations: a fundamentally new understanding of diffuse glioma? Lancet Oncol. 2011;12(1):83-91.

69. Dang L, White DW, Gross S, Bennett BD, Bittinger MA, Driggers EM, et al. Cancer-associated *IDH1* mutations produce 2-hydroxyglutarate. Nature. 2010;465(7300):966.

70. Turcan S, Rohle D, Goenka A, Walsh LA, Fang F, Yilmaz E, et al. *IDH1* mutation is sufficient to establish the glioma hypermethylator phenotype. Nature. 2012;483(7390):479-83.

71. Xu Y, Hu B, Choi AJ, Gopalan B, Lee BH, Kalady MF, et al. Unique DNA methylome profiles in CpG island methylator phenotype colon cancers. Genome Res. 2012;22(2):283-91.

72. Hartmann C, Meyer J, Balss J, Capper D, Mueller W, Christians A, et al. Type and frequency of *IDH1* and *IDH2* mutations are related to astrocytic and oligodendroglial differentiation and age: a study of 1,010 diffuse gliomas. Acta Neuropathol. 2009;118(4):469-74.

73. Mardis ER, Ding L, Dooling DJ, Larson DE, McLellan MD, Chen K, et al. Recurring mutations found by sequencing an acute myeloid leukemia genome. N Engl J Med. 2009;361(11):1058-66.

74. Yan H, Parsons DW, Jin G, McLendon R, Rasheed BA, Yuan W, et al. *IDH1* and *IDH2* mutations in gliomas. N Engl J Med. 2009;360(8):765-73.

75. Sanson M, Marie Y, Paris S, Idbaih A, Laffaire J, Ducray F, et al. Isocitrate dehydrogenase 1 codon 132 mutation is an important prognostic biomarker in gliomas. J Clin Oncol. 2009;27(25):4150-4.

76. Wick W, Hartmann C, Engel C, Stoffels M, Felsberg J, Stockhammer F, et al. NOA-04 randomized phase III trial of sequential radiochemotherapy of anaplastic glioma with procarbazine, lomustine, and vincristine or temozolomide. J Clin Oncol. 2009;27(35):5874-80.

77. Beiko J, Suki D, Hess KR, Fox BD, Cheung V, Cabral M, et al. *IDH1* mutant malignant astrocytomas are more amenable to surgical resection and have a survival benefit associated with maximal surgical resection. Neuro Oncol. 2014;16(1):81-91.

78. Cairncross JG, Wang M, Jenkins RB, Shaw EG, Giannini C, Brachman DG, et al. Benefit from procarbazine, lomustine, and vincristine in oligodendroglial tumors is associated with mutation of IDH. J Clin Oncol. 2014;32(8):783-90.

79. Weller M, Felsberg J, Hartmann C, Berger H, Steinbach JP, Schramm J, et al. Molecular predictors of progression-free and overall survival in patients with newly diagnosed glioblastoma: a prospective translational study of the German Glioma Network. J Clin Oncol. 2009;27(34):5743-50.

80. Gan HK, Kaye AH, Luwor RB. The *EGFR*vIII variant in glioblastoma multiforme. J Clin Neurosci. 2009;16(6):748-54.

81. Lee JC, Vivanco I, Beroukhim R, Huang JH, Feng WL, DeBiasi RM, et al. Epidermal growth factor receptor activation in glioblastoma through novel missense mutations in the extracellular domain. PLoS Med. 2006;3(12):e485.

82. Ekstrand AJ, Sugawa N, James CD, Collins VP. Amplified and rearranged epidermal growth factor receptor genes in human glioblastomas reveal deletions of sequences encoding portions of the N- and/or C-terminal tails. Proc Natl Acad Sci U S A.1992;89(10):4309-13.

83. Huang HS, Nagane M, Klingbeil CK, Lin H, Nishikawa R, Ji XD, et al. The enhanced tumorigenic activity of a mutant epidermal growth factor receptor common in human cancers is mediated by threshold levels of constitutive tyrosine phosphorylation and unattenuated signaling. J Biol Chem. 1997;272(5):2927-35.

84. Shinojima N, Tada K, Shiraishi S, Kamiryo T, Kochi M, Nakamura H, et al. Prognostic value of epidermal growth factor receptor in patients with glioblastoma multiforme. Cancer Res. 2003;63(20):6962-70.

85.   Huncharek M, Kupelnick B. Epidermal growth factor receptor gene amplification as a prognostic marker in glioblastoma multiforme: results of a meta-analysis. Oncology research. 2000;12(2):107-12.

86.   Mellinghoff IK, Wang MY, Vivanco I, Haas-Kogan DA, Zhu S, Dia EQ, et al. Molecular determinants of the response of glioblastomas to *EGFR* kinase inhibitors. N Engl J Med. 2005;353(19):2012-24.

87.   Li G, Wong AJ. EGF receptor variant III as a target antigen for tumor immunotherapy. Expert review of vaccines. 2008;7(7):977-85.

88.   van den Bent MJ, Brandes AA, Rampling R, Kouwenhoven MC, Kros JM, Carpentier AF, et al. Randomized phase II trial of erlotinib versus temozolomide or carmustine in recurrent glioblastoma: EORTC brain tumor group study 26034. J Clin Oncol. 2009;27(8):1268-74.

89.   Uhm JH, Ballman KV, Wu W, Giannini C, Krauss JC, Buckner JC, et al. Phase II evaluation of gefitinib in patients with newly diagnosed Grade 4 astrocytoma: Mayo/North Central Cancer Treatment Group Study N0074. International journal of radiation oncology, biology, physics. 2011;80(2):347-53.

90.   Thiessen B, Stewart C, Tsao M, Kamel-Reid S, Schaiquevich P, Mason W, et al. A phase I/II trial of GW572016 (lapatinib) in recurrent glioblastoma multiforme: clinical outcomes, pharmacokinetics and molecular correlation. Cancer chemotherapy and pharmacology. 2010;65(2):353-61.

91.   Sharma SV, Bell DW, Settleman J, Haber DA. Epidermal growth factor receptor mutations in lung cancer. Nat Rev Cancer. 2007;7(3):169-81.

92.   Jones DT, Kocialkowski S, Liu L, Pearson DM, Backlund LM, Ichimura K, et al. Tandem duplication producing a novel oncogenic BRAF fusion gene defines the majority of pilocytic astrocytomas. Cancer Res. 2008;68(21):8673-7.

93.   Pfister S, Janzarik WG, Remke M, Ernst A, Werft W, Becker N, et al. BRAF gene duplication constitutes a mechanism of MAPK pathway activation in low-grade astrocytomas. J Clin Invest. 2008;118(5):1739-49.

94.   Bar EE, Lin A, Tihan T, Burger PC, Eberhart CG. Frequent gains at chromosome 7q34 involving BRAF in pilocytic astrocytoma. J Neuropathol Exp Neurol. 2008;67(9):878-87.

95.   Becker AP, Scapulatempo-Neto C, Carloni AC, Paulino A, Sheren J, Aisner DL, et al. KIAA1549: BRAF Gene Fusion and FGFR1 Hotspot Mutations Are Prognostic Factors in Pilocytic Astrocytomas. J Neuropathol Exp Neurol. 2015;74(7):743-54.

96.   Tatevossian RG, Lawson AR, Forshew T, Hindley GF, Ellison DW, Sheer D. MAPK pathway activation and the origins of pediatric low-grade astrocytomas. Journal of cellular physiology. 2010;222(3):509-14.

97.   Esteller M, Garcia-Foncillas J, Andion E, Goodman SN, Hidalgo OF, Vanaclocha V, et al. Inactivation of the DNA-repair gene *MGMT* and the clinical response of gliomas to alkylating agents. N Engl J Med. 2000;343(19):1350-4.

98.   Nakagawachi T, Soejima H, Urano T, Zhao W, Higashimoto K, Satoh Y, et al. Silencing effect of CpG island hypermethylation and histone modifications on O6- methylguanine-DNA methyltransferase (*MGMT*) gene expression in human cancer. Oncogene. 2003;22(55):8835-44.

99.   Bady P, Sciuscio D, Diserens AC, Bloch J, van den Bent MJ, Marosi C, et al. *MGMT* methylation analysis of glioblastoma on the Infinium methylation BeadChip identifies two distinct CpG regions associated with gene silencing and outcome, yielding a prediction model for comparisons across datasets, tumor grades, and CIMP-status. Acta Neuropathol. 2012;124(4):547-60.

100. Esteller M, Risques RA, Toyota M, Capella G, Moreno V, Peinado MA, et al. Promoter hypermethylation of the DNA repair gene O(6)-methylguanine-DNA methyltransferase is associated with the

presence of G:C to A:T transition mutations in p53 in human colorectal tumorigenesis. Cancer Res. 2001;61(12):4689-92.

101. Weller M, Stupp R, Reifenberger G, Brandes AA, van den Bent MJ, Wick W, et al. *MGMT* promoter methylation in malignant gliomas: ready for personalized medicine? Nature reviews Neurology. 2010;6(1):39-51.

102. Malley DS, Hamoudi RA, Kocialkowski S, Pearson DM, Collins VP, Ichimura K. A distinct region of the *MGMT* CpG island critical for transcriptional regulation is preferentially methylated in glioblastoma cells and xenografts. Acta Neuropathol. 2011;121(5):651-61.
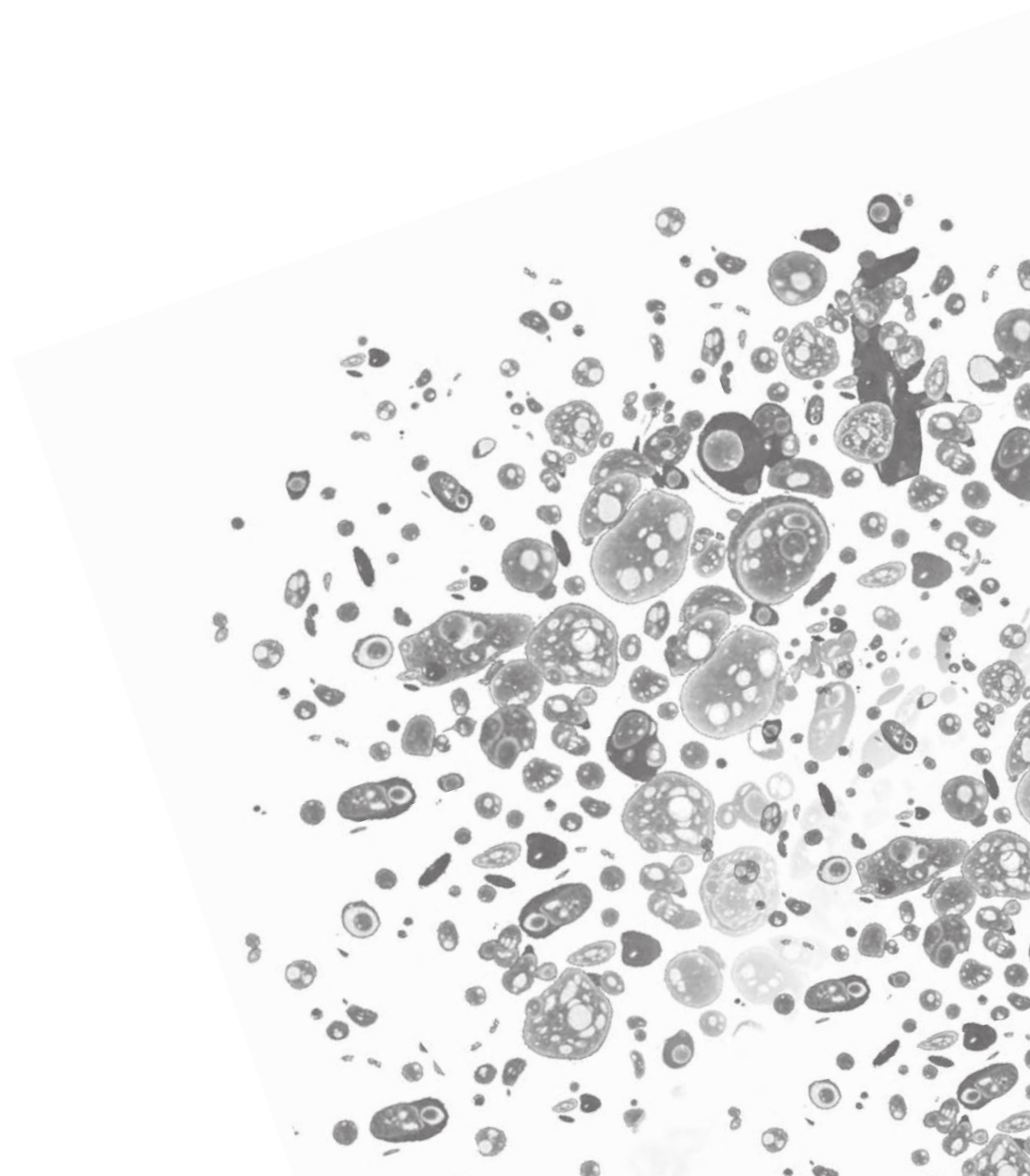
CHAPTER 1

Intrinsic molecular subtypes of glioma are prognostic and predict benefit from adjuvant procarbazine, lomustine, and vincristine chemotherapy in combination with other prognostic factors in anaplastic oligodendroglial brain tumors: a report from EORTC study 26951

Lale Erdem-Eraslan, Lonneke A. Gravendeel, Johan de Rooi, Paul H.C. Eilers, Ahmed Idbaih, Wim G.M. Spliet, Wilfred F.A. den Dunnen, Johannes L. Teepen, Pieter Wesseling, Peter A.E. Sillevis Smitt, Johan M. Kros, Thierry Gorlia, Martin J. van den Bent, and Pim J. French
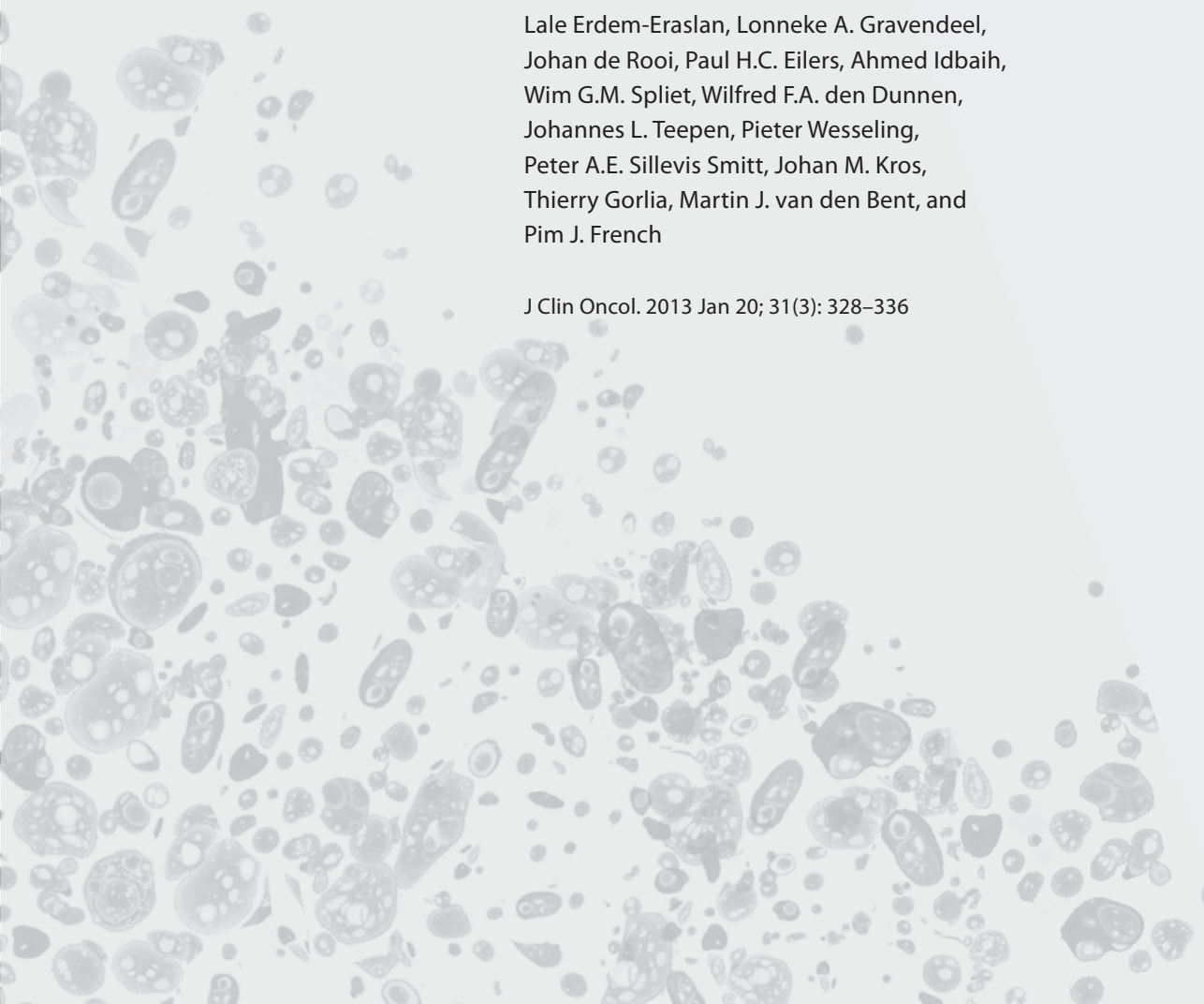
ABSTRACT

Purpose

Intrinsic glioma subtypes (IGSs) are molecularly similar tumors that can be identified based on unsupervised gene expression analysis. Here, we have evaluated the clinical relevance of these subtypes within European Organisation for Research and Treatment of Cancer (EORTC) 26951, a randomized phase III clinical trial investigating adjuvant procarbazine, lomustine, and vincristine (PCV) chemotherapy in anaplastic oligoden-droglial tumors. Our study includes gene expression profiles of formalin-fixed, paraffin-embedded (FFPE) clinical trial samples.

Patients and Methods

Gene expression profiling was performed in 140 samples, 47 fresh frozen samples and 93 FFPE samples, on HU133_Plus_2.0 and HuEx_1.0_st arrays, respectively.

Results

All previously identified six IGSs are present in EORTC 26951. This confirms that different molecular subtypes are present within a well-defined histologic subtype. Intrinsic subtypes are highly prognostic for overall survival (OS) and progression-free survival (PFS). They are prognostic for PFS independent of clinical (age, performance status, and tumor location), molecular (1p/19q loss of heterozygosity [LOH], *IDH1* mutation, and *MGMT* methylation), and histologic parameters. Combining known molecular (1p/19q LOH, *IDH1*) prognostic parameters with intrinsic subtypes improves outcome prediction (proportion of explained variation, 30% *v* 23% for each individual group of factors). Specific genetic changes (*IDH1*, 1p/19q LOH, and *EGFR* amplification) segregate into different subtypes. We identified one subtype, IGS-9 (characterized by a high percentage of 1p/19q LOH and *IDH1* mutations), that especially benefits from PCV chemotherapy. Median OS in this subtype was 5.5 years after radiotherapy (RT) alone versus 12.8 years after RT/PCV (P = .0349; hazard ratio, 2.18; 95% CI, 1.06 to 4.50).

Conclusion

Intrinsic subtypes are highly prognostic in EORTC 26951 and improve outcome prediction when combined with other prognostic factors. Tumors assigned to IGS-9 benefit from adjuvant PCV.

INTRODUCTION

Unsupervised analysis of gene expression profiling identifies subgroups of tumors that are molecularly similar. This approach has been used to identify distinct intrinsic subtypes of cancer and provides an objective method to classify tumors (1–4). In gliomas, the identified intrinsic subtypes reportedly correlate better with patient prognosis than histology (5–9). Intrinsic glioma subtypes (IGSs) are not only similar on the RNA level, but specific genetic changes also segregate in distinct intrinsic subtypes (8,10). Therefore, it is likely that each molecular subtype will require its own treatment paradigm.

True validation of the prognostic relevance of the IGSs requires analysis on homogeneously and prospectively treated patients, ideally within a randomized clinical trial. One of the main problems in analyzing clinical trial samples is that they are often of poor quality; most are formalin-fixed, paraffin-embedded (FFPE) samples (11).

However, recent technologic advances have enabled high-throughput analysis of FFPE material, including expression arrays (12–14). In a large cohort of paired fresh frozen (FF)-FFPE samples, we recently demonstrated that differences in mRNA expression are retained in FFPE samples. Importantly, the assignment to one of six IGSs was identical between the FF-FFPE matched samples in 87% of cases (15), and the intrinsic subtypes remain highly prognostic for survival. These results demonstrate that FFPE material can be used for expression profiling.

Not all patients with glioma respond similarly to treatment. For example, glioblastomas with a methylated O6-methylguanine-methyltransferase (*MGMT*) promoter respond better to treatment with temozolomide (16,17). In oligodendrogliomas, uncontrolled trials indicated that loss of heterozygosity (LOH) on 1p/19q is predictive for response to procarbazine, lomustine, and vincristine (PCV) chemotherapy (18,19). Selection of patients who benefit most from particular therapeutic regimens helps to improve treatment efficacy and to potentially avoid toxicity in patients who are unlikely to benefit from that therapy anyway.

European Organisation for Research and Treatment of Cancer (EORTC) 26951 is a randomized phase III clinical trial investigating whether the addition of PCV chemotherapy to radiotherapy (RT) would improve overall survival (OS) and progression-free survival (PFS) in patients with anaplastic oligodendroglioma (AOD) or anaplastic mixed oligoastrocytoma (AOA). This trial showed that the addition of six cycles of PCV after 59.4 Gy of RT increases OS and PFS in these tumors (20). However, some patients seemed to benefit more from the addition of PCV treatment than others (21).

Here, we have evaluated the clinical relevance of intrinsic subtypes within EORTC 26951. Our study is the first to use gene expression profiling on FFPE clinical trial samples. Our data validate that intrinsic subtypes of glioma are prognostic for survival. Intrinsic subtypes improve outcome prediction when combined with other known prognostic

parameters (1p/19q LOH and *IDH1* mutation), although this increase is not significant. Our data also indicate that patients with tumors assigned to a specific intrinsic subtype benefit from PCV treatment.

PATIENTS AND METHODS

Patient Samples

Patients were considered eligible for EORTC 26951 if they had been diagnosed by the local pathologist with an AOD or an AOA according to the 1993 WHO classification. Details of the eligibility criteria and the CONSORT flow diagram have been described previously (21) and are shown in Figure 1. A central pathology review was conducted on 345 of 368 samples and on 136 of 140 samples used in the present study. Four samples were omitted in the multivariate analysis that included review diagnosis as a factor.

Figure 1.
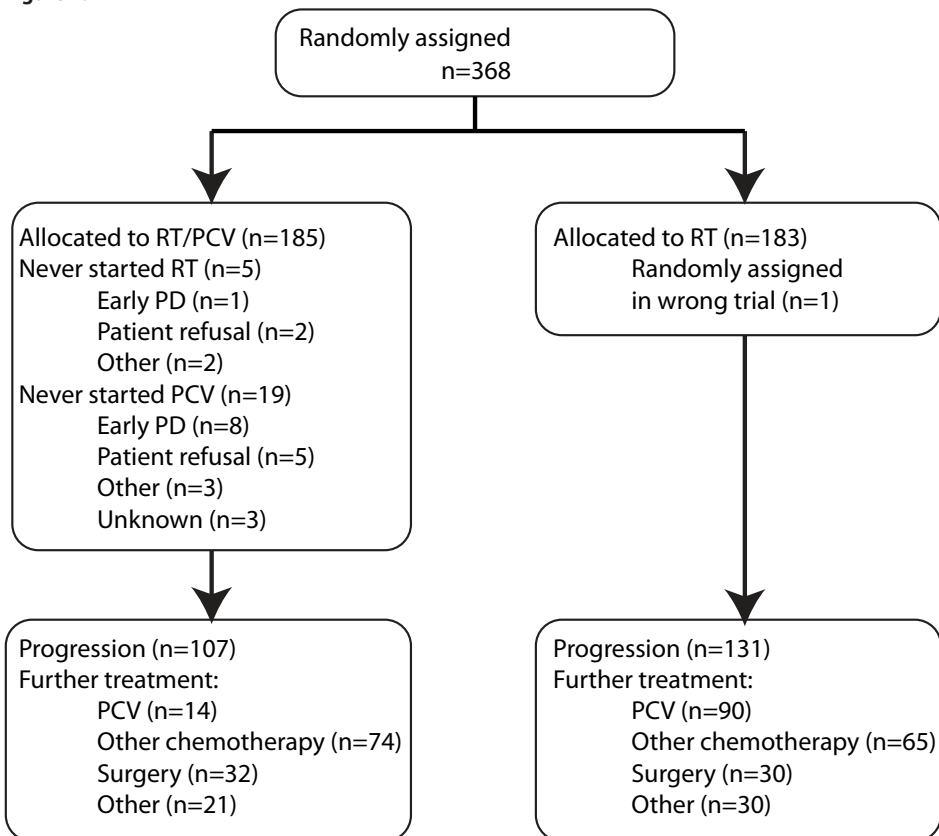
CONSORT diagram. PCV, procarbazine, lomustine, and vincristine; PD, progressive disease; RT, radiotherapy.

All analysis using histologic diagnosis made use of the review diagnosis. Patient and sample characteristics are detailed in the Data Supplement. Analysis of 1p/19q LOH, *EGFR* amplification, *IDH1* mutations, and *MGMT* promoter methylation on EORTC 26951 samples has been described previously (21–23).

RNA Isolation and Array Hybridization

Total RNA extraction, purification, and quantification from FF and FFPE material were reported previously (8,15). RNA (150 ng) from FF and FFPE tissues was used for expression profiling. FF samples (n = 47) were profiled as described on HU133plus 2.0 arrays (Affymetrix, High Wycombe, United Kingdom) (8); FFPE samples (n = 93) were profiled using HuEx_1.0_st arrays (Affymetrix) in combination with Nugen Ovation kits (Nugen, San Carlos, CA), as reported (13,15).

Statistical Analysis

Samples were assigned to one of the six intrinsic molecular subtypes of glioma using ClusterRepro (an R package; http://crantastic.org/packages/clusterRepro) as described previously, omitting control cluster 0 (8,24). Previously, these intrinsic subtypes were designated cluster followed by the cluster number (0, 9, 16, 17, 18, 22, or 23). Here, we annotate these clusters as IGSs followed by the same cluster number (eg, IGS-9). Other groups have also described molecular classification methods (7,9),(10); the overlap with The Cancer Genome Atlas classification is detailed in the Data Supplement (for other comparisons, see Gravendeel et al (8)). Samples assigned to IGS-9 and IGS-17 generally are assigned to the proneural subtype, IGS-18 to the classical subtype, and IGS-23 to the mesenchymal subtype. Neural subtypes are assigned to either IGS-17 or IGS-23.

Differences between the Kaplan-Meier survival curves were calculated using the log- rank (Mantel-Cox) test using GraphPad Prism version 5.00 for Windows (GraphPad Software, San Diego, CA). Comparisons between frequencies were calculated using the Fisher's exact test. In this exploratory analysis, $P < .05$ was considered to indicate significant differences. The importance of groups of prognostic factors was compared using the percentage of explained variation (PEV) developed by Heinze and Schemper (25) for Cox regression using SAS macros (SAS Institute, Cary, NC). A PEV of at least 20% is considered a minimum requirement for a model to provide sufficiently precise individual PFS or OS predictions (26,27). PFS and OS were computed from random assignment to date of event (progression and/or death) or censored at the date of last visit.

RESULTS

Patients and Samples

Out of 368 patients within the EORTC 26951 trial, a total of 140 samples of were available for the current study; for the other patients, the amount of material was insufficient. Of the samples, 47 were FF and 93 were FFPE. Seventy-three patients had been assigned to the RT plus PCV chemotherapy arm, and 67 patients had been assigned to the RT only arm. Our cohort of samples from the EORTC 26951 study did not differ from the entire EORTC 26951 cohort (368 patients) with respect to age, sex, performance status, diagnosis, tumor location, *IDH1* mutation, 1p/19q LOH, *EGFR* amplification, *MGMT* promoter methylation, OS, and PFS (Table 1). However, OS within the RT only treatment arm of included patients was worse compared with OS in patients not included (OS: 1.6 *v* 3.7 years, respectively; *P* = .009; hazard ratio [HR], 1.59; 95% CI, 1.12 to 2.25; PFS: 0.8 *v* 1.4 years, respectively; *P* = .012; HR, 1.55; 95% CI, 1.10 to 2.17), even when corrected for known clinical (age, extent of resection, sex, and performance status) and molecular (1p/19q LOH) characteristics and histologic review diagnosis. There were no such differences in the RT-PCV arm. This effect is likely a result of difference in patient selection in the hospitals but not related to tissue sampling. Of note, at the time of random assignment, patients were stratified per center. Of the included samples, there were no differences in clinical, molecular, or histologic characteristics between the two treatment arms (Data Supplement). A detailed analysis of patients included versus not included is shown in the Data Supplement.

Intrinsic Subtypes Are Prognostic for OS and PFS

Expression profiling was performed on a total of 140 samples of patients treated within EORTC 26951. All expression profiles were then assigned to one of six predefined intrinsic subtypes. These molecularly similar intrinsic subtypes were identified previously and are based on unsupervised gene expression analysis (8). All six IGSs were identified, which shows that patients with different molecular subtypes were enrolled within this trial under the same histopathologic diagnosis. After assignment, IGS-9, IGS-16, IGS-17, IGS-18, IGS-22, and IGS-23 contained 50, two, 26, 27, eight, and 27 patients, respectively. The histologic composition (both original and review diagnosis) of subtypes is depicted in the Data Supplement. The intrinsic subtypes were highly prognostic for both OS and PFS. The median OS times for IGS-9, IGS-17, IGS-18, and IGS-23 were 8.5, 2.8, 1.2, and 1.0 years, respectively; and the median PFS times were 5.7, 1.8, 0.5, and 0.5 years, respectively (Fig 2). IGS-16 and IGS-22 contained too few samples to draw conclusions. Details for IGS-22 are listed in the Data Supplement. The subtype-specific differences in survival were highly similar to previously reported differences using FF archival samples and confirm the prognostic power of intrinsic subtyping (8). Even within the 1p/19q

**Table 1.** Comparison of baseline characteristics.

		Baseline characteristics			
		Included in the cluster analysis			
		No	Yes	Total	
		N=228 (%)	N=140 (%)	N=368 (%)	P-value
Age	Median Range	49.5 19.4 - 68.7	49.4 18.6 - 68.7	49.5 18.6 - 68.7	0.57
	Obs (O)	228	140	368	
Sex	Male	123 (53.9)	89 (63.6)	212 (57.6)	0.08
	Female	105 (46.1)	51 (36.4)	156 (42.4)	
Performance status	0.	81 (35.5)	53 (37.9)	134 (36.4)	0.75
	1.0	107 (46.9)	64 (45.7)	171 (46.5)	
	2.0	36 (15.8)	22 (15.7)	58 (15.8)	
Histological diagnoses	AOD	173 (75.9)	93 (66.4)	266 (72.3)	0.04
	AOA>25% O	53 (23.2)	47 (33.6)	100 (27.2)	
Central diagnosis	AOD	100 (43.9)	76 (54.3)	176 (47.8)	0.02
	AOA	46 (20.2)	36 (25.7)	82 (22.3)	
	LGG	28 (12.3)	11 (7.9)	39 (10.6)	
	HGG	26 (11.4)	13 (9.3)	39 (10.6)	
	Other	10 (4.4)	0 (0.0)	10 (2.7)	
	Missing	18 (7.9)	4 (2.9)	22 (6.0)	
Tumor location	Elsewhere	119 (52.2)	71 (50.7)	190 (51.6)	0.83
	Frontal	109 (47.8)	69 (49.3)	178 (48.4)	
IDH1 mutation	Normal	41 (18.0)	58 (41.4)	99 (26.9)	0.37
	Mutated	39 (17.1)	44 (31.4)	83 (22.6)	
1p19q LOH	Non codeleted	141 (61.8)	95 (67.9)	236 (64.1)	0.51
	Codeleted	44 (19.3)	36 (25.7)	80 (21.7)	
EGFR mutation	Normal	111 (48.7)	82 (58.6)	193 (52.4)	0.76
	Amplified	32 (14.0)	26 (18.6)	58 (15.8)	
MGMT promoter methylation	Unmethylated	14 (6.1)	17 (12.1)	31 (8.4)	0.61
	Methylated	57 (25.0)	64 (45.7)	121 (32.9)	
PFS	Obs (O);HR (95% CI)	181; 1.00	117; 1.16 (0.92, 1.46)		0.21
	Median (95% CI) (months)	19.65 (15.38, 33.35)	14.52 (9.63, 21.13)		
	% at 2 Year(s) (95% CI)	48.02 (41.39, 54.34)	39.29 (31.20, 47.26)		
OS	Obs (O); HR (95% CI)	168; 1.00	113; 1.25 (0.99, 1.59)		0.06
	Median (95% CI) (months)	43.89 (30.03, 61.17)	26.87 (18.69, 38.31)		
	% at 2 Year(s) (95% CI)	63.44 (56.81, 69.33)	51.43 (42.87, 59.33)		

Abbreviations: Obs: observation events; AOD: anaplastic oligodendroglioma; AOA: anaplastic oligoastrocy-toma; LGG: low grade glioma; HGG: glioblastomas and anaplastic astrocytoma; HR: hazard ratio; CI: confidence interval; PFS: progression-free survival; OS: overall survival. $P<0.01$ is considered statistically significant. The missing values are not included in the table and are the remaining percentages.

codeleted patient cohort, IGS subtyping remained prognostic. Conversely, 1p/19q status was also prognostic within patients assigned to IGS-9 (Data Supplement).

In multivariate analysis, intrinsic subtype was a significant prognostic factor that was independent from clinical (age, sex, performance status, and type of surgery), molecular (1p/19q LOH), and histologic (local diagnosis or review diagnosis) parameters (Table 2). Tissue type (FF or FFPE) was not a prognostic variable in univariate or multivariate analysis. When *IDH1* mutation status was included in this analysis, intrinsic subtyping remained an independent prognostic factor for PFS ($P = .003$) but not OS ($P = .052$).

Figure 2.
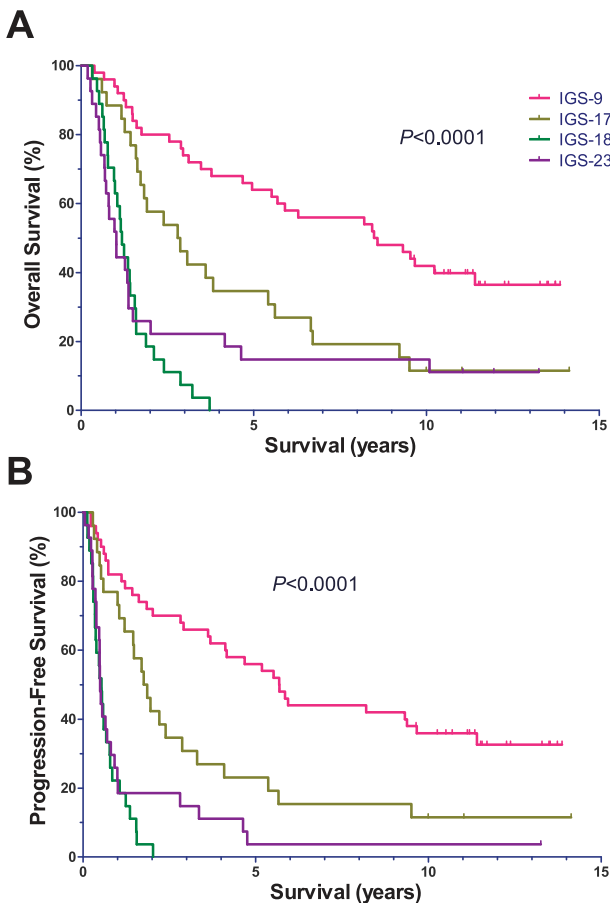
Kaplan-Meier survival curves of (A) overall survival (OS) and (B) progression-free survival (PFS) of the four major intrinsic glioma subtypes (IGSs) to which the patients from the European Organisation for Research and Treatment of Cancer (EORTC) 26951 trial were assigned. Survival is depicted as time (years) since random assignment. The four IGSs were highly prognostic for both OS and PFS because patient prognosis was different for each IGS. Only two and eight samples were assigned to IGS-16 and IGS-22, respectively (not shown).

Table 2. Analysis of OS by intrinsic subtyping

Number of observations	126
Number of failures	102

|	P-value	HR	95% CI for HR
Intrinsic subtype	0.001	1.06	1.03 - 1.12
Age	0.002	1.03	1.01 - 1.05
Sex	0.530	0.87	0.57 - 1.34
Type of surgery	0.016	0.67	0.49 - 0.93
Performance status	0.011	1.46	1.09 - 1.94
1p19qLOH	0.000	0.32	0.17 - 0.59
Review diagnosis	0.086	0.82	0.66 - 1.03

Abbreviations: HR: hazard ratio (compared to RT only arm); CI: confidence interval. Calculations are based on 126 observations. Type of surgery categories included: biopsy, partial resection and total resection. Performance status is based on WHO-ECOG scoring (0, 1 or 2) as described in(20). All categories were used as variable in the analysis.

When *MGMT* promoter methylation was included, intrinsic subtyping remained an independent prognostic factor for both PFS ($P < .001$) and OS ($P = .008$), although the number of patients analyzed became relatively small (n = 80). Of note, even in the confirmed AOD tumors at central pathology review, each histologic subtype was found to contain several intrinsic subtypes. Within the group of central pathology review–confirmed AOD and AOA tumors or within the group of tumors with 1p/19q LOH, intrinsic subtype remains an independent prognostic factor.

Distribution of 1p/19q LOH ($P < .001$), *MGMT* ($P = .007$), *IDH1* ($P < .001$), and *EGFR* ($P <.001$) was significantly different between clusters. 1p/19q LOH was significantly more frequently present in tumors assigned to IGS-9 (29 of 46 samples, 63%) compared with IGS-17 (six of 25 samples, 24%), IGS-18 (zero of 26 samples, 0%), and IGS-23 (zero of 25 samples, 0%; Fig 3). *EGFR* amplification was predominantly observed in IGS-18 (14 of 24 samples, 58%) and, to a lesser extent, in IGS-23 (eight of 21 samples, 38%). *EGFR* amplification was rarely observed in samples assigned to IGS-9 (three of 39 samples, 7.6%) and IGS-17 (zero of 19 samples, 0%). IGS-9 and IGS-17 were more often associated with *MGMT* methylation and/or *IDH1* mutation compared with IGS-18 and IGS-23 (Fig 3 and Data Supplement). As previously reported, CpG island methylation phenotype–positive tumors segregated in IGS-9 and IGS-17, whereas CpG island methylation phenotype–negative tumors segregated in IGS-18 and IGS-23 (17).

Molecular parameters (28) (*IDH1* and 1p/19q LOH) and intrinsic subtypes are both important prognostic factors. To assess the added predictive value for PFS of intrinsic subtyping, we combined molecular (*IDH1* and 1p/19q LOH) data with intrinsic subtypes

Figure 3.
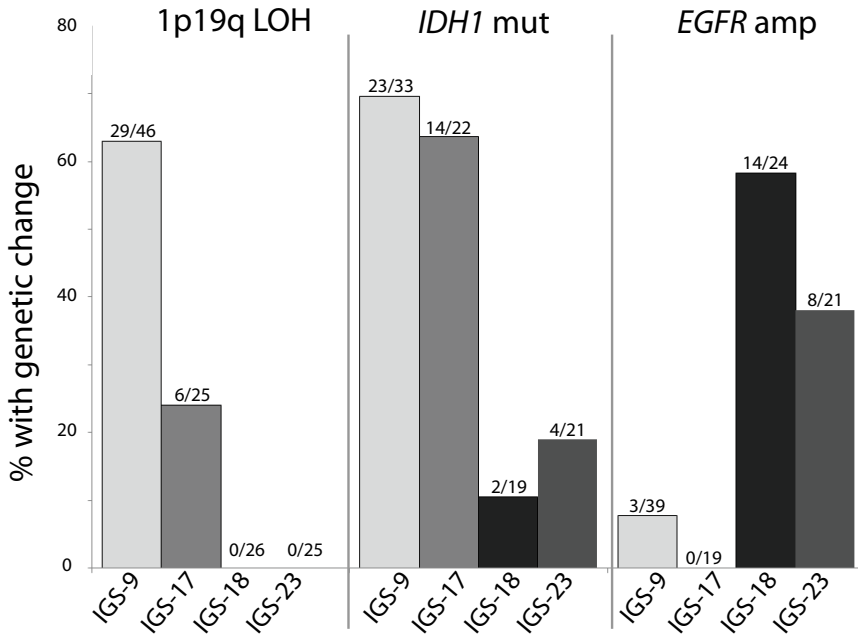
Genetic differences between intrinsic glioma subtypes (IGSs). Specific genetic changes segregate into distinct IGSs. 1p/19q loss of heterozygosity (LOH) was predominantly observed in tumors assigned to IGS-9 and, to a lesser extent, tumors assigned to IGS-17 but was not seen in tumors assigned to IGS-18 and IGS-23. *IDH1* mutations (mut) were significantly more observed in samples assigned to IGS-9 and IGS-17 compared with IGS-18 and IGS-23. *EGFR* amplification (amp) was predominantly identified in IGS-18 and IGS-23 but rarely identified in samples assigned to IGS-9 and IGS-17. This segregation was highly similar to that reported by us previously using archival samples and demonstrates that each IGS has a different set of causal genetic changes (8).

and assessed the PEV by the two models. Both molecular parameters and intrinsic subtypes had comparable PEV (Data Supplement). This does not mean that both models explain the same variability. However, the combined model has a larger PEV of 30% compared with 23% for each individual group of factors, although this difference is not statistically significant.

Prediction of Benefit From Adjuvant PCV

We then evaluated whether the benefit from adjuvant PCV chemotherapy was specific to selected intrinsic subtypes. The addition of adjuvant PCV improved OS in samples assigned to IGS-9 (12.8 years in the RT-PCV arm *v* 5.5 years in the RT only arm; *P* = .035; HR, 2.18; 95% CI, 1.06 to 4.50); an improvement was also observed for PFS (12.8 years in the RT-PCV arm *v* 3.6 years in the RT only arm; *P* = .0018; HR, 3.18; 95% CI, 1.54 to 6.59). Data are shown in Figure 4 and Table 3. PCV treatment also improved PFS, but not OS, in

samples assigned to IGS-18 (0.8 years in the RT-PCV arm *v* 0.4 years in the RT only arm; *P* = .028; HR, 2.51; 95% CI, 1.10 to 5.69). A trend toward an increase in both OS and PFS was observed between the two treatment arms in samples assigned to IGS-17 (OS: 5.4 *v* 1.8 years in RT-PCV and RT only arms, respectively; *P* = .096; HR, 2.21; 95% CI, 0.87 to 5.60; PFS: 2.2 *v* 1.0 years in RT-PCV and RT only arms, respectively; *P* = .109; HR, 2.12; 95% CI, 0.85 to 5.30). No difference in PFS or OS was observed between the treatment arms in samples assigned to IGS-23. Interaction tests for the effects of treatment across intrinsic subtypes were not significant for both PFS and OS (Data Supplement).

**Table 3.** Median Overall and Progression-free survival per treatment arm.

	Overall survival				Progression-free survival			
	Median survival (years)		Hazard Ratio, [95%CI]	P-value	Median survival (years)		Hazard Ratio, [95% CI]	P-value
	RT	RT/PCV			RT	RT/PCV		
IGS-9	5.5	12.8	2.18; [1.06, 4.50]	0.0349	3.6	12.8	3.18; [1.54, 6.59]	0.0018
IGS-17	1.8	5.4	2.21; [0.87, 5.60]	0.0962	1.0	2.2	2.12; [0.85, 5.30]	0.1086
IGS-18	1.1	1.4	1.43; [0.66, 3.12]	0.3669	0.4	0.8	2.51; [1.10, 5.69]	0.0280
IGS-23	1.1	1.0	0.89; [0.39, 2.02]	0.7771	0.6	0.5	0.98; [0.44, 2.18]	0.9678

Abbreviations: IGS: intrinsic glioma subtype; RT: radiotherapy; RT/PCV: radiotherapy followed by procarbazine, lomustine and vincristine chemotherapy.

DISCUSSION

In this study, we performed intrinsic subtyping within a prospective clinical trial, EORTC 26951. Our data demonstrate that all six IGSs are present in EORTC 26951, despite the fact that only AODs and AOAs (as diagnosed by the local pathologist) were included in this study. After central pathology review, each histologic diagnosis still contained various intrinsic subtypes. Similar to reports in archival samples, the intrinsic subtypes are an independent prognostic factor both for OS and PFS. Combining known molecular (1p/19q LOH and *IDH1*) prognostic parameters with intrinsic subtypes improves outcome prediction, although this difference is not significant (PEV of 30% *v* 23% for individual groups of factors).

Histologic classification of gliomas is troublesome and subject to interobserver variation (29). In this study, we confirm that expression profiling, compared with the diagnoses made by the local pathologists, is a more accurate and objective method to classify gliomas (6–10,30–34). Also similar to reports on archival samples, specific genetic changes (*IDH1*, 1p/19q LOH, and *EGFR* amplification) segregate into different subtypes. Therefore, intrinsic subtypes are not only similar in their RNA expression profile, but are also similar on the DNA level in their genetic aberrations. Our data validate

Figure 4.
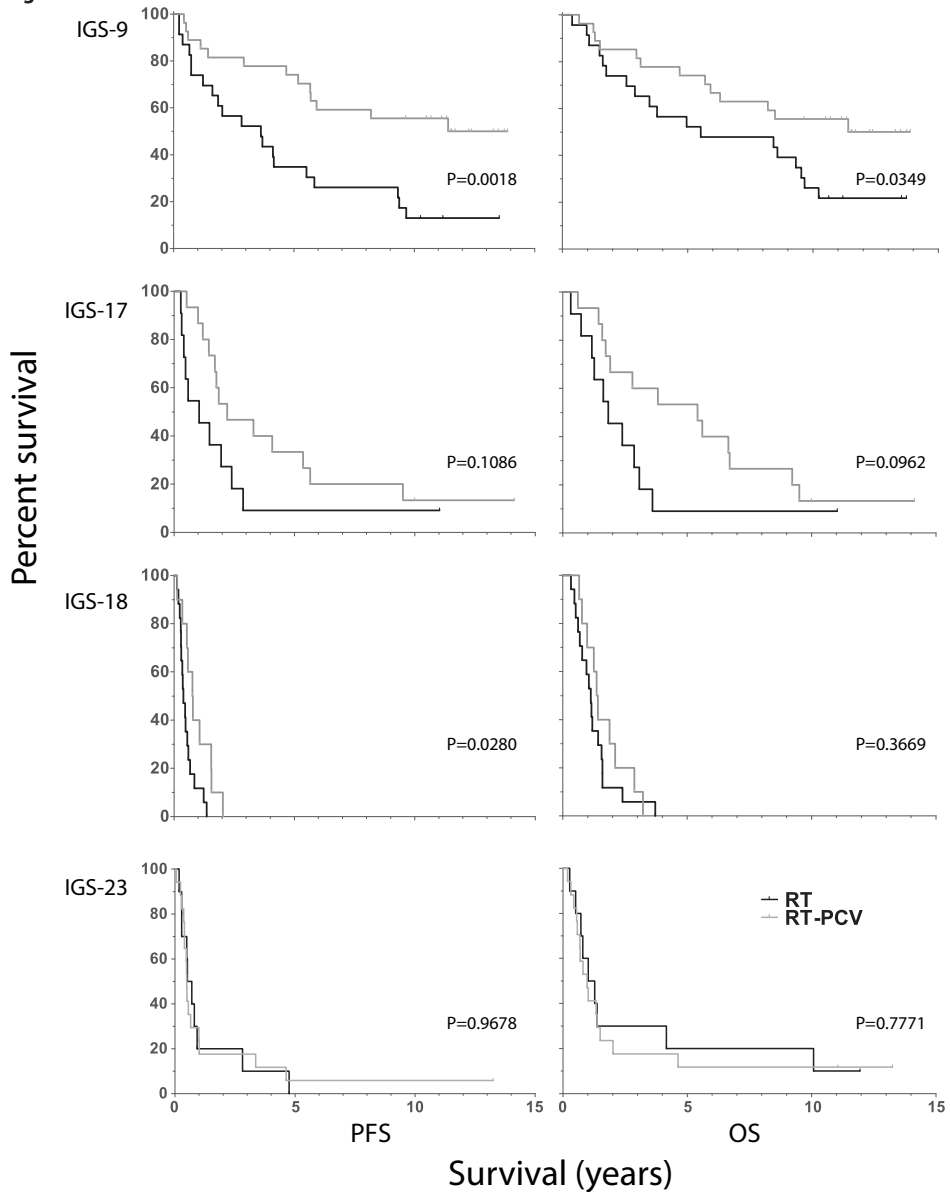
Kaplan-Meier survival curves of the four intrinsic glioma subtypes (IGSs) per treatment arm. (A and B) Adjuvant procarbazine, lomustine, and vincristine (PCV) chemotherapy improved overall survival (OS) and progression-free survival (PFS) in samples assigned to IGS-9. (C and D) A trend toward an increase in both OS and PFS is seen between the two treatment arms in samples assigned to IGS-17. (E and F) Adjuvant PCV also improved PFS, but not OS, in samples assigned to IGS-18. (G and H) No difference between the two treatment arms was observed for both OS and PFS in samples assigned to IGS-23. Patients with one specific IGS (IGS-9) seem to benefit from adjuvant PCV chemotherapy, whereas patients with tumors assigned to IGS-23 do not. In this figure, survival is depicted as time (years) since random assignment. RT, radiotherapy.

the prognostic significance of intrinsic subtypes, and therefore intrinsic subtyping can be used to determine the molecular heterogeneity of samples included in clinical trials.

As said, clinical trial samples are often of poor quality because most are FFPE samples (11). However, recent technologic advances have indicated that expression profiling is feasible on FFPE material (12,13,15).

One of the limitations of the current study is that we were unable to determine the intrinsic subtype of all samples from EORTC 26951. Although most characteristics of samples included versus those not included are similar, this argues for a validation of our results in an independent cohort.

1p/19q and *IDH* are powerful low-cost tools for molecular classification. However, these single molecular markers provide limited information and may miss, for example, tumors with only partial 1p/19q deletions (35). In addition, approximately 30% of tumors with 1p/19q LOH do not have an *IDH1* mutation. Because of these limitations, we believe that single molecular marker analysis will be replaced by high-throughput assays. Here, we demonstrate that IGS classification improves outcome prediction and thus provides additional value for patients. Long-term follow-up of this trial shows that adjuvant PCV improves OS in AOA and AOD. Here, we further demonstrate that not all patients benefit equally from this treatment. Samples assigned to IGS-9 (characterized by a high percentage of 1p/19q LOH and *IDH1* mutations) significantly benefit from PCV chemotherapy, whereas samples assigned to IGS-23 do not show any improvement in outcome (neither PFS nor OS). This outcome for IGS-9 samples is remarkable because there was a large degree of crossover in the RT only arm at time of progression (21).

Tumors with 1p/19q LOH have been reported to show durable responses to chemotherapy (18,19,36). Independently, both the EORTC 26951 trial and its North American counterpart Radiation Therapy Oncology Group (RTOG) 9402 have shown that the addition of PCV to RT improved OS in 1p/19q codeleted oligodendrogliomas (37,38). Our data validate these observations because IGS-9 contains gliomas with the highest percentage 1p/19q LOH. Moreover, the median survival time between the RT-PCV and RT only arm is highly comparable to the median survival observed in RTOG 9402 (14.7 years in the RT-PCV arm *v* 7.3 years in the RT only arm in the RTOG 9402 trial and 12.8 years in the RT-PCV arm *v* 5.5 years in the RT only arm for IGS-9 samples in the EORTC 26951 trial). It should be noted that not all tumors assigned to IGS-9 had 1p/19q LOH (19 of 46 tumors), and conversely, not all tumors with 1p/19q LOH were assigned to IGS-9 (29 of 36 tumors). Similarly, 18 of 55 tumors assigned to IGS-9 or IGS-17 did not have an *IDH1* mutation, and seven of 44 tumors with an *IDH1* mutation were not assigned to IGS-9 or IGS-17. Although we show that combining known molecular (1p/19q LOH and *IDH1*) prognostic parameters with intrinsic subtypes improves outcome prediction, which of these techniques can best predict response to PCV chemotherapy remains to be determined; numbers in the current study are too low for a formal comparison.

Identifying patients who do not benefit from PCV chemotherapy is of equal clinical relevance. In our study, samples assigned to IGS-18 or IGS-23 showed no benefit from PCV chemotherapy in OS (although an increase in PFS was observed for IGS-18). In RTOG 9402, OS was not improved by PCV chemotherapy in AODs and AOAs that retained either 1p and/or 19q. Combined, these data indicate that patients harboring an AOD or AOA that have retained 1p and/or 19q, assigned to IGS-18 or IGS-23, do not show a benefit in OS from PCV chemotherapy.

Samples assigned to IGS-17 showed a trend toward improved outcome from PCV chemotherapy, both in PFS and OS. IGS-17 contains predominantly tumors that have retained 1p/19q but have *IDH1* mutations. A similar trend toward improved outcome was observed in the entire EORTC 26951 cohort tumors with retained 1p/19q and mutated *IDH1*. Nevertheless, our sample cohort is relatively modest in size (N = 140), and our analysis is post hoc (retrospective testing), which is hypothesis generating. Therefore, our data should be validated in an additional independent cohort to firmly establish the predictive effect of these intrinsic molecular subtypes.

Interestingly, in a separate clinical trial (EORTC 22981/26981) on glioblastoma, patients with tumors assigned to IGS-18 also did not show a marked response to the addition of temozolomide to RT (8,39). In this study, too few samples were assigned to other subtypes to draw firm conclusions. It should be noted that there are some important differences between EORTC 26951 and EORTC 22981/26981. For example, EORTC 22981/26981 examined the efficacy of temozolomide chemotherapy in combination with RT as opposed to PCV. However, PCV and temozolomide are both alkylating agents with similar mechanism of action. Another important difference is the histologic subtype investigated; only glioblastomas were included in EORTC 22981/26981, whereas EORTC 26951 included AODs and AOAs. However, intrinsic subtypes have similar molecular and clinical characteristics and are independent of histologic diagnosis. Therefore, we hypothesize that samples assigned to a defined intrinsic subtype will show similar responses to similar chemotherapy regimens regardless of histologic diagnosis.

In summary, we demonstrate, on clinical trial samples and using FFPE material, that intrinsic molecular subtypes are highly prognostic for OS and PFS. Our data indicate that at least one intrinsic subtype of glioma responds favorably to PCV chemotherapy. Intrinsic subtypes are easily determined, and therefore, this approach provides a novel, straightforward, and promising way to improve outcome prediction when combined with other prognostic factors.

REFERENCES

1. Valk PJ, Verhaak RG, Beijen MA, et al. Prognostically useful gene-expression profiles in acute myeloid leukemia. N Engl J Med. 2004;350:1617–1628.

2. Sørlie T, Perou CM, Tibshirani R, et al. Gene expression patterns of breast carcinomas distinguish tumor subclasses with clinical implications. Proc Natl Acad Sci U S A. 2001;98:10869–10874.

3. Northcott PA, Korshunov A, Witt H, et al. Medulloblastoma comprises four distinct molecular variants. J Clin Oncol. 2011;29:1408–1414.

4. French PJ, Peeters J, Horsman S, et al. Identification of differentially regulated splice variants and novel exons in glial brain tumors using exon expression arrays. Cancer Res. 2007;67:5635–5642.

5. French PJ, Swagemakers SM, Nagel JH, et al. Gene expression profiles associated with treatment response in oligodendrogliomas. Cancer Res. 2005;65:11335–11344.

6. Nutt CL, Mani DR, Betensky RA, et al. Gene expression-based classification of malignant gliomas correlates better with survival than histological classification. Cancer Res. 2003;63:1602–1607.

7. Phillips HS, Kharbanda S, Chen R, et al. Molecular subclasses of high-grade glioma predict prognosis, delineate a pattern of disease progression, and resemble stages in neurogenesis. Cancer Cell. 2006;9:157–173.

8. Gravendeel LA, Kouwenhoven MC, Gevaert O, et al. Intrinsic gene expression profiles of gliomas are a better predictor of survival than histology. Cancer Res. 2009;69:9065–9072.

9. Li A, Walling J, Ahn S, et al. Unsupervised analysis of transcriptomic profiles reveals six glioma subtypes. Cancer Res. 2009;69:2091–2099.

10. Verhaak RG, Hoadley KA, Purdom E, et al. Integrated genomic analysis identifies clinically relevant subtypes of glioblastoma characterized by abnormalities in PDGFRA, *IDH1*, *EGFR*, and NF1. Cancer Cell. 2010;17:98–110.

11. Masuda N, Ohnishi T, Kawamoto S, et al. Analysis of chemical modification of RNA from formalin-fixed samples and optimization of molecular biology applications for such samples. Nucleic Acids Res. 1999;27:4436–4443.

12. Hoshida Y, Villanueva A, Kobayashi M, et al. Gene expression in fixed tissues and outcome in hepatocellular carcinoma. N Engl J Med. 2008;359:1995–2004.

13. Hall JS, Leong HS, Armenoult LS, et al. Exon-array profiling unlocks clinically and biologically relevant gene signatures from formalin-fixed paraffin-embedded tumour samples. Br J Cancer. 2011;104:971–981.

14. Linton KM, Hey Y, Saunders E, et al. Acquisition of biologically relevant gene expression data by Affymetrix microarray analysis of archival formalin-fixed paraffin- embedded tumours. Br J Cancer. 2008;98:1403–1414.

15. Gravendeel LA, de Rooi JJ, Eilers PH, et al. Gene expression profiles of gliomas in formalin-fixed paraffin-embedded material. Br J Cancer. 2012;106:538–545.

16. Hegi ME, Diserens AC, Gorlia T, et al. *MGMT* gene silencing and benefit from temozolomide in glioblastoma. N Engl J Med. 2005;352:997–1003.

17. van den Bent MJ, Gravendeel LA, Gorlia T, et al. A hypermethylated phenotype is a better predictor of survival than *MGMT* methylation in anaplastic oligodendroglial brain tumors: A report from EORTC study 26951. Clin Cancer Res. 2011;17:7148–7155.

18. Cairncross JG, Ueki K, Zlatescu MC, et al. Specific genetic predictors of chemotherapeutic response and survival in patients with anaplastic oligodendrogliomas. J Natl Cancer Inst. 1998;90:1473–1479.

19. van den Bent MJ, Looijenga LH, Langenberg K, et al. Chromosomal anomalies in oligodendroglial tumors are correlated with clinical features. Cancer. 2003;97:1276–1284.

20. van den Bent MJ, Brandes AA, Taphoorn MJ, et al. Adjuvant procarbazine, lomustine, and vincristine chemotherapy in newly diagnosed anaplastic oligodendroglioma: Long-term follow-up of EORTC Brain Tumor Group study 26951. J Clin Oncol. [epub ahead of print on October 15, 2012]

21. van den Bent MJ, Carpentier AF, Brandes AA, et al. Adjuvant procarbazine, lomstine, and vincristine improves progression-free survival but not overall survival in newly diagnosed anaplastic oligodendrogliomas and oligoastrocytomas: A randomized European Organisation for Research and Treatment of Cancer phase III trial. J Clin Oncol. 2006;24:2715–2722.

22. Kouwenhoven MC, Gorlia T, Kros JM, et al. Molecular analysis of anaplastic oligodendroglial tumors in a prospective randomized study: A report from EORTC study 26951. Neuro Oncol. 2009;11:737–746

23. Idbaih A, Dalmasso C, Kouwenhoven M, et al. Genomic aberrations associated with outcome in anaplastic oligodendroglial tumors treated within the EORTC phase III trial 26951. J Neurooncol. 2011;103:221–230.

24. Kapp AV, Tibshirani R. Are clusters found in one dataset present in another dataset? Biostatistics. 2007;8:9–31.

25. Heinze G, Schemper M. Comparing the importance of prognostic factors in Cox and logistic regression using SAS. Comput Methods Programs Biomed. 2003;71:155–163.

26. Schemper M, Henderson R. Predictive accuracy and explained variation in Cox regression. Biometrics. 2000;56:249–255.

27. Dunkler D, Michiels S, Schemper M. Gene expression profiling: Does it add predictive accuracy to clinical characteristics in cancer prognosis? Eur J Cancer. 2007;43:745–751.

28. van den Bent MJ, Dubbink HJ, Marie Y, et al. *IDH1* and *IDH2* mutations are prognostic but not predictive for outcome in anaplastic oligodendroglial tumors: A report of the European Organization for Research and Treatment of Cancer Brain Tumor Group. Clin Cancer Res. 2010;16:1597–1604.

29. Kros JM, Gorlia T, Kouwenhoven MC, et al. Panel review of anaplastic oligodendroglioma from European Organization For Research and Treatment of Cancer Trial 26951: Assessment of consensus in diagnosis, influence of 1p/19q loss, and correlations with outcome. J Neuropathol Exp Neurol. 2007;66:545–551.

30. Freije WA, Castro-Vargas FE, Fang Z, et al. Gene expression profiling of gliomas strongly predicts survival. Cancer Res. 2004;64:6503–6510.

31. Louis DN, Ohgaki H, Wiestler OD, et al. The 2007 WHO classification of tumours of the central nervous system. Acta Neuropathol. 2007;114:97–109.

32. Madhavan S, Zenklusen JC, Kotliarov Y, et al. Rembrandt: Helping personalized medicine become a reality through integrative translational research. Mol Cancer Res. 2009;7:157–167.

33. Shirahata M, Iwao-Koizumi K, Saito S, et al. Gene expression-based molecular diagnostic system for malignant gliomas is superior to histological diagnosis. Clin Cancer Res. 2007;13:7341–7356.

34. Shirahata M, Oba S, Iwao-Koizumi K, et al. Using gene expression profiling to identify a prognostic molecular spectrum in gliomas. Cancer Sci. 2009;100:165–172.

35. Idbaih A, Kouwenhoven M, Jeuken J, et al. Chromosome 1p loss evaluation in anaplastic oligodendrogliomas. Neuropathology. 2008;28:440–443.

36. Kouwenhoven MC, Kros JM, French PJ, et al. 1p/19q loss within oligodendroglioma is predictive for response to first line temozolomide but not to salvage treatment. Eur J Cancer. 2006;42:2499–2503.

37. Intergroup Radiation Therapy Oncology Group Trial 9402, Cairncross G, Berkey B, et al. Phase III trial of chemotherapy plus radiotherapy compared with radiotherapy alone for pure and mixed anaplastic oligodendroglioma: Intergroup Radiation Therapy Oncology Group Trial 9402. J Clin Oncol. 2006;24:2707–2714.

38. Cairncross G, Wang M, Shaw E, et al. Phase III trial of chemoradiotherapy for anaplastic oligodendroglioma: Long-term results of RTOG 9402. J Clin Oncol. [epub ahead of print on Oct 15, 2012]

39. Murat A, Migliavacca E, Gorlia T, et al. Stem cell-related "self-renewal" signature and high epidermal growth factor receptor expression associated with resistance to concomitant chemoradiotherapy in glioblastoma. J Clin Oncol. 2008;26:3015–3024.
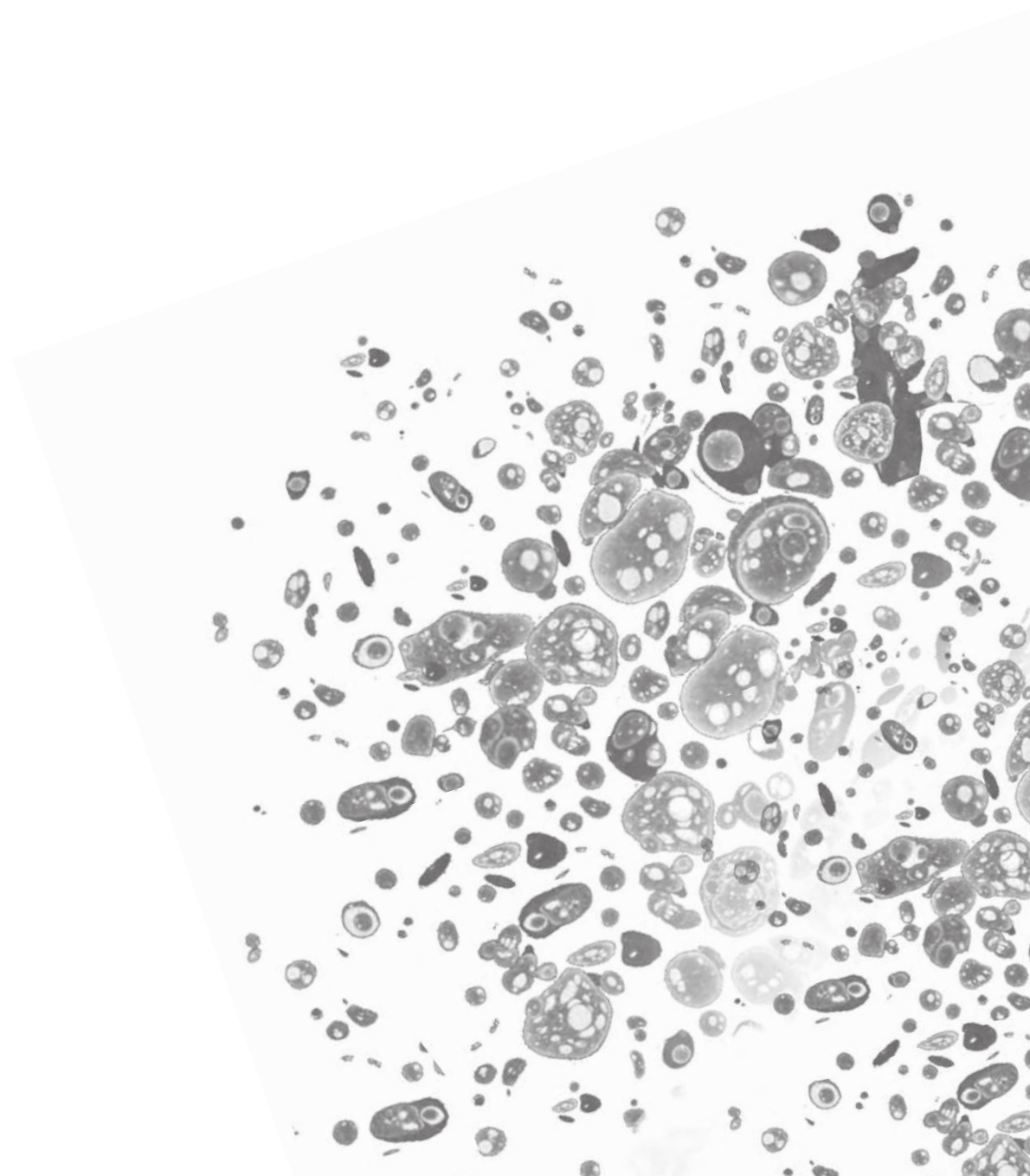
CHAPTER 2

## MGMT-STP27 Methylation Status as Predictive Marker for Response to PCV in Anaplastic Oligodendrogliomas and Oligoastrocytomas. A Report from EORTC Study 26951

Martin J. van den Bent, Lale Erdem-Eraslan,
Ahmed Idbaih, Johan de Rooi, Paul H.C. Eilers,
Wim G.M. Spliet, Wilfred F.A. den Dunnen,
Cees Tijssen, Pieter Wesseling,
Peter A.E. Sillevis Smitt, Johan M. Kros,
Thierry Gorlia, and Pim J. French
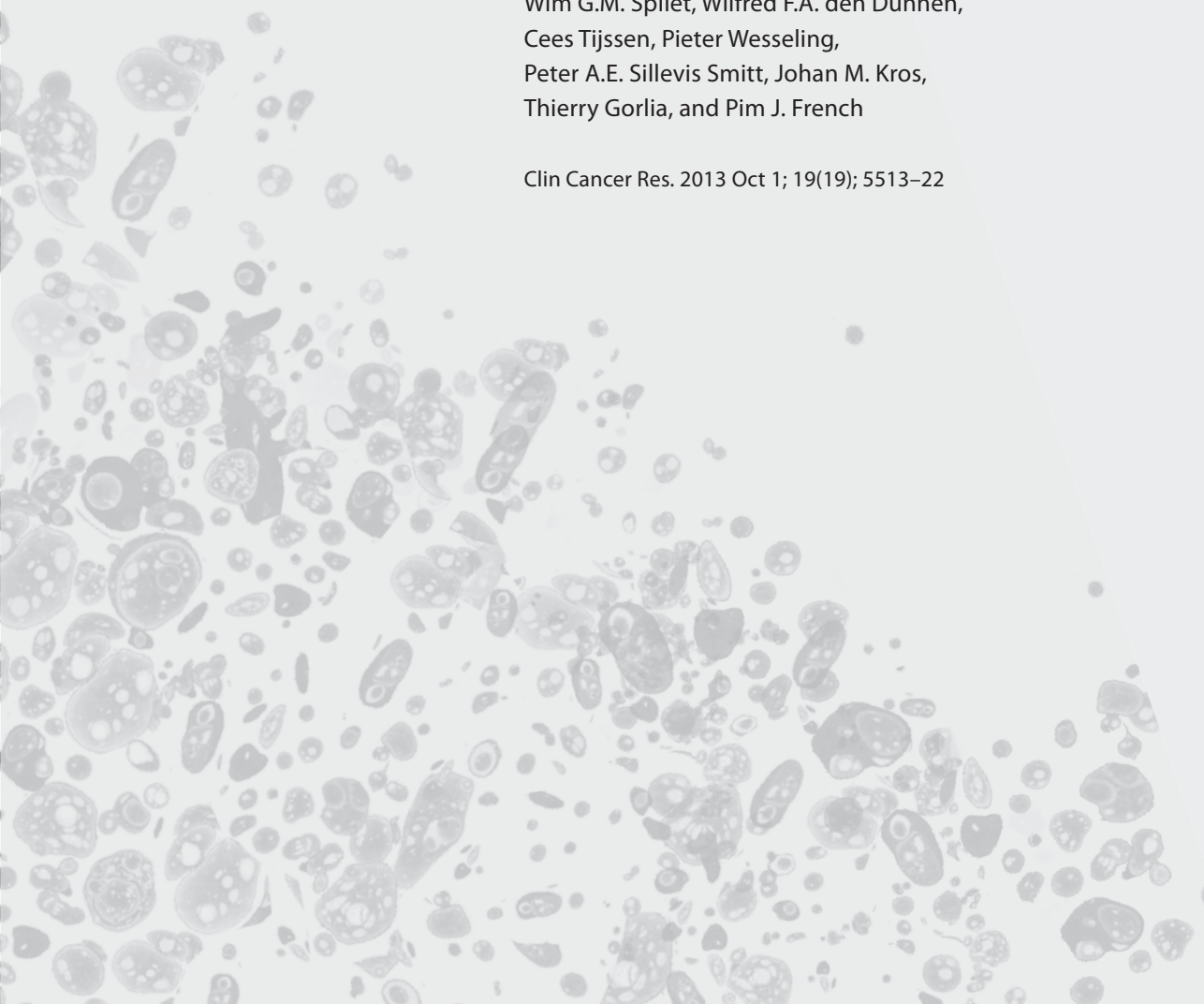
ABSTRACT

Purpose

The long-term follow-up results from the EORTC 26951 trial showed that the addition of procarbazine, CCNU, and vincristine (PCV) after radiotherapy increases survival in anaplastic oligodendrogliomas/oligoastrocytomas (AOD/AOA). However, some patients appeared to benefit more from PCV treatment than others.

Experimental Design

We conducted genome-wide methylation profiling of 115 samples included in the EORTC 26951 trial and extracted the CpG island hypermethylated phenotype (CIMP) and *MGMT* promoter methylation (*MGMT*-STP27) status.

Results

We first show that methylation profiling can be conducted on archival tissues with a performance that is similar to snap-frozen tissue samples. We then conducted methylation profiling on EORTC 26951 clinical trial samples. Univariate analysis indicated that CIMP+ or *MGMT*-STP27 methylated tumors had an improved survival compared with CIMP− and/or *MGMT*-STP27 unmethylated tumors [median overall survival (OS), 1.05 vs. 6.46 years and 1.06 vs. 3.8 years, both $P < 0.0001$ for CIMP and *MGMT*-STP27 status, respectively]. Multivariable analysis indicates that CIMP and *MGMT*-STP27 are significant prognostic factors for survival in presence of age, sex, performance score, and review diagnosis in the model. CIMP+ and *MGMT*-STP27 methylated tumors showed a clear benefit from adjuvant PCV chemotherapy: the median OS of CIMP+ samples in the RT and RT-PCV arms was 3.27 and 9.51 years, respectively ($P = 0.0033$); for *MGMT*-STP27 methylated samples, it was 1.98 and 8.65 years. There was no such benefit for CIMP- or for *MGMT*-STP27 unmethylated tumors. *MGMT*-STP27 status remained significant in an interaction test ($P = 0.003$). Statistical analysis of microarray (SAM) identified 259 novel CpGs associated with treatment response.

Conclusions

MGMT-STP27 may be used to guide treatment decisions in this tumor type.

INTRODUCTION

In 1995, a large European phase III clinical trial ("EORTC 26951") was initiated to examine the effects of adjuvant procarbazine, CCNU, and vincristine (PCV) chemotherapy in anaplastic oligodendroglial tumors [oligodendrogliomas (AOD) and oligoastrocytomas (AOA); (1). The long-term follow-up of this study shows that adjuvant PCV chemotherapy given after radiotherapy improves overall survival (OS) in this tumor type (2). Molecular analysis has shown that in particular patients in which the tumor has a combined deletion of the 1p and 19q chromosomal arms (1p/19q co-deleted tumors) appeared to benefit from the addition of PCV treatment. A trial with similar inclusion criteria and treatment protocol, RTOG 9402, showed comparable results: patients with oligodendroglioma who harbor tumors with a 1p/19q co-deletion showed a benefit from neoadjuvant PCV chemotherapy (3, 4). Combined, these trials have changed the standard of care for 1p/19q co-deleted tumors.

Results from both trials also indicate that a subset of patients benefit from (neo-) adjuvant PCV even though the tumor has retained 1p and/or 19q. In search for markers that identify those responsive patients, post hoc analysis on material from the EORTC 26951 trial has shown that *IDH1* mutational status and *MGMT* promoter methylation may be correlated to increased benefit to adjuvant PCV chemotherapy (5, 6). Statistical tests for interaction remained however negative, perhaps due to the relatively small number of patients of whom material could be analyzed. Similarly, gene expression profiling showed that tumors assigned to "intrinsic glioma subtype-9" (IGS-9, containing a high percentage of tumors with 1p/19q codeletion) showed benefit from adjuvant PCV chemotherapy (7). However, tumors assigned to IGS-17 (of which the majority had retained 1p and/or 19q) also showed a trend toward benefit from adjuvant PCV. These findings suggest there may be alternative molecular factors that predict benefit from adjuvant PCV chemotherapy.

In 2011, we have reported on a study in which genome-wide methylation profiling was conducted on snap-frozen tissue samples of patients included in the EORTC 26951 trial. Similar to other studies, we found a strong correlation between a genome-wide hypermethylation phenotype ("CIMP") and survival (8–11). However, preliminary analysis also indicated that CIMP status may be predictive for response to PCV chemotherapy. Unfortunately, the number of samples derived from the EORTC 26951 trial was too small ($n = 50$) to draw firm conclusions. At the time, analysis of additional samples was difficult as remaining samples were all fixed in formalin and embedded in paraffin (FFPE). However, recent technological advances suggest that FFPE tissues can be now used for genome-wide methylation analysis which increases the number of EORTC 26951 samples available for methylation profiling.

Apart from the potential predictive value of CIMP status, methylation of the *MGMT* promoter has been established as a predictive marker for outcome to chemo-irradiation with temozolomide in gliomas (12–14). In patients treated within EORTC 26951, we were unable to establish such an association between *MGMT* promoter methylation and benefit from adjuvant PCV chemotherapy (6). However, the assay used for our study (MS-MLPA, methylation-specific multiplex ligation-dependent probe amplification) interrogated different CpG sites than the assay used for the studies whereby *MGMT* promoter methylation status predicted benefit from chemotherapy (MS-PCR). Two regions within the *MGMT* promoter are correlated with mRNA expression levels, *DMR1* and *DMR2*, of which the latter is interrogated by MS-PCR (15). Recently, a study identified 2 CpG sites that are correlated to *MGMT* RNA expression levels and patient survival (16). These CpGs are located on the Humanmethylation 27 and 450 arrays. These CpG sites lie within *DMR1* and *DMR2* and are not assessed by the MS-MLPA assay that we used to assess *MGMT* promoter methylation. A prediction model, *MGMT*-STP27, was generated to determine the *MGMT* promoter methylation status from the methylation data. We used this model as an alternative method to assess *MGMT* promoter methylation and compared it with our MS-MLPA findings.

MATERIALS AND METHODS

Patient samples

Patients were considered eligible in the EORTC 26951, if they had been diagnosed by the local pathologist with an AOD or an AOA according to the 1993 WHO classification. Details of the eligibility criteria and the consolidated standards on reporting trials (Consort) flow diagram have been described previously (1). All samples that could be retrieved from this study were included ($n = 115$). A central pathology review was conducted on 345 of 368 samples, 113 of 115 for samples used in present study. The 2 cases were omitted in the multivariate analysis that included review diagnosis as factor. All analyses using histologic diagnosis made use of the review diagnosis. Patient/sample characteristics are detailed in Supplementary Table S1. Analysis of 1p/19qLOH, *EGFR* amplification, *IDH1* mutations (as determined by direct sequencing of the c.395G mutation hotspot), and *MGMT* promoter methylation as assessed by MLPA on EORTC 26951 samples were described previously (1, 6, 17–19). Areas with high tumor content (>70%–80%) were highlighted by the pathologist (J.M. Kros) before conducting the *IDH1* mutation analysis.

Six additional samples were collected from the Erasmus MC brain tumor tissue bank to test the performance of Illumina 450 k beadchips. One part of these tumors was fixed in formalin and embedded in paraffin, the other was snap frozen and stored at −80°C.

Patients provided written informed consent according to national and local regulations for the clinical study and correlative tissue studies.

Nucleic acid isolation and array hybridization

For FF tissues, gDNA was isolated from 5 to 40 cryostat sections of 40-μm thickness using the QIAamp DNA Mini Kit (Qiagen) according to the manufacturer's instructions. For FFPE tissue, gDNA was isolated from 8 to 10 sections of 10-μm thickness from paraffin blocks using the QIAamp FFPE DNA Kit. Methylation profiling was conducted using 1 μg of gDNA which was subjected to bisulfite modification using the EZ DNA Methylation Kit (Zymo Research Company). Bisulfite-converted DNA was then hybridized to Illumina Infinium HumanMethylation 27 arrays (Illumina) by Service XS or to Infinium HumanMethylation 450 arrays (Illumina) run by ArosAB according to standard Illumina protocols. Data from 50 Infinium HumanMethylation 27 arrays samples were previously reported (11). All array data is available via the NCBI GEO datasets, accession number GSE48462. Infinium HumanMethylation 27 arrays interrogate 27,578 CpG sites across 14,476 genes; the 450 arrays interrogate >485.000 CpG sites and contain most, but not all, of 27 k array content. The 450 k array contains 1,432 of 1,503 probesets used to determine CIMP status.

Statistical analysis

Samples were assigned to either the CIMP+ or CIMP−subtype using ClusterRepro (an R package) based on the nearest centroid as described previously (20) according to the 1,503 CpGs described by the TCGA (10). The *MGMT* promoter methylation status (*MGMT*-STP27) was extracted from 2 CpG sites on the methylation array (*cg*12434587 and *cg*12981137) as described (16). Differences between the Kaplan–Meier survival curves were calculated by the log-rank (Mantel–Cox) test using GraphPad Prism version 5.00 for Windows, GraphPad Software. Comparisons between frequencies were calculated by the Fisher exact test in which $P < 0.05$ was considered to indicate significant differences. Progression-free survival (PFS) and overall survival (OS) were computed from randomization to date of event (progression and/or death) or censored at the date of last visit. To assess interfactor relationship, we used the well-established Spearman correlation coefficient (SCC) which provided for binary and ordinal factors the same measures of association as the phi coefficient. With the available sample size, clinically relevant coefficient (SCC ≥ 0.4) all had a significance lower than a conservative threshold of 1% ($P < 0.01$). The log-rank test for interaction was used to compare treatment effect in different molecular subsets. Significance analysis of microarrays (SAM) was conducted using SAMR, an R package, making use of censored survival outcome (21, 22). M-values of methylation were used for SAM analysis (23); CpGs located on the X or Y chromosomes were removed from all analysis. The variance inflation factor (VIF) was assessed

to determine the severity of multicolinearity between factors. For a factor, VIF = 4 ($\sqrt{4}$ = 2) means that the SE of the coefficient of that factor is 2 times as large as it would be if it was uncorrelated to other factors. A VIF bigger than 2 is considered as large. Pathway analysis was conducted using IPA (Ingenuity Systems).

RESULTS

Evaluation of the suitability of FFPE material for genome-wide methylation profiling

Most clinical trial samples are fixed in formalin and embedded in paraffin. Our first experiments therefore evaluated the suitability of FFPE material for genome-wide methylation profiling. For this, we generated methylation profiles of 6 glioma samples, using 3 to 5 replicates per sample. Replicates included (i) fresh-frozen (FF) samples ($n = 4$), (ii) FFPE of sections cut from a paraffin block ($n = 6$), (iii) FFPE of sections that were scraped from microscope slides to allow selecting for the area with highest tumor density ($n = 6$), (iv) a technical replicate of ii ($n = 3$), and (v) technical replicates of iii ($n= 4$). The time in paraffin of these samples was between 15 and 17 years.

A first evaluation showed that the signal intensities of the methylated and unmethylated probes of the array were higher in the FF samples than in the FFPE samples (6,882 ± 931 vs. 3,946 ± 1,438, $P = 0.002$; Supplementary Figure S1). Within the FFPE samples, scraped sections showed a significantly lower intensity than the whole FFPE sections (2,797 ± 962 vs. 5,096 ± 672, $P < 0.001$). Despite of these differences in signal intensities, there was no obvious difference between the different tissue sources in the beta values [methylated/(methylated + unmethylated), Supplementary Figure S1]. Indeed, reproducibility between the beta values of technical replicates was high: $R^2 = 0.987 \pm 0.009$ (range, 0.969–0.994). Reproducibility between the beta values of whole tissue sections and scraped microscope slides was also high: $R^2 = 0.976 \pm 0.012$ (range, 0.960–0.985), which indicates that the enrichment for areas with high tumor content only marginally influences results in these samples.

When comparing the beta values of the FF samples with those of the FFPE samples, we also observed a high correlation between the replicates $R^2 = 0.961 \pm 0.023$ (range, 0.919–0.987) when using all the 480 k CpG sites. This is remarkably high, especially when considering the time samples were stored in paraffin (15–17 years). This long storage time therefore does not significantly compromise on the performance of the platform. The high correlation between all replicates is also shown in an unsupervised clustering analysis conducted on the 2,000 most variable CpG sites in which samples from the same replicate clustered closely together (Figure 1). These data show that the Illumina

humanmethylation450 platform can be used to study CpG methylation on both FF and FFPE samples.

Previous methylation data on EORTC 26951 samples were generated using the HumanMethylation27 beadchip. To determine whether the methylation array used for FFPE profiling (HumanMethylation450) is comparable to the HumanMethylation27 beadchip, we analyzed 48 FFPE samples on both platforms. A high sample correlation in all samples across the 2 array types was observed when using the beta values of probesets that

Figure 1.
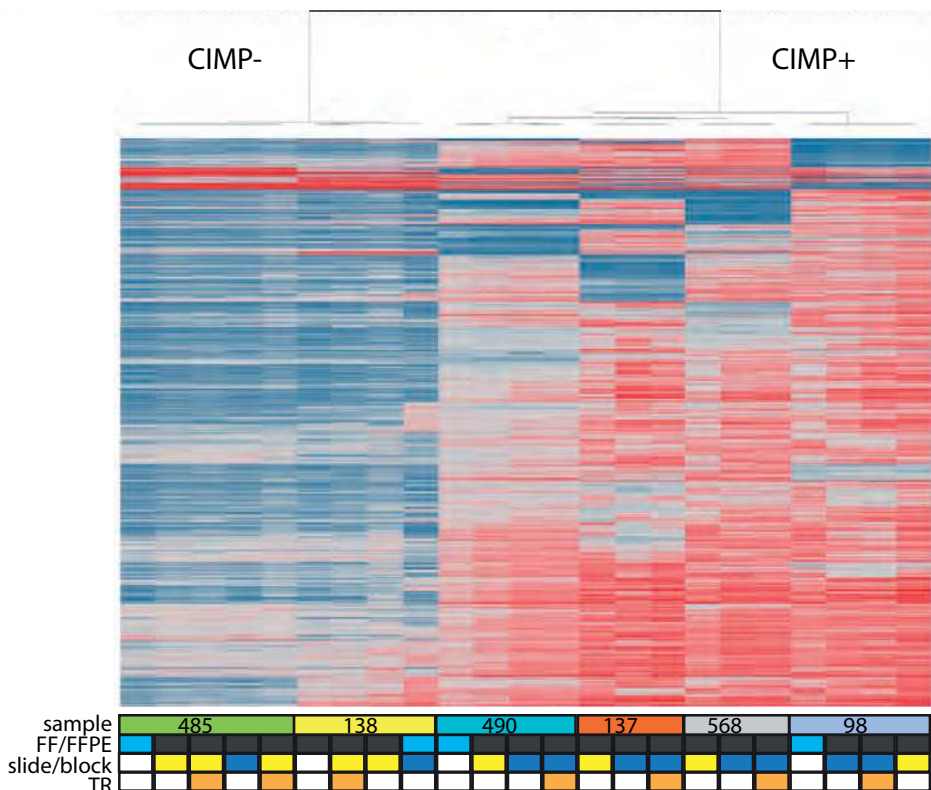
Hierarchical clustering of methylation profiles highlights similarity between FF and FFPE replicates from the same sample. Methylation profiles of 6 glioma samples were generated, labels for each sample are color coded below the plots. Replicates included (i) FF samples ($n = 4$), (ii) FFPE of sections cut from a paraffin block ($n = 6$), (iii) FFPE of sections that were scraped from microscope slides to allow selecting for the area with highest tumor density ($n = 6$), (iv) a technical replicate of ii ($n = 3$), and (v) technical replicates of iii ($n = 4$). The time in paraffin of these samples was between 15 and 17 years. The 2,000 most variable CpGs per sample are clustered with red corresponding to high M-values (methylated) and blue to low Beta-values (unmethylated). Hierarchical clustering of these 2,000 most variable CpG sites shows that the replicates from the same sample cluster together regardless of tissue origin (FF or FFPE) or whether FFPE samples were derived from tissue blocks (b) or scraped from tissue sections (s). TR, technical replicate.

are overlapping on both platforms ($n = 25,978$), $R^2 = 0.960 \pm 0.020$ (range, 0.854–0.982). These data show that the performance of the HumanMethylation450 beadchip is similar to the HumanMethylation27 beadchip.

We then conducted methylation profiling on 66 samples of the EORTC 26951 trial. Of these, 8 were FF and run on HumanMethylation27 beadchips, 59 were FFPE and run on HumanMethylation450 beadchips. Data were combined with 50 samples that were analyzed previously using FF samples on HumanMethylation27 beadchips (11). Data are available via NCBI GEO datasets, GSE48462. Samples 21 and 224 were run on both platforms, data from the HumanMethylation 450 beadchips for these two samples were used in the analysis. This sample cohort did not differ from the entire EORTC patient cohort with respect to age, sex, performance status, diagnosis, tumor location, *IDH1* mutation status, 1p/19q codeletion status, *EGFR* amplification, or *MGMT* promoter methylation status as assessed by MLPA (Supplementary Table S2). Our patient cohort however contained fewer biopsies and more total resections ($P = 0.005$). In addition, the treatment effect of patients included in this study was larger than the treatment effect of patients not included (Supplementary Figure S2): Median OS of patients included in the RT and RT-PCV arm was 1.6 and 5.7 years, whereas in patients not included it was 3.5 and 3.2 years. The correlation between *MGMT*-STP27 and *MGMT*-MLPA, CIMP, *IDH1* mutation, and 1p/19q codeletion were, although significant, modest in strength [Spearman correlation coefficient *MGMT*-MLPA = 0.56, ($P < 0.0001$; with CIMP 0.39 ($P < 0.0001$), with *IDH1* 0.42 ($P < 0.0001$), and with 1p/19q 0.29 ($P = 0.002$)].

CIMP and *MGMT* methylation status are predictive for benefit from PCV chemotherapy

Of the 115 samples that were profiled, 66 were CIMP+ and 49 CIMP−. The *MGMT* promoter methylation status (*MGMT*-STP27) extracted from the genome-wide methylation data identified 88 of 115 samples with a methylated *MGMT* promoter and 27 of 115 with an unmethylated promoter. CIMP and *MGMT*-STP27 status were correlated: of the 66 CIMP+ samples, 60 had a methylated *MGMT* promoter, 6 were unmethylated. Of the 49 CIMP-samples, 28 had a methylated *MGMT* promoter, 21 were unmethylated. 1p/19q codeletion was identified in 29 of 111 samples. All of the 48 CIMP− had retained 1p/19q as did 34 of 63 CIMP+ samples. Twenty-six of 27 *MGMT*-STP27 unmethylated samples had retained 1p/19q as did 56 of 84 *MGMT*-STP27 methylated samples. Correlation of CIMP and *MGMT*-STP27 status with other molecular markers and associated survival data are shown in Supplementary Table S3.

Univariate analysis indicates that patients with CIMP+ tumors have a more favorable prognosis than CIMP− tumors (6.65 vs. 1.05 years for OS and 3.69 vs. 0.50 years for PFS; Table 1 and Figure 2). Similarly, *MGMT*-STP27 methylated samples have a more favorable prognosis than *MGMT*-STP27 unmethylated samples (3.8 vs. 1.06 years for OS and 1.86
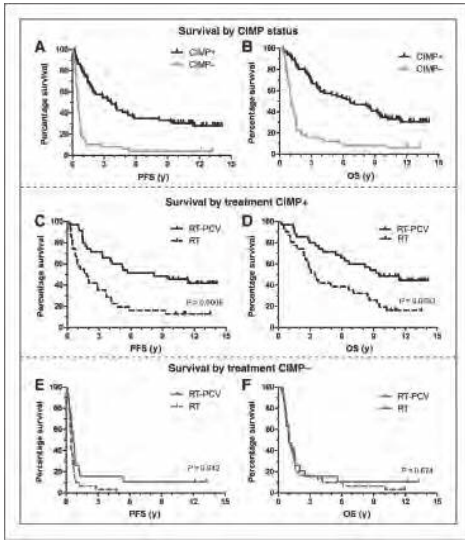
Figure 2.

CIMP status is prognostic for survival in samples of the EORTC 26951 clinical trial. Kaplan–Meier survival curves show that patients harboring CIMP+ tumors have a better prognosis than patients with CIMP− tumors. A, PFS. B, OS. C–F, CIMP status is predictive for benefit to adjuvant PCV chemotherapy. Kaplan–Meier survival curves showing that patients harboring CIMP+ tumors benefit both in PFS (C) and in OS (D) following adjuvant PCV chemotherapy. Patients harboring CIMP− tumors show modest improvement in PFS (E) but not in OS (F) following adjuvant PCV chemotherapy. For all graphs: black lines indicate the CIMP+ samples, gray lines indicate the CIMP− samples. Dashed lines are RT only, uninterrupted lines RT-PCV.

vs. 0.65 years for PFS; Table 1 and Figure 3). Multivariate analysis indicates that CIMP and *MGMT*-STP27 status are prognostic factors for survival in the presence of clinical and histological parameters (age, sex, performance score, type of surgery, and review diagnosis, Table 1). They are no longer independent prognostic variables when all clinical and molecular parameters and histology are included in the analysis (Table 1). In all analyses, all factors except STP27 (max 1.6) had a large VIF (>2). A limitation of these multivariable analyses is a limited sample size ($n = 115$) and presence of severe multicolinearity which might explain why CIMP and STP27 lost significance in the "all factors" analyses.

When stratified for treatment, patients with CIMP+ tumors showed a clear benefit from adjuvant PCV chemotherapy, both for OS and PFS (Table 2, Figure 2). For example, the median OS of CIMP+ samples in the RT and RT-PCV arms was 3.47 and 9.51 years, respectively. For CIMP− tumors, there was no such benefit for OS, although there was a slight increase in PFS 0.68 vs. 0.47 years. These data show that CIMP-positive status is predictive, at least for OS, for benefit from adjuvant PCV in patients treated within EORTC 26951. The interaction test, however, remained above the threshold of significance ($P = 0.07$, Figure 4)

A more pronounced benefit from treatment was observed in *MGMT*-STP27 methylated samples (Figure 3): Median OS of *MGMT*-STP27 methylated samples in the RT and RT-PCV arms was 1.98 and 8.65 years, respectively. For PFS, it was 0.73 and 5.36 years. For *MGMT*-STP27 unmethylated, there was no such benefit, neither for OS nor for PFS. *MGMT*-STP27 status was highly significant in the interaction test ($P = 0.003$, Figure 4).

Table 1. Uni and multivariable analysis of molecular and clinical factors

OS analysis		CIMP status				MGMT-STP27 status		
n (events)		HR (95% CI)	P	VIF		HR (95% CI)	P	VIF
Univariate	CIMP status	0.21 (0.13–0.34)	**<0.001**		STP27	0.26 (0.14–0.48)	**<0.001**	
Molecular	CIMP status	0.56 (0.29–1.05)	0.073	4.4	STP27	0.66 (0.39–1.11)	0.12	1.6
107 (84)	IDH1 mut	0.64 (0.32–1.27)	0.2	5.7	IDH1 mut	0.5 (0.29–0.85)	**0.012**	3.5
	1p19q LOH	0.47 (0.24–0.92)	**0.027**	3.2	1p19q LOH	0.43 (0.23–0.83)	**0.011**	3.1
Clinical	CIMP status	0.26 (0.16–0.44)	**<0.001**	2.1	STP27	0.49 (0.29–0.83)	**0.009**	1.4
112 (89)	Age	1.02 (1–1.04)	0.136	11.9	Age	1.02 (1–1.04)	0.065	11.3
	Sex	1.12 (0.7–1.79)	0.643	3.1	Sex	0.85 (0.54–1.34)	0.495	3
	Performance	0.75 (0.56–1.02)	0.063	2.3	Performance	0.72 (0.53–0.98)	**0.037**	2.3
	Surgery	0.54 (0.35–0.82)	**0.004**	8.9	Surgery	0.69 (0.46–1.03)	0.068	8.9
	Review diagn.	1.16 (0.89–1.53)	0.276	3.6	Review diagn.	1.3 (0.99–1.71)	0.057	3.6
All	CIMP status	0.54 (0.26–1.11)	0.097	4.5	STP27	0.88 (0.50–1.59)	0.681	1.6
104 (82)	IDH1 mut	0.56 (0.28–1.11)	0.096	5.9	IDH1 mut	0.40 (0.24–0.69)	**0.001**	3.6
	1p19q LOH	0.45 (0.22–0.93)	**0.032**	6.3	1p19q LOH	0.41 (0.20–0.83)	**0.014**	6.3
	Age	1.02 (1–1.05)	**0.034**	11.4	Age	1.03 (1.01–1.05)	**0.014**	11.3
	Sex	1.22 (0.73–2.02)	0.448	3.1	Sex	1.08 (0.66–1.76)	0.757	3
	Performance	0.76 (0.55–1.05)	0.099	2.4	Performance	0.77 (0.56–1.06)	0.111	2.4
	Surgery	0.56 (0.36–0.88)	**0.011**	9.6	Surgery	0.64 (0.42–0.96)	**0.031**	9.5
	Review diagn.	1.1 (0.83–1.47)	0.497	4.2	Review diagn.	1.16 (0.87–1.55)	0.32	4.3

Table 1. Uni and multivariable analysis of molecular and clinical factors (continued)

PFS analysis		CIMP status				MGMT-STP27 status		
n (events)		HR (95% CI)	P	VIF		HR (95% CI)	P	VIF
Univariate	CIMP status	0.18 (0.11–0.29)	**<0.001**		STP27	0.27 (0.15–0.5)	**<0.001**	
Molecular	CIMP status	0.51 (0.27–0.96)	**0.036**	4.4	STP27	0.80 (0.47–1.35)	0.402	1.6
107 (87)	IDH1 mut	0.69 (0.35–1.37)	0.283	5.7	IDH1 mut	0.49 (0.28–0.83)	**0.009**	3.5
	1p19q LOH	0.41 (0.21–0.79)	**0.009**	3.2	1p19q LOH	0.38 (0.20–0.73)	**0.004**	3.1
Clinical	CIMP status	0.27 (0.17–0.44)	**<0.001**	2.1	STP27	0.51 (0.31–0.85)	**0.009**	1.4
112 (92)	Age	1 (0.98–1.02)	0.803	11.9	Age	1.01 (0.99–1.03)	0.412	11.3
	Sex	0.91 (0.57–1.45)	0.693	3.1	Sex	0.73 (0.47–1.14)	0.165	3
	Performance	0.71 (0.53–0.97)	**0.03**	2.3	Performance	0.70 (0.52–0.95)	**0.025**	2.3
	Surgery	0.65 (0.44–0.97)	**0.033**	8.9	Surgery	0.76 (0.52–1.1)	0.145	8.9
	Review diagn.	1.15 (0.88–1.5)	0.311	3.6	Review diagn.	1.3 (1–1.68)	0.053	3.6
All	CIMP status	0.55 (0.27–1.10)	0.091	4.5	STP27	1.00 (0.58–1.75)	0.989	1.6
104 (85)	IDH1 mut	0.61 (0.30–1.22)	0.159	5.9	IDH1 mut	0.42 (0.24–0.72)	**0.002**	3.6
	1p19q LOH	0.43 (0.21–0.90)	**0.025**	6.3	1p19q LOH	0.41 (0.20–0.83)	**0.014**	6.3
	Age	1.01 (0.99–1.03)	0.348	11.4	Age	1.01 (0.99–1.03)	0.162	11.3
	Sex	1 (0.6–1.65)	0.992	3.1	Sex	0.89 (0.55–1.46)	0.651	3
	Performance	0.76 (0.55–1.04)	0.093	2.4	Performance	0.77 (0.56–1.06)	0.113	2.4
	Surgery	0.7 (0.47–1.04)	0.079	9.6	Surgery	0.76 (0.52–1.12)	0.167	9.5
	Review diagn.	1.09 (0.83–1.45)	0.528	4.2	Review diagn.	1.17 (0.89–1.55)	0.256	4.3

NOTE: Multivariate analysis including molecular parameters (Molecular), clinical parameters (Clinical) or including all molecular and clinical parameters and review diagnosis (All). Calculations are based on 107, 112, and 104 observations, respectively (between brackets: number of events). Depicted are the results for OS (top) and PFS (bottom). Type of surgery categories included: biopsy, partial resection, and total resection. Performance status is based on WHO-ECOG scoring (0, 1, or 2); all categories were used as variables in the analysis. Age was used as continuous variable. Values in bold are significant at P < 0.05.
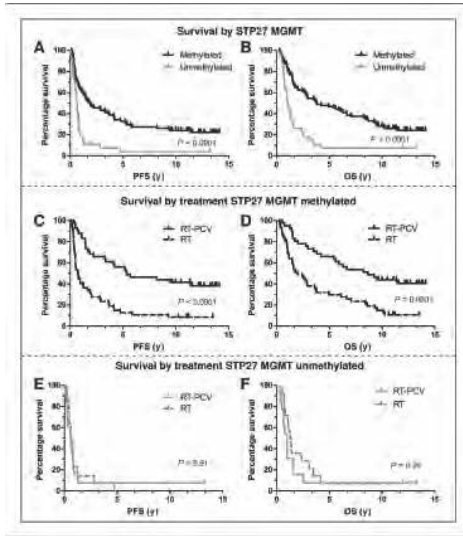
Figure 3.

MGMT-STP27 status is prognostic for survival in samples of the EORTC-26951 clinical trial. Kaplan–Meier survival curves show that patients harboring *MGMT*-STP27 methylated tumors have a better prognosis than patients that with *MGMT*-STP27 unmethylated tumors. A, PFS. B, OS. C–F, *MGMT*-STP27 status is predictive for benefit to adjuvant PCV chemotherapy. Kaplan–Meier survival curves showing that patients harboring *MGMT*-STP27 methylated tumors benefit both in PFS (C) and in OS (D) following adjuvant PCV chemotherapy. Patients harboring *MGMT*-STP27 unmethylated tumors do not show benefit from adjuvant PCV chemotherapy both in PFS (E) and in OS (F). For all graphs: black lines indicate the *MGMT*-STP27 methylated samples, gray lines indicate the *MGMT*-STP27 unmethylated samples. Dashed lines are RT only, uninterrupted lines RT-PCV.

Identification of CpG sites associated with survival and response to treatment

SAM analysis identified a total of 13,852 CpG sites that are associated with survival when using the entire dataset. This large number of CpGs (approximately half of all probesets on the array) is related to the tumors' CIMP status and is illustrative for the large differences between these 2 subtypes. SAM analysis also identified 13 probesets and 3,921 probesets associated with survival in the CIMP− and in the CIMP+ subtype, respectively. Hierarchical clustering based on these CpGs identified 2 distinct subtypes that indeed correlated with survival in our dataset (Supplementary Figure S3).

We next aimed to identify CpG sites associated with benefit from treatment. For this, we first conducted SAM analysis to identify CpG sites associated with survival in the RT-PCV arm and then removed all CpGs that were associated with survival in the RT-only arm. To increase stringency, SAM analysis on the RT-only arm was conducted used relaxed criteria [false discovery rate (fdr) cutoff of 0.05], whereas stringent criteria were used to identify CpGs in the RT-PCV arm (fdr cutoff of 0.001). Our analysis identified 13,912 and 3,308 CpGs associated with survival in the RT and RT-PCV arms, respectively. Most of the 3,308 CpGs identified by analysis of the RT-PCV arm were also present in the 13,912 CpGs identified by analysis of the RT arm. However, 259 CpGs were uniquely associated with survival in the RT-PCV arm (Supplementary Table S4).

The strongest differentially methylated CpG site identified this way was cg12981137, a probeset that is 1 of the 2 CpGs used to determine the tumors' *MGMT*-STP27 status. The top networks associated with the 259 CpGs associated with treatment response involve "lipid metabolism," "cancer," "cellular development," and "cellular movement" as determined by Ingenuity Pathway Analysis.

Figure 4.
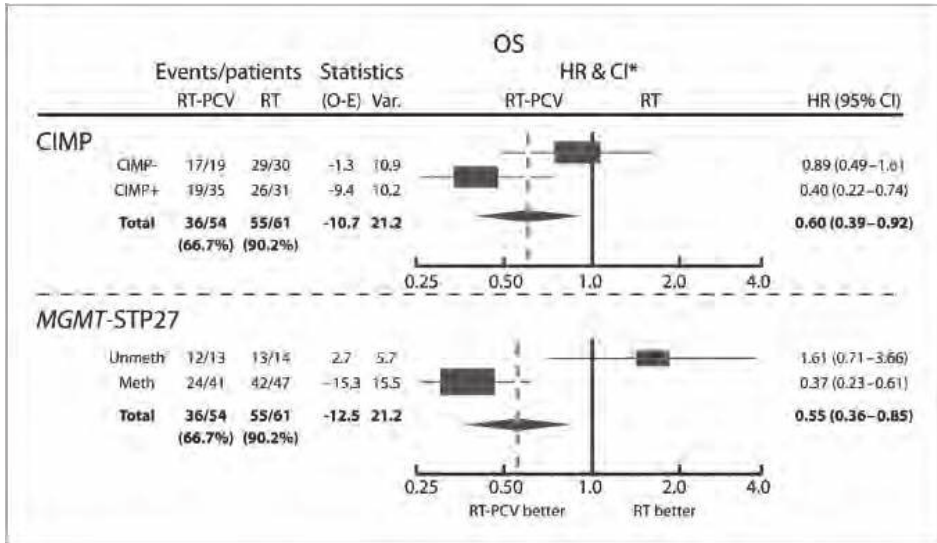
Forest plots of relative risk of CIMP and *MGMT*-STP27 in the RT and RT-PCV treatment arms. The interaction test for CIMP status of borderline significance, $P = 0.07$, $\chi2$ 3.37, degrees of freedom (df) = 1. For *MGMT*-STP27, the interaction test was significant $P = 0.003$, $\chi2$ 8.93, df=1.

Table 2. CIMP and *MGMT*-STP27 status predict benefit from adjuvant PCV treatment

	PFS				OS			
	RT	RT-PCV	HR (95% CI)	P	RT	RT-PCV	HR (95% CI)	P
CIMP								
Pos	1.84	8.2	0.34 (0.18–0.62)	0.0005	3.47	9.51	0.40 (0.22–0.74)	0.0033
Neg	0.47	0.68	0.54 (0.30–0.98)	0.042	1.84	1.06	0.88 (0.49–1.60)	0.67
	0.73	5.36	0.30 (0.18–0.50)	<0.0001	1.98	8.65	0.37 (0.23–0.61)	0.0001
Unmeth	0.62	0.65	0.95 (0.44–2.10)	0.91	1.32	0.96	1.61 (0.71–3.65)	0.26

DISCUSSION

In this study, we have conducted genome-wide methylation profiling on samples treated within EORTC study 26951 on adjuvant PCV chemotherapy in anaplastic oligo-dendroglial tumors. Although the study was set up to further explore the predictive significance of CIMP status, the results show a more predictive value of *MGMT* promoter methylation status as calculated from the methylation array data. Our data expand on the predictive power of *MGMT* promoter methylation status by showing it not only pre-dicts benefit from temozolomide chemotherapy in patients with glioblastoma (12–14) but also predicts benefit from PCV chemotherapy in patients with AOA and AOD. Of note, the *MGMT*-STP27 has thus far only been tested on snap-frozen tissue samples (16).

Interestingly, previous experiments on EORTC 26951 clinical trial material failed to identify a predictive effect of *MGMT* promoter methylation status. In the previous study, however, *MGMT* promoter methylation status was determined using MLPA which interrogates a different set of CpG sites than *MGMT*-STP27 (16, 24). Indeed, the Spearman correlation between MS-MLPA and *MGMT*-STP27 was only 0.56. This confirms that different CpG sites within the *MGMT* promoter have different predictive power for outcome to alkylating chemotherapy. Other studies that confirmed the predictive power of *MGMT* promoter methylation also examined CpG sites that are different from those examined by the MLPA assay (12–14, 25). For example, the NOA-08 study has validated the role of *MGMT* determination in newly diagnosed glioblastoma (14). In addition to examining different CpG sites, the previous OS analysis of the MS-MSLPA on *MGMT* promoter methylation was based on the outcome data of the 2006 report on EORTC 26951. With longer follow-up, a long-term benefit of adjuvant PCV chemotherapy has been established, in particular of the 1p1/9q co-deleted tumors.

Bady and colleagues have conducted an analysis of the best CpG sites to predict *MGMT* promoter methylation status on the Illumina Beadchip27 and 450 platforms (16). However, it is possible that other CpGs that lie within the *MGMT* promoter provide an even greater predictive power than those of *MGMT*-STP27. To determine this, a further detailed analysis of the *MGMT* promoter region needs to be conducted in which methylation on all CpGs, but especially those in *DMR1* and *DMR2*, are correlated to patient outcome. Data should then be validated on material derived from an independent trial.

Our observation that CIMP+ tumors benefit from adjuvant PCV chemotherapy is in line with other data obtained in anaplastic oligodendrogliomas: 1p/19q codeleted tumors are virtually all CIMP+, and we and others have reported that anaplastic oligodendrogliomas with 1p/19q codeletion benefit from (neo) adjuvant PCV (4, 19, 26; see also ref. 27). Finally, the gene expression subtypes in the EORTC 26951 trial that benefit from adjuvant PCV (IGS-9 and IGS-17) are also CIMP+ (7).

CIMP status is also highly correlated with *IDH1* mutation status (Spearman correlation, $\rho = 0.77$), although 14/60 CIMP+ tumors are *IDH1* wild-type. Recent evidence indicates that the hypermethylated phenotype is caused by metabolic changes due to mutations in the *IDH1* gene (28–30). Previous analyses on EORTC 26951 trial material also showed an association between *IDH1* mutations and treatment response. However, impact on outcome to PCV from both *IDH1* mutation status and CIMP status remained nonsignificant in tests for interaction (5, 11). Apart from the present observation that CIMP status is predictive for benefit from adjuvant PCV chemotherapy, we also show that CIMP status is prognostic for survival. These data have been corroborated in other studies (8, 10, 11).

The 14 samples in our study that were *IDH1* wt but CIMP+ may be the result of assay sensitivity (either in the determination of *IDH1* or CIMP status), presence of other mutations producing *R*-2-hydroxyglutarate [either rare mutations in *IDH1* (31) or mutations in

IDH2] or a true positive finding that there are indeed CIMP+ tumors that are *IDH1* wt. It should be noted that other groups have also identified CIMP+ tumors that are *IDH1* wt. For example, in their original manuscript, the TCGA has identified 2 of 12 CIMP+ tumors that are *IDH1* wt (10). This ratio of CIMP+ but *IDH1* wt tumors is highly similar to that found in present study (14 of 63 or 22%).

Exploratory analysis of our dataset identified a set of CpGs that are associated with benefit from adjuvant PCV chemotherapy. One of the CpG sites identified by our analysis was cg12981137 which was the strongest candidate indentified by this analysis. This probeset is located within the *MGMT* promoter region and is a part of the previously defined *MGMT*-STP27 2 CpG site predictor profile of response to chemotherapy in glioblastoma. The second CpG of the *MGMT*-STP27 predictor was associated with survival in both treatment arms and therefore was not specific for OS benefit after RT-PCV. For all of the identified 259 CpGs associated with treatment response, it was always the methylated form that was associated with benefit from treatment.

One limitation of our study is that we were only able to analyze a subset of patients treated within EORTC 26951, although most characteristics of samples included versus those not included are similar. However, treatment effect of patients included is larger than patients not included (Supplementary Figure S2). Also, our sample cohort is relatively modest in size (115) and our analysis is post hoc (retrospective testing). Our results therefore require validation in an additional independent cohort to firmly establish the predictive effect of CIMP status, *MGMT*-STP27 status, and the CpGs associated with treatment response.

The practical consequence of our study is that the *MGMT* promoter methylation status needs to be determined in AOD. At present, there are different techniques available that determine the methylation status, and several of these are also currently being used in routine diagnostics. However, as some methylation sites within the *MGMT* promoter region have less predictive power than others, care should be taken to ensure that the correct CpG sites are interrogated. The use of Illumina beadchips as a diagnostic tool may be practically difficult to implement but this technique does offer the advantage that additional markers (such as CIMP status) may be added to the predictive (or prognostic) profile. In addition, methylation arrays can also be used to determine gross genomic changes such as 1p19q LOH. If the transition of glioma diagnostics toward more molecular-based diagnosis continues, these types of platforms may be rational.

In summary, we confirm, on clinical trial samples and using FFPE material, that CIMP status is prognostic for overall survival in the EORTC 26951 clinical trial. Although CIMP status is correlated to benefit to PCV chemotherapy, our data show a significant predictive effect of the *MGMT*-STP27 status, although validation on an independent dataset is warranted. As only the *MGMT*-STP27 methylated samples show benefit from PCV, *MGMT*-STP27 could be used to guide treatment decisions in this tumor type.

REFERENCES

1. van den Bent MJ, Carpentier AF, Brandes AA, Sanson M, Taphoorn MJ, Bernsen HJ, et al. Adjuvant procarbazine, lomustine, and vincristine improves progression-free survival but not overall survival in newly diagnosed anaplastic oligodendrogliomas and oligoastrocytomas: a randomized European Organisation for Research and Treatment of Cancer phase III trial. J Clin Oncol 2006;24:2715–22.

2. van den Bent MJ, Brandes AA, Taphoorn MJ, Kros JM, Kouwenhoven MC, Delattre JY, et al. Adjuvant procarbazine, lomustine, and vincristine chemotherapy in newly diagnosed anaplastic oligodendroglioma: long-term follow-up of EORTC brain tumor group study 26951. J Clin Oncol 2013;31:344–50.

3. Cairncross G, Berkey B, Shaw E, Jenkins R, Scheithauer B, Brachman D, et al. Phase III trial of chemotherapy plus radiotherapy compared with radiotherapy alone for pure and mixed anaplastic oligodendroglioma: Intergroup Radiation Therapy Oncology Group Trial 9402. J Clin Oncol 2006;24:2707–14.

4. Cairncross G, Wang M, Shaw E, Jenkins R, Brachman D, Buckner J, et al. Phase III trial of chemoradiotherapy for anaplastic oligodendroglioma: long-term results of RTOG 9402. J Clin Oncol 2013;31:337–43.

5. van den Bent MJ, Dubbink HJ, Marie Y, Brandes AA, Taphoorn MJ, Wesseling P, et al. *IDH1* and *IDH2* mutations are prognostic but not predictive for outcome in anaplastic oligodendroglial tumors: a report of the European Organization for Research and Treatment of Cancer Brain Tumor Group. Clin Cancer Res 2010;16:1597–604.

6. van den Bent MJ, Dubbink HJ, Sanson M, van der Lee-Haarloo CR, Hegi M, Jeuken JW, et al. *MGMT* promoter methylation is prognostic but not predictive for outcome to adjuvant PCV chemotherapy in anaplastic oligodendroglial tumors: a report from EORTC Brain Tumor Group Study 26951. J Clin Oncol 2009;27:5881–6.

7. Erdem-Eraslan L, Gravendeel LA, de Rooi J, Eilers PH, Idbaih A, Spliet WG, et al. Intrinsic molecular subtypes of glioma are prognostic and predict benefit from adjuvant procarbazine, lomustine, and vincristine chemotherapy in combination with other prognostic factors in anaplastic oligodendroglial brain tumors: a report from EORTC study 26951. J Clin Oncol 2013;31:328–36.

8. Christensen BC, Smith AA, Zheng S, Koestler DC, Houseman EA, Marsit CJ, et al. DNA methylation, isocitrate dehydrogenase mutation, and survival in glioma. J Natl Cancer Inst 2011;103:143–53.

9. Martinez R, Martin-Subero JI, Rohde V, Kirsch M, Alaminos M, Fernandez AF, et al. A microarray-based DNA methylation study of glioblastoma multiforme. Epigenetics 2009;4:255–64.

10. Noushmehr H, Weisenberger DJ, Diefes K, Phillips HS, Pujara K, Berman BP, et al. Identification of a CpG island methylator phenotype that defines a distinct subgroup of glioma. Cancer Cell 2010;17:510 22.

11. van den Bent MJ, Gravendeel LA, Gorlia T, Kros JM, Lapre L, Wesseling P, et al. A hypermethylated phenotype is a better predictor of survival than *MGMT* methylation in anaplastic oligodendroglial brain tumors: a report from EORTC study 26951. Clin Cancer Res 2011;17:7148–55.

12. Hegi ME, Diserens AC, Gorlia T, Hamou MF, de Tribolet N, Weller M, et al. *MGMT* gene silencing and benefit from temozolomide in glioblastoma. N Engl J Med 2005;352:997–1003.

13. Malmstrom A, Gronberg BH, Marosi C, Stupp R, Frappaz D, Schultz H, et al. Temozolomide versus standard 6-week radiotherapy versus hypofractionated radiotherapy in patients older than 60 years with glioblastoma: the Nordic randomised, phase 3 trial. Lancet Oncol 2012;13:916–26.

14. Wick W, Platten M, Meisner C, Felsberg J, Tabatabai G, Simon M, et al. Temozolomide chemotherapy alone versus radiotherapy alone for malignant astrocytoma in the elderly: the NOA-08 randomised, phase 3 trial. Lancet Oncol 2012;13:707–15.

15. Malley DS, Hamoudi RA, Kocialkowski S, Pearson DM, Collins VP, Ichimura K . A distinct region of the *MGMT* CpG island critical for transcriptional regulation is preferentially methylated in glioblastoma cells and xenografts. Acta Neuropathol 2011;121:651–61.

16. Bady P, Sciuscio D, Diserens AC, Bloch J, van den Bent MJ, Marosi C, et al. *MGMT* methylation analysis of glioblastoma on the Infinium methylation BeadChip identifies two distinct CpG regions associated with gene silencing and outcome, yielding a prediction model for comparisons across datasets, tumor grades, and CIMP-status. Acta Neuropathol 2012;124:547–60.

17. Idbaih A, Dalmasso C, Kouwenhoven M, Jeuken J, Carpentier C, Gorlia T, et al. Genomic aberrations associated with outcome in anaplastic oligodendroglial tumors treated within the EORTC phase III trial 26951. J Neurooncol 2011;103:221–30.

18. Kouwenhoven MC, Gorlia T, Kros JM, Ibdaih A, Brandes AA, Bromberg JE, et al. Molecular analysis of anaplastic oligodendroglial tumors in a prospective randomized study: A report from EORTC study 26951. Neuro-oncology 2009;11:737–46.

19. van den Bent MJ, Hoang-Xuan K, Brandes AA, Kros JM, Kouwenhoven MC, Taphoorn MJ, et al. Long-term follow-up results of EORTC 26951: A randomized phase III study on adjuvant PCV chemotherapy in anaplastic oligodendroglial tumors (AOD). J Clin Oncol 30, 2012 (suppl; abstr 2).

20. Kapp AV, Tibshirani R . Are clusters found in one dataset present in another dataset? Biostatistics (Oxford, England) 2007;8:9–31.

21. Taylor J, Tibshirani R, Efron B . The 'miss rate' for the analysis of gene expression data. Biostatistics (Oxford, England) 2005;6:111–7.

22. Tusher VG, Tibshirani R, Chu G . Significance analysis of microarrays applied to the ionizing radiation response. Proc Natl Acad Sci U S A 2001;98:5116–21.

23. Du P, Zhang X, Huang CC, Jafari N, Kibbe WA, Hou L, et al. Comparison of Beta- value and M-value methods for quantifying methylation levels by microarray analysis. BMC Bioinformatics 2010;11:587.

24. Weller M, Stupp R, Reifenberger G, Brandes AA, van den Bent MJ, Wick W, et al. *MGMT* promoter methylation in malignant gliomas: ready for personalized medicine? Nat Rev Neurol 2010;6:39–51.

25. Esteller M, Risques RA, Toyota M, Capella G, Moreno V, Peinado MA, et al. Promoter hypermethylation of the DNA repair gene O(6)-methylguanine-DNA methyltransferase is associated with the presence of G:C to A:T transition mutations in p53 in human colorectal tumorigenesis. Cancer Res 2001;61:4689–92.

26. Cairncross JG, Ueki K, Zlatescu MC, Lisle DK, Finkelstein DM, Hammond RR, et al. Specific genetic predictors of chemotherapeutic response and survival in patients with anaplastic oligodendrogliomas. J Natl Cancer Inst 1998;90:1473–9.

27. Mokhtari K, Ducray F, Kros JM, Gorlia T, Idbaih A, Taphoorn M, et al. Alpha- internexin expression predicts outcome in anaplastic oligodendroglial tumors and may positively impact the efficacy of chemotherapy: European organization for research and treatment of cancer trial 26951. Cancer 2012;117:3014–26.

28. Figueroa ME, Abdel-Wahab O, Lu C, Ward PS, Patel J, Shih A, et al. Leukemic *IDH1* and *IDH2* mutations result in a hypermethylation phenotype, disrupt TET2 function, and impair hematopoietic differentiation. Cancer Cell 2010;18:553–67.

29. Turcan S, Rohle D, Goenka A, Walsh LA, Fang F, Yilmaz E, et al. *IDH1* mutation is sufficient to establish the glioma hypermethylator phenotype. Nature 2012;483:479–8.

30. Xu W, Yang H, Liu Y, Yang Y, Wang P, Kim SH, et al. Oncometabolite 2- hydroxyglutarate is a competitive inhibitor of alpha-ketoglutarate-dependent dioxygenases. Cancer Cell 2011;19:17–30.

31. Ward PS, Cross JR, Lu C, Weigert O, Abel-Wahab O, Levine RL, et al. Identification of additional *IDH* mutations associated with oncometabolite R(-)-2-hydroxyglutarate production. Oncogene 2012;31:2491–8.
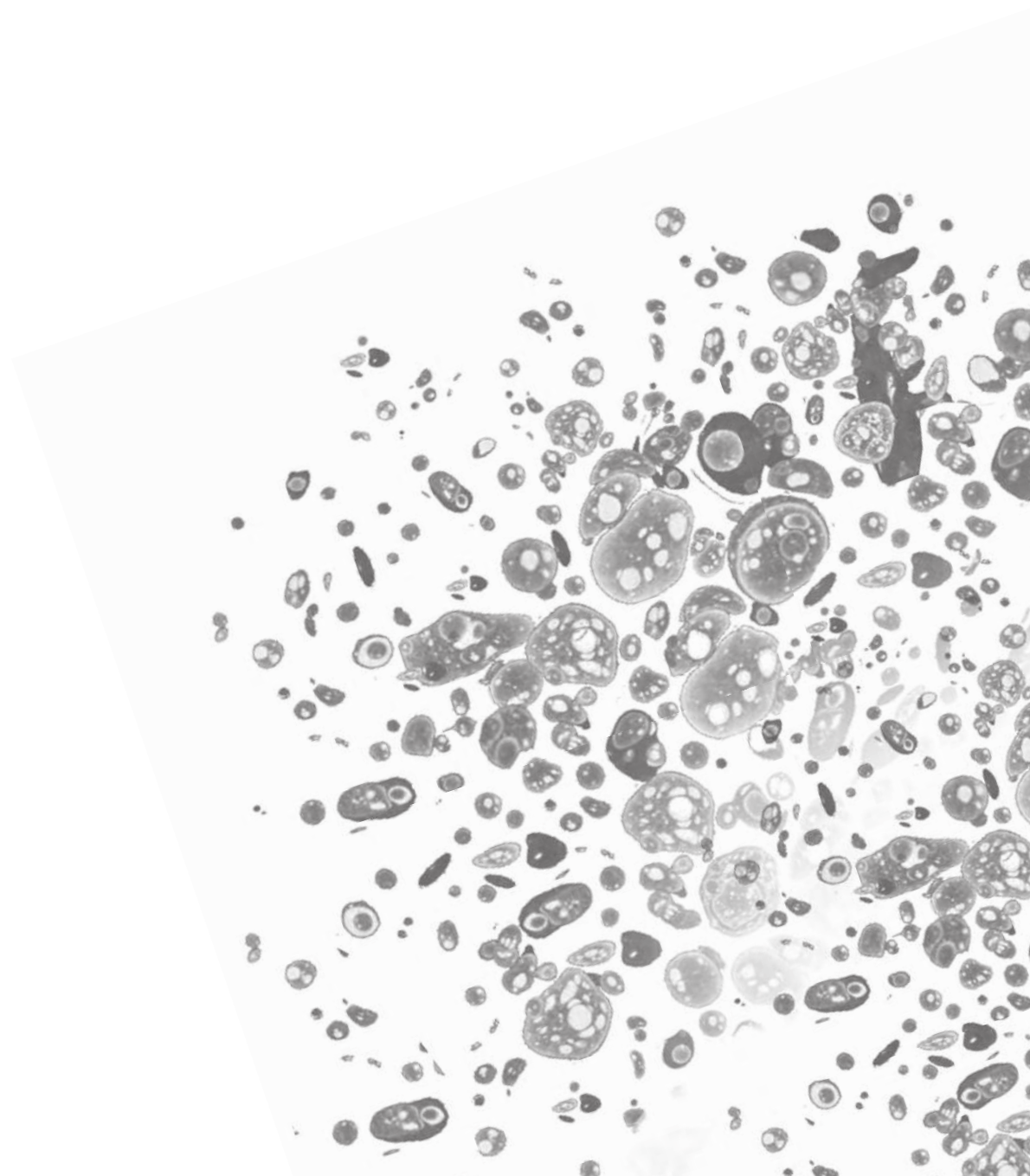
CHAPTER 3

Identification of recurrent GBM patients who may benefit from Bevacizumab and CCNU. A report from the BELOB trial conducted by the Dutch Neurooncology Group

Lale Erdem-Eraslan, Martin J. van den Bent,
Youri Hoogstrate, Hina Naz-Khan,
Andrew Stubbs, Peter van der Spek,
René Böttcher, Ya Gao, Maurice de Wit,
Walter Taal, Hendrika M Oosterkamp,
Annemiek Walenkamp, Laurens V. Beerepoot,
Monique C.J. Hanse, Jan Buter, Aafke H. Honkoop,
Bronno van der Holt, René M. Vernhout,
Peter A.E. Sillevis Smitt, Johan M. Kros,
Pim J. French

ABSTRACT

The results from the randomized phase II BELOB trial provided evidence for a potential benefit of bevacizumab (beva; a humanized monoclonal antibody against circulating VEGF-A) when added to CCNU chemotherapy in recurrent GBM patients. In this study, we have performed gene expression profiling (DASL and RNA-seq) on formalin fixed, paraffin embedded (FFPE) tumor material from patients treated within the BELOB trial to identify recurrent GBM patients who benefit most from combined beva/CCNU treatment. We first extensively validate the use of FFPE tissues for expression profiling on both DASL and RNA-seq. Our data show that tumors assigned to IGS-18 or 'classical' GBMs show a significant benefit in progression free survival (PFS) and a trend towards benefit in overall survival (OS) from beva+CCNU treatment; other subtypes do not show such benefit. In particular, expression of *FMO4* and *OSBPL3* were associated with treatment response. All molecular glioma subtypes are evenly distributed along the different study arms and the improved outcome in the beva/CCNU arm therefore is not explained by an uneven distribution of prognostically favorable subtypes. Analysis of RNA-seq data highlighted genetic changes, including mutations, gene fusions (and identification of the exact genomic breakpoint), and copy number changes (albeit with limited resolution) within this well-defined cohort of tumors. When validated in an independent dataset, the predictive markers identified in this study will allow selection of recurrent GBM patients that benefit from beva+CCNU treatment.

INTRODUCTION

Glioblastomas (GBMs) are the most common and aggressive type of glial brain tumors (1). The current standard of care for GBM patients includes surgical resection followed by combined chemo-irradiation with temozolomide (2). However, GBMs invariably relapse and when this progression occurs, treatment options are limited. Nitrosoureas (in particular lomustine and carmustine), retreatment with (dose intense) temozolomide, re-irradiation, and re-resection are treatments that are often employed but have limited activity (3). Progression-free survival of recurrent GBM patients is in the range of 2-4 months, and post-progression survival of about 6-8 months, with conventional chemotherapy (4).

GBMs are histologically characterized by endothelial proliferation and necrosis. At the molecular level, they are characterized by hypoxia induced- and HIF-1alfa dependent upregulation of Vascular Endothelial Growth Factor (*VEGF*) production by tumor cells, which subsequently induces new blood vessel formation (5). Because of the extensive endothelial proliferation that characterizes GBM, soon after the discovery of *VEGF* and its significance for the angiogenesis of tumor growth it has been hypothesized that GBM would provide a good target for anti-angiogenic treatments.

In spite of some initially promising results in uncontrolled trials however, recent data suggests that the effects of angiogenesis inhibition on overall survival (OS) is limited in both primary and recurrent GBM patients (6-9) ENREF_6. For example, bevacizumab, a humanized monoclonal antibody against circulating *VEGF*, failed to demonstrate significant improvement of survival in newly diagnosed GBM patients in two large randomized phase III clinical trials (10, 11). Similarly, cediranib, a pan VEGFR inhibitor, did not improve outcome in recurrent GBM patients (12). Although the overall effects of angiogenesis inhibition may be disappointing, it is possible that subsets of patients do obtain some clinical benefit (for examples in glioma see (13-16). For bevacizumab, gene expression analysis provided preliminary evidence of benefit in distinct molecular subtypes of GBMs (17, 18).

Recently, results were reported for the BELOB trial, a trial from the Dutch Neuro- Oncology Group (LWNO), in which patients were randomly assigned to treatment with lomustine (CCNU), bevacizumab (beva) or a combination of CCNU with beva (beva/CCNU) (19). The trial results were intriguing as they indicate a potential survival benefit of beva/CCNU in recurrent GBM patients. In this study, we have performed gene expression profiling and RNA-sequencing on tumor samples derived from patients treated within the BELOB trial to identify recurrent GBM patients who benefit from combined beva/CCNU treatment. Our results show that of the different molecular subtypes of GBM (20, 21) 'classical' GBMs or those assigned to IGS-18 showed a trend towards benefit from treatment; other subtypes did not show such benefit. When validated in an independent

dataset, our data will allow selection of recurrent GBM patients that benefit from beva/CCNU combination treatment.

MATERIALS AND METHODS

Patients were eligible for the BELOB trial if they were ≥18 years and had a first recurrence of GBM after temozolomide and radiotherapy treatment. Details of the study have been described previously (19). We also selected 37 paired FF-FFPE samples from the Erasmus University Medical Center glioma tumor archive, with FF and the FFPE samples taken as parallel biopsies from the same tumor. All of the FF–FFPE sample pairs were described previously to assess the performance of HuEx_1.0_St arrays (Affymetrix) (20, 22). Use of patient material was approved by the Institutional Review Board of the respective hospitals and patients provided written informed consent according to national and local regulations for the clinical study and correlative tissue studies.

Total RNA extraction, purification, and quantification from FF and FFPE material were reported previously (22). 250 ng of purified RNA was used for labeling and hybridization on DASL beadchips (run by Service XS, Leiden, the Netherlands); 500 ng was used for RNA-sequencing on an Illumina TruSeq and ~35-40 million 40 base paired end-reads were generated per sample. RNA-seq (n=96) was run by Expression Analysis (Durham, NC). DNA extraction was performed using the Allprep FFPE DNA/RNA FFPE kit (Qiagen, Venlo, the Netherlands) according to the manufacturers' instructions. RNA expression profiles were then assigned to one of six intrinsic molecular subtypes of glioma (omitting IGS-0), or to one of four glioma subtypes as defined by the TCGA, using the ClusterRepro R package (http://crantastic.org/packages/clusterRepro) (23). Expression data is available at the NCBI Geo datasets, accession number GSE72951. Gene expression levels (Ref-seq genes) were extracted from the RNA-seq data using featureCounts (24), after alignment on hg19 with Tophat2 (25) of clipped/trimmed reads as provided by the manufacturer. VarScan 2 was used to identify SNVs and indels in the RNA-seq data (26-28), Annovar was used to annotate the SNVs (29). Candidate SNVs were filtered for SNVs that are present in the 1000 genomes database, and for changes that would result in a change in the primary protein sequence. We further focused on those that are either absent from dbSNP138 or are present in the COSMIC database (30, 31). *ANKRD36* was removed from this analysis: 497 mutations in 94 samples were identified in this gene, which is likely due to misalignment of homologous and/or non-refseq genes (e.g. *ANKRD36B* or *FLJ54441*). Candiate fusion genes were detected using ChimeraScan V0.4.5 on hg19 (32). RT-PCR was used to confirm fusion candidates, Sanger sequencing was performed to confirm genetic changes.

Differences between the Kaplan-Meier survival curves were calculated using the log- rank (Mantel-Cox) test using GraphPad Prism version 5.00 for Windows (GraphPad Software, San Diego, CA). For all analysis, OS and PFS were calculated from point of first recurrence. The significance of prognostic factors was determined with a multivariate analysis using Cox regression. In this analysis treatment was coded as 1. Beva/CCNU, 2. CCNU and 3. Beva. Comparisons between frequencies were assessed by the Fisher's exact test or the chi square test (where indicated). SAM analysis was performed using SAMR, an R package. The SAM approach to identify genes associated with treatment response is similar to previously reported using methylation arrays (33). Pathway analysis was performed using Ingenuity IPA (Qiagen, Venlo, the Netherlands) using genes differentially expressed between IGS-18 and all other subtypes at P<0.01 and > 2x fold change in expression level.

RESULTS

DASL and RNA-seq performance on FFPE samples and sample assignment

As RNA isolated from samples that are fixed in formalin and embedded in paraffin (FFPE) is degraded, we first ran a series of tests to determine the suitability of using DASL arrays and RNA-seq on FFPE isolated RNA. In this analysis we compared performance of the two platforms between technical and biological replicates, and compared the performance between snap frozen and archival samples that were stored >15 years in paraffin. Results are highlighted in the supplementary data results figures S1-S3. Our experiments demonstrate that both DASL beadchips and RNA-seq can be used to perform gene expression profiling and assignment to specific molecular subtypes using FFPE tissues, even when the tissues were stored up to 20 years in paraffin.

Molecular subtypes of glioma in BELOB trial tumor samples

All available BELOB trial samples (114/152) were assigned to molecular subtypes as defined by 'Gravendeel' (IGS-9, 17, 18, 22 and 23) and 'Verhaak' (Proneural, Neural, Classical and Mesenchymal) (20, 21) (table 2). The patient characteristics of tumor samples included in the current study did not differ from the entire BELOB patient cohort with respect to age, sex, performance score, *MGMT* promoter methylation and survival (table 1). Material was unavailable for the remaining 38 tumor samples. As can be expected, most samples were assigned to the prognostically unfavorable subtypes IGS-18 and IGS-23; GBMs are often assigned to these molecular subtypes (supplementary table 3). Few samples were assigned to the prognostically favorable subtypes IGS-9 and IGS-17. All subtypes, including the prognostically favorable samples, were evenly distributed along the different study arms and the improved outcome in the Beva/CCNU arm therefore is

not explained by a skewed distribution of these samples. When samples were assigned according to the TCGA classification of GBMs, most samples are assigned to the TCGA 'Classical' and 'Mesenchymal' subtypes and few to the 'proneural' and 'neural' subtypes (table 2). From the point of 1st recurrence, the timepoint used for all analysis in current manuscript, the survival (both OS and PFS) between molecular subtypes was not significantly different Supplementary figure S4.

Table 1. Patient data

	Current study			Patients from the BELOB trial not included in present study			
	N=114			N=38			
	Beva	CCNU	BC	Beva	CCNU	BC	
	35 (30)	37 (32)	43 (37)	15 (46)	9 (27)	9 (27)	
	N(%)	N(%)	N(%)	N(%)	N(%)	N(%)	P
Age, years							
Median	58	57	57	58	56	57.5	0.25
Range	37-77	28-73	24-73	38-72	46-68	41-72	
Sex							
Male	21 (60)	20 (54)	30 (70)	11 (73)	7 (70)	3 (33)	0.29
Female	14 (40)	17 (46)	13 (30)	4 (26)	3 (30)	6 (67)	
Performance status							
0	11 (31)	13 (35)	10 (23)	2 (13)	2 (20)	4 (44)	0.52
1	19 (54)	19 (51)	27 (63)	13 (87)	7 (70)	5 (56)	
2	5 (14)	5 (13)	6 (14)	0 (0)	1 (10)	0 (0)	
IDH1 mutation							
Normal	31 (89)	32 (88)	38 (88)	7 (47)	7 (70)	4 (44)	0.73
Mutated	1 (3)	2 (6)	4 (9)	0 (0)	1 (10)	0 (0)	
Missing	3 (9)	2 (6)	1 (2)	8 (53)	2 (20)	5 (56)	
MGMT promoter methylation							
Unmethylated	18 (51)	18 (49)	24 (56)	6 (40)	3 (30)	2 (22)	0.91
Methylated	16 (46)	18 (49)	18 (42)	2 (13)	5 (50)	3 (33)	
Missing/unvalid	1 (3)	1 (3)	1 (2)	7 (47)	2 (20)	4 (44)	
Median Survival (months)							
Progression-free survival	3.0	1.9	4.1	2.7	1.4	7.9	
Overall survival	8.3	7.9	10.8	5.9	6.9	13.6	

Abbreviations: Beva: bevacizumab; CCNU: Lomustine; BC: Bevacizumab and CCNU; P<0.05 is considered a statistically significant between patients included vs not included

Table 2. Sample assignment

	Proneural	Neural	Classical	Mesenchymal	Total
IGS-0	1	3	0	0	4
IGS-9	2	0	0	0	2
IGS-17	2	4	1	0	7
IGS-18	1	1	68	0	70
IGS-22	2	0	1	0	3
IGS-23	0	1	7	19	27
Total	8	9	77	19	113

Similar to previously reported, specific genetic changes segregate into distinct intrinsic subtypes (supplementary figure S5). For example, *IDH1* mutations were present in eight BELOB tumor samples (expression data are available for seven), and were identified predominantly in prognostically favorable subtypes IGS-9 (2/4, 50%), IGS-17 (3/9, 33%) and at much lower frequency in IGS-18 (1/72) and IGS-23 (1/28) (P<0.001 IGS-9+17 *v.* IGS-18+23). Similarly, *IDH1* mutations were predominantly found in 'proneural' GBMs (3/8). *EGFR* amplification is a common event in IGS-18 and in 'classical' GBMs (20, 34), and is associated with mRNA upregulation and with an accumulation of genetic changes in this locus (34). In the current dataset, samples assigned to either IGS-18 or 'classical' GBMs indeed have a significantly higher expression of *EGFR* (14.2 *v.* 12.8 for IGS-18 *v.* any other subtype on DASL, P<0.001 students t-test; data are identical for 'classical' *v.* any other subtype). Samples assigned to IGS-18 (or 'classical' GBMs) also have a significantly higher frequency of genetic changes in the *EGFR* locus as determined by RNA-seq (31/47 in IGS-18 *v.* 5/29 in any of the other subtypes, P<0.001, Fisher exact test). Similar for 'classical' *v.* other GBMs: 34/51 v 2/24 (P<0.001). The assignment of tumors to specific molecular subtypes therefore corresponds to the histological diagnosis (i.e. predominantly prognostically poor subtypes) and to the type of genetic changes found (i.e. specific genetic changes segregate within defined molecular subtypes).

Response to treatment

The molecular subtypes of gliomas identified in BELOB tumor samples were then stratified according to treatment arm. In this retrospective analysis, samples assigned to IGS-18 showed a trend towards benefit from the combination of bevacizumab and CCNU (median OS 7.9, 8.3 and 11.9 months in the CCNU, beva and beva/CCNU arms respectively P=0.09, figure 1). This trend was absent when grouping all samples not assigned to IGS-18 (median OS 10.1, 8.9 and 6.3 months in the CCNU, beva and beva/CCNU arms respectively P=0.85); too few samples assigned to IGS-9, IGS-17, IGS-22 or IGS-23 to assess treatment response in individual subtypes. A significant benefit in progression free survival (PFS) was observed for tumor samples assigned to IGS-18: survival of samples

assigned to IGS-18 was 1.4, 2.9 and 4.2 months in the CCNU, beva and beva/CCNU arms respectively (P=0.0004), for non-IGS-18 samples it was 2.8, 4.1 and 3.7 months (P=0.23, figure 1).

Figure 1.
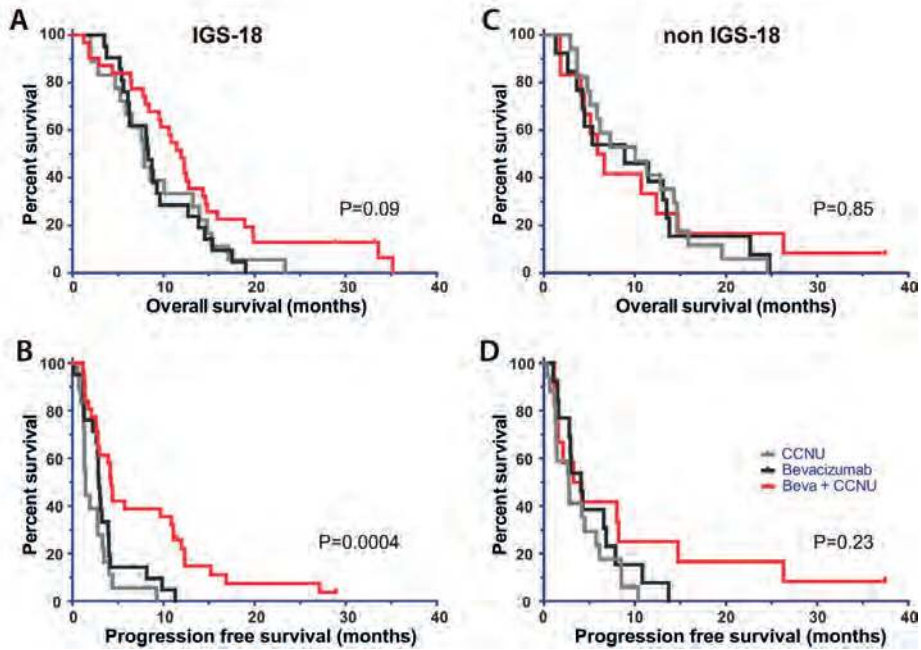
Distinct molecular subtypes of GBM show a trend towards benefit from Beva/CCNU treatment. The molecular subtypes of glioma were stratified according to treatment arm. Tumors assigned to IGS-18 show a trend towards benefit from Beva/CCNU treatment in both OS (A) and PFS (B). Tumors assigned to other subtypes combined do not show such benefit (C and D).

Analysis of subtypes defined by the TCGA showed similar results: 'classical' GBMs showed a trend towards improved survival from the combination of bevacizumab and CCNU (median OS 8.2, 8.3 and 11.9 months in the CCNU, Beva and Beva/CCNU arms respectively P=0.097, median PFS 1.7, 3.0 and 4.2 months, P=0.001, supplementary figure S6). This trend was absent when grouping all 'non-classical' GBMs (median OS 8.7, 7.1 and 5.9 months in the CCNU, beva and beva/CCNU arms respectively P=0.90, median PFS 2.7, 3.0 and 3.7, P=0.29); too few samples were 'mesenchymal', 'proneural' or 'neural' to assess treatment response in individual subtypes. These data suggest that recurrent GBM patients whose tumors are assigned to IGS-18 or are 'classical' GBMs may benefit from the combination of bevacizumab and CCNU whereas tumors assigned to other subtypes do not show such benefit.

We next aimed to identify genes and molecular pathways that were associated with treatment response on overall survival. We first performed SAM analysis and identified two genes (*FMO4* and *OSBPL3*) that are associated with overall survival specifically in the beva/CCNU treatment arm (using a false discovery rate cutoff of 0.05). SAM analysis failed to identify genes associated with survival in the CCNU and beva monotherapy arms of this study. As the two genes are associated with survival only in the beva/CCNU treatment arm, these genes may be considered specifically associated with response to treatment (figure 2). Indeed, clustering samples based on *FMO4* and *OSBPL3* expression divided samples in two major subtypes (figure 2). Overall survival between the two subtypes was similar for patients treated with either CCNU or beva monotherapy (median survival of 8.3 *v.* 8.5 and 6.1 *v.* 10.1 months for CCNU and beva monotherapy respectively, P=0.57). However, survival between the two subtypes significantly differed for patients treated with beva/CCNU (median survival of 6.1 *v.* 12.4 months, P<0.0001). There is no

Figure 2.
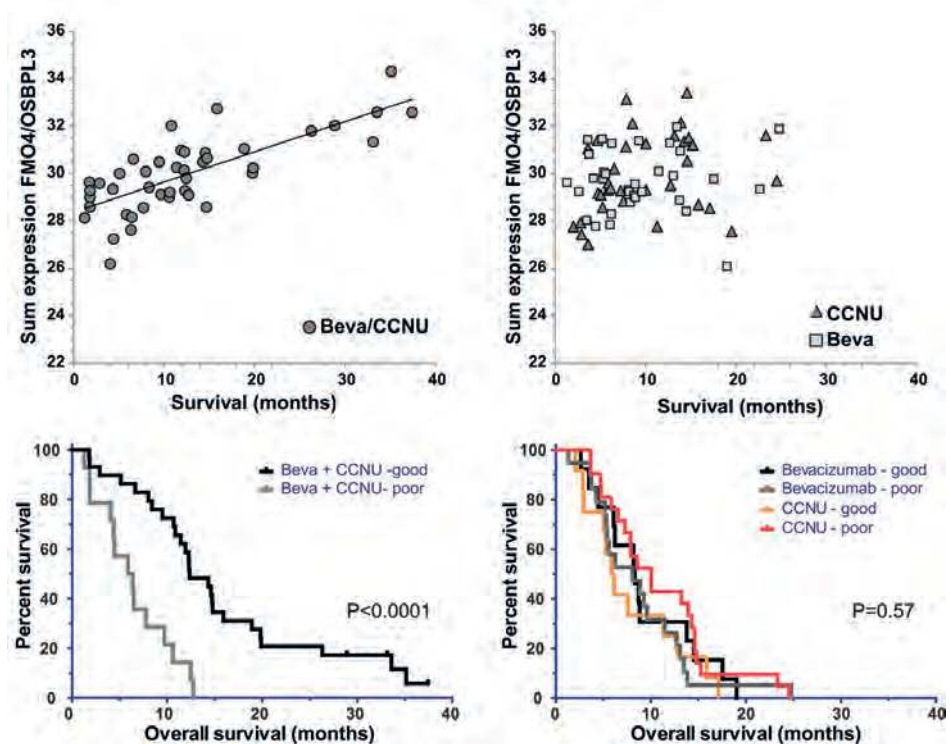
SAM analysis identified two genes (*FMO4* and *OSBPL3*) that are associated with overall survival specifically in the Beva/CCNU treatment arm. Unsupervised hierarchical clustering based on these two genes separates tumors in two major subtypes. Subsequent stratification of tumors by treatment shows that *FMO4*/*OSBPL3* expression predicts response in the Beva/CCNU arm (left) but not in the other (Beva or CCNU monotherapy) arms (right).

difference in gene expression levels of these two genes between the different molecular subtypes (supplementary data figure s8).

Because tumors assigned to IGS-18 show a trend towards benefit from beva/CCNU, we also performed pathway analysis on genes differentially expressed between IGS-18 and all other molecular subtypes. Pathway analysis was performed using our previously reported dataset containing snap frozen tumor samples (20). A total of 241 differentially expressed genes and seventeen differentially activated pathways were identified. Pathways included those that are involved in a.o. cellular assembly, cancer, cellular growth and proliferation. We then used the entire set of genes of each individual pathway (also including genes not differentially expressed between IGS-18 and other molecular subtypes) to screen whether the pathway is associated with response to beva/CCNU treatment. Four of these pathways were associated with response to beva/CCNU treatment, the other thirteen pathways showed little association (supplementary table 4, supplementary figure S7a and b). Functions of the four pathways associated with response to beva/CCNU combination treatment were often overlapping and include functional descriptors such as 'cellular assembly and organization', 'growth and proliferation' and 'tissue/organ morphology'.

Univariate analysis highlighted that in BELOB samples, *MGMT* promoter methylation (P=0.01), *IDH1* mutation status (P=0.04), treatment (P=0.04) and *FMO4/OSBPL3* expression (P<0.0001) were factors significantly correlated with OS. It should be noted however that the study was not powered to perform comparative analysis. Multivariate analysis including these factors showed *MGMT* promoter methylation, treatment and *FMO4/OSBPL3* expression as independent prognostic factors associated with overall survival (table 3A; supplementary table 5). The interaction between *FMO4/OSBPL3* expression and treatment was significant confirming the notion that high *FMO4/OSBPL3* expression is associated with treatment response in the bev/CCNU arm. Factors associated with PFS in a univariate analysis were *MGMT* promoter methylation (P=0.004), *IDH1* mutation status (P=0.017), performance status (P=0.013), intrinsic subtype (P=0.018), treatment (P=0.006) and *FMO4/OSBPL3* expression (P=0.0004). Multivariate analysis including these factors showed *MGMT* promoter methylation, *IDH1* mutation status and treatment as independent prognostic factors associated with PFS (table 3B). The interaction between *FMO4/OSBPL3* expression and treatment was also significant for PFS in this analysis confirming association of *FMO4/OSBPL3* expression with bev/CCNU treatment.

In patients of the TCGA database that received bevacizumab at any time during the treatment, a non-significant tendency towards increased survival was observed in tumors with high expression of *FMO4* or *OSBPL3* (strongest in GBMs assigned to IGS-18: median survival of 1.21 v 1.50 years for both *FMO4* and *OSBPL3*, supplementary figure S9). High expression of *FMO4* or *OSBPL3* was not associated with increased survival in the entire TCGA GBM dataset. We should stress that these data should be interpreted

with caution: the number of patients receiving bevacizumab (and assigned to IGS-18) is small (n=18), patients did not receive uniform treatment, and bevacizumab may have been given at a time-point different from the BELOB study.

Table 3a. Multivariate analysis of factors associated with overall survival

	Haz. Ratio	Std Err.	z	P>|z|	95% Conf. Interval	
MGMT	0.60	0.22	-2.35	0.019	0.39	0.92
IDH1	0.45	0.55	-1.46	0.144	0.15	1.32
Treatment	1.34E+07	4.03	4.07	0.000	4.95E+03	3.63E+10
FMO4/OSBPL3	0.79	0.12	-1.89	0.059	0.63	1.01
TRT * F/O	0.43	0.21	-4.09	0.000	0.28	0.64

Trt * F/O: interaction term treatment and *FMO4/OSBPL3* expression

Table 3b. Multivariate analysis of factors associated with progression free survival

	Haz. Ratio	Std Err.	z	P>|z|	95% Conf. Interval	
MGMT	0.55	0.22	-2.68	0.007	0.36	0.85
IDH1	0.31	0.56	-2.06	0.039	0.10	0.95
Performance	3.91	1.05	1.30	0.194	0.50	30.73
IGS-subtype	1.07	0.09	0.77	0.443	0.90	1.27
Treatment	1.05E+08	4.37	4.23	0.000	2.01E+04	5.45E+11
FMO4/OSBPL3	1.08	0.13	0.57	0.566	0.84	1.38
TRT * F/O	0.37	0.23	-4.36	0.000	0.24	0.58

Trt * F/O: interaction term treatment and *FMO4/OSBPL3* expression

Mutations and structural rearrangements

Mutation analysis using RNA-seq data identified a total of 45 mutations in 13 genes (out of the 71 genes frequently mutated in GBMs (34).) in 78 BELOB trial samples (table 4). Genes include *EGFR* (n=29, with often multiple mutations in a single sample), *PTEN* (n=10 of which 4 result in a premature stop codon), *TP53* (n=4), and *NF1* (n=2). The frequency of most mutations is slightly lower than previously reported (34) and can be explained because many genes are expressed at low levels, especially when one allele is lost as is the case in many tumor suppressor genes. In addition, homozygous deletions will not be identified by RNA-seq. However, a low frequency for several genes also reflects the high number of "classical" GBMs in our dataset: *PIK3CA*, *PIK3R1* and *TP53* mutations are common to "proneural" GBMs, *NF1* mutations are common to "mesenchymal' GBMs (21). The mutations per sample, along with the clinical data and molecular subtype are shown in figure 3. The type and frequency of mutations identified corresponds to those reported previously for GBMs, although RNA-seq is likely to underestimate the mutation frequencies in genes expressed at low level, particularly in tumor suppressor genes (34, 35).

Table 4. Frequency of mutations identified by RNA-seq

Gene	mutated samples (n)	frequency (%)	Brennan frequency (%)
EGFR *	29	37.2	32.6
PTEN	10	13.0	32
TP53	5	6.5	34.4
NF1 **	2	3.8	13.7
IDH1	2	2.6	5.2
RPL5	2	2.6	2.7
ATRX	2	2.6	5.8
PIK3R1	1	1.3	11.7
ZNF844	1	1.3	2.1
RB1	1	1.3	9.3
ABCC9	1	1.3	4.8
PDGFRA	2	2.6	4.5
SCN9A	1	1.3	3.8
ANKRD36	0	0.0	1.7
PIK3CA	0	0.0	12
SEMA3C	0	0.0	3.8
CD3EAP	0	0.0	1
CARD6	0	0.0	2.4

* for many mutations in EGFR, the frequency was below the minimal allele frequency used by varscan. For this analysis we also included hotspot mutations at low frequency. ** one tumor harboured two mutations in NF1.

We also used RNA-seq to identify (large) chromosomal losses: regions with chromosomal loss will be represented by RNA-seq as regions absent in heterozygous SNPs. Allele specific expression will also be reflected as a region absent in heterozygous SNPs (such as occurs in females on the X-chromosome), but this occurs a minority of genes only (36). Our algorithm was tested by comparing control samples of which SNP data was also present from snap frozen samples (see ref (37), Supplementary figure S10). The only frequent LOH observed was LOH of chromosome 10 and was observed at significantly higher frequency in samples assigned to IGS-18 (34/43, 79%) compared to IGS-23 (6/16, 38%) or other molecular subtypes (1/9, 11%, P<0.001 chi- square test).

ChimeraScan identified a total of 8879 candidate fusion genes (range 12-209). Within the technical and biological replicates, the overlap in identified candidates was low (39.6 ± 9.7%) but improved significantly when additional filters were applied (at least ten reads covering the breakpoint of which at least two chimeric reads), to 95±9.2%. When applying these filters to the entire dataset, and removing falsely called fusion transcripts due to alternative splicing events and those that occur in repetitive sequences, 28 candidate fusion genes remained (Supplementary table 6). These fusion candidates include the known fusion genes FGFR3-TACC (n=2) and EGFR-SEPT14 (n=2) (38-40) ENREF 28. WIF1 and VSTM2A were identified as a novel fusion partner of EGFR.

Figure 3.
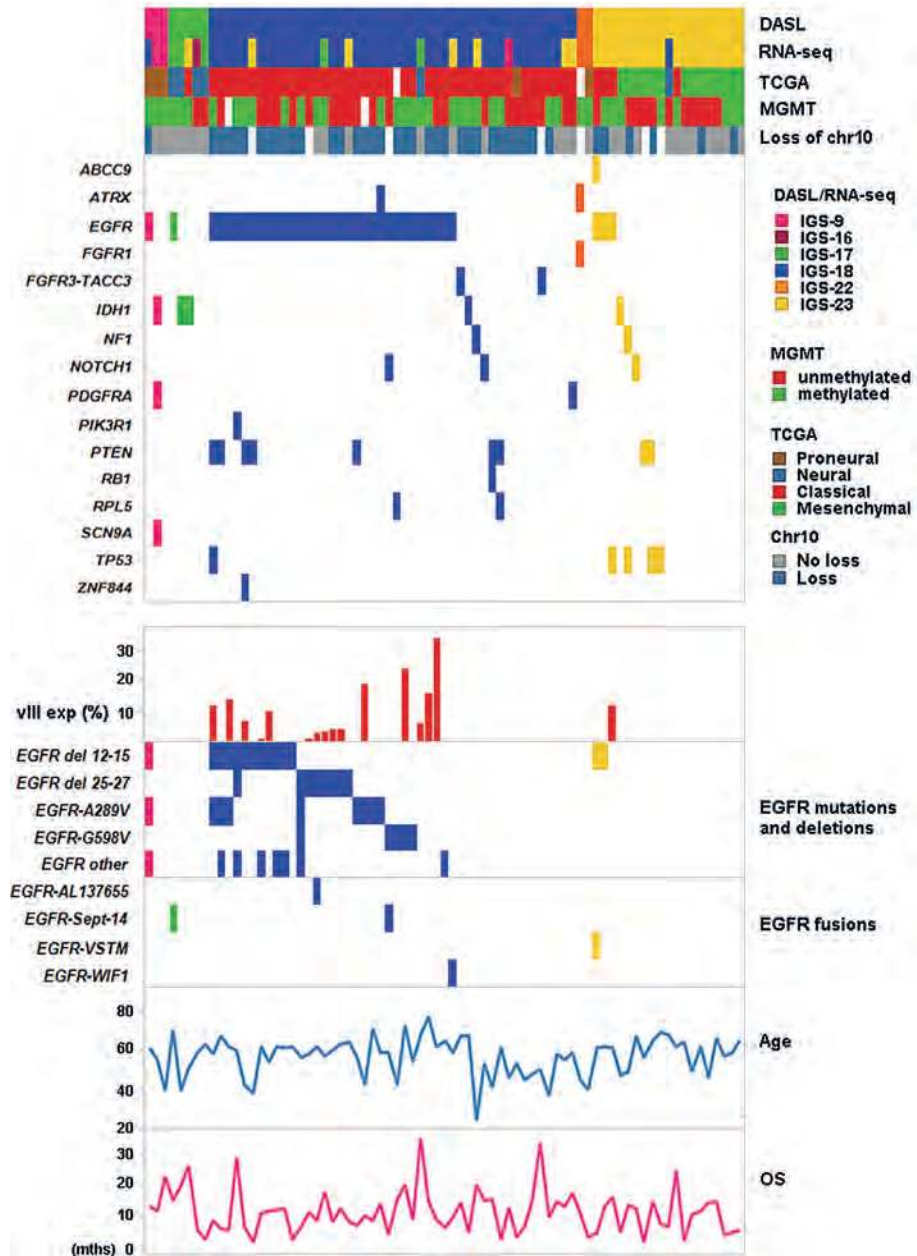
Summary of molecular and clinical parameters of patients with available RNA-seq data. Top rows depict molecular subtypes according to Gravendeel et al(20) (DASL expression and RNA seq) and according to Verhaak et al (21). *MGMT* promoter methylation was reported previously (19). LOH of Chr 10 was extracted from RNA-seq data based on monoallelic expression. Top boxed area depicts genetic changes found by RNA-seq. The specific genetic changes in *EGFR* is depicted in the lower boxed region and includes mutations, intragenic deletions and fusion genes.

All remaining fusion genes were unique events though some fusion partners (*NUP107*, *VOPP1*, *GRB10*, *LANCL2*, *MLLT3* and *VSTM2A*) were identified in two samples. Fusion genes are incorporated, alongside with clinical and other molecular data in figure 3. Fusion genes involving *NUP107* surround the *MDM2* locus, and it is possible they occur secondary to a high copy amplification of this locus (both samples express high levels of *MDM2*). There are four samples with *NUP107* fusion genes in the TCGA dataset, all of which have high copy *MDM2* amplification (34). By analogy, both *PSPH* and *VOPP1* are located close to the *EGFR* locus and, in the TCGA dataset, fusions involving *PSPH* or *VOPP1* are either associated with *EGFR* amplification or are direct fusion partner of *EGFR*.

Analysis of intronic reads can identify the genomic breakpoint of fusion genes

Sequencing of total RNA results in a large proportion of intronic reads (41). This is likely caused by the use of random primers for cDNA synthesis; in random primed cDNA synthesis both the mature and unspliced mRNAs are converted into cDNA. In general, introns are spliced out only after transcription of the entire intron. Therefore, on a population level, the 5' end of an intron will have a higher read-depth than the 3' end (41). This is particularly visible in transcripts with long introns (42), as the half-life of an intron is determined by its length and by the rate of RNA polymerase II transcription, ~3.5-4 kb/hr (43, 44). Of note, we have observed exceptions to this rule, arguing for intra-intronic splicing events (see supplementary figure S11 for some examples). Additional calculations on the rate of transcription and the level of expression is depicted in Supplementary figure S12.

We hypothesized that the presence of the pre-mRNA transcripts can be used to identify intronic genomic breakpoints of fusion genes: where in intact introns there is a relatively stable coverage of pre-mRNA levels, the levels of pre-mRNA may suddenly change at the exact genomic breakpoint of a fusion gene. Indeed, such sudden decreases/increases of pre-mRNA levels are often present in the introns of the fusion genes identified by ChimeraScan. PCR using primers spanning the putative breakpoint confirmed the presence and location of the genomic break (supplementary figure S13).

DISCUSSION

In this study we have performed gene expression profiling and RNA-sequencing on tumor material derived from patients treated within the BELOB trial in order to identify recurrent GBM patients who benefit from combined CCNU and bevacizumab treatment. Our results indicate that patients with a specific molecular subtype of glioma, IGS-18 or 'classical GBMs', may show more benefit from beva/CCNU treatment. In particular, the expression of *FMO4* and *OSBPL3* are correlated with benefit from this combination treatment. It should be noted however that our data analysis is post-hoc and confirmation in

an independent dataset is therefore required. The in-depth analysis of the transcriptome by RNA-seq also highlighted genetic changes (mutations, indels, gene fusions (including identification of the exact genomic breakpoint) and copy number changes (albeit with limited resolution)) within this well-defined cohort of tumors.

Recently, data were reported on two large randomized phase III clinical trials that investigated the role of the addition of bevacizumab to temozolomide chemo- radio-therapy in newly diagnosed GBM patients (10, 11). Unfortunately, the results show that the combination treatment did not result in an increased overall survival of patients. Subsequent translational research however, did identify subgroups of patients that showed benefit from beva + temozolomide treatment (17, 18). For example, Sulman et al. provided evidence, in the RTOG 0825 study, that 'mesenchymal' GBMs performed particularly poor on the combination treatment (18). Although these data were generated on newly diagnosed GBMs, our data on recurrent GBMs largely corroborate these findings: no trend towards treatment benefit was identified in 'non-classical' GBMs (most of which were mesenchymal tumors, though numbers are too small to draw firm conclusions). Recently, Phillips et al, in the AvaGlio study, demonstrated that G-CIMP-'proneural' GBMs benefitted from beva + temozolomide (17). Our dataset however, contains very few 'proneural' GBMs, which may be related to the observation that these tumors have the worst prognosis of all GBM subtypes and may simply not qualify for second line treatment (34). Based on data provided in current manuscript, it would be interesting to see whether in those studies tumors assigned to IGS-18 also show benefit from the addition of bevacizumab to chemotherapy.

Of note, in a recent retrospective analysis, patients with tumors assigned to IGS-18 or classical GBMs had worse outcome compared to those assigned to IGS-22/23 when treatment with a combination of beva and irinotecan (45).

SAM analysis identified two genes that were associated with survival specifically in the beva/CCNU combination arm. Flavin-containing monooxygenase 4 (*FMO4*) is a protein that catalyzes the NADPH-dependent oxygenation of drugs, pesticides and xenobiotics (46). *FMO4* is part of a protein family (*FMO1-5*) that, after cytochrome P450, is the second largest protein family involved in drug metabolism. *FMO* oxidation increases the polarity of (nitrogen-containing) substrates, which aids excretion and detoxification, but may also catalyze drugs into more active forms. Since *FMO4* expression is involved in drug metabolism and is associated with survival in the beva+CCNU arm, it is possible that *FMO4* expression may render tumors more sensitive to CCNU treatment (when in combination with beva).

OSBPL3 is one of the twelve members of the oxysterol binding protein (*OSBP*) related protein (ORP) family that play a role in lipid metabolism, vesicle trafficking and cell signaling (47). *OSBPL3* binds to the phosphoinositides PIP2 and PIP3 and can interact with the small GTPase R-RAS (48, 49). *OSBPL3* was shown to play a role in the regulation

of the actin cytoskeleton and cellular adhesion (49). Since a set of tumors respond to bevacizumab by increased migration/invasion and vessel co-option (50, 51) and *VEGF* directly inhibits glioma invasion (52), it is possible that increased *OSBPL3* expression increases cellular adhesion and so reduces the migratory capacity of tumor cells. Perhaps a combination of altered migration and drug metabolism renders tumors in the beva+CCNU arm more sensitive to this treatment.

One of the peculiarities of our dataset is that it contained an overrepresentation of tumors assigned to IGS-18 or 'classical' GBMs where in general, GBMs are roughly equally distributed across the various molecular subtypes (20, 21, 53, 54). We are confident however of the molecular classification as described in current manuscript: there was a high correlation in tumor assignment between snap frozen and FFPE samples and between different methods (DASL and RNA-seq) and genetic changes in the *EGFR* locus (and 10q LOH) are a hallmark of IGS-18 or 'classical' GBMs and most tumors assigned to IGS-18 or 'classical' GBMs indeed harbor genetic changes in this gene. This segregation of genetic changes was also observed for *IDH1*. The higher frequency of tumors assigned to IGS-18 or 'classical' GBMs may reflect a sample bias of current study. However, in a study analyzing *EGFR* amplification in matched primary and recurrent tumors, we also find a high frequency of *EGFR* amplification at initial diagnosis (~70%, van den Bent et al., accepted for publication). It is therefore possible that (*EGFR*-amplified-) tumors assigned to IGS-18 are more prone to receiving re- treatment at tumor recurrence. For example, G-CIMP- proneural GBMs are selected against as they have poorest prognosis of all GBM subtypes (34).

A limitation of our study is the use of primary tumor tissue for classification, whereas the recurrent tumor was treated. In 2006, a study identifying three molecular subtypes of glioma included analysis of 26 (unselected) matched primary and recurrent tumor pairs (54). This study showed that at progression, gliomas shift from a proneural towards a mesenchymal subtype. However, it also demonstrated that 18/26 (70%) tumors remain in the same subtype (a similar retention of molecular subtype is observed when these tumors to molecular subtypes as defined by Gravendeel et al supplementary table 7). More specifically, within the eight tumors assigned to IGS-18 at initial diagnosis in this study, six remained in IGS-18 at tumor recurrence. A study performed by our group included seven repeat samples and both tumors assigned to IGS-18 at initial diagnosis remained in IGS-18 at tumor recurrence (20). Moreover, we have recently performed analysis of the *EGFR* locus in 55 uniformly treated primary recurrent tumor pairs (van den Bent et al., accepted for publication). *EGFR* amplification can be used as surrogate marker for IGS-18 tumors: retention of *EGFR* amplification status at tumor recurrence therefore is suggestive for retention of the intrinsic glioma subtype. The data from this study indicate that the *EGFR* status of the tumor remains similar at the point of recurrence in 47/55 matched tumor pairs. These studies suggest that in many tumors, the

molecular subtype largely remains identical at tumor progression (even though they may shift towards a more mesenchymal phenotype).

A second limitation of this study is that material was available for only a subset (114/152) of BELOB trial samples. Although we did not identify differences in patient characteristics of tumor samples included vs not included (table 1), the use of only a subset of patients may have introduced a sample bias.

Recurrent fusion genes identified in our dataset (*FGFR3-TACC3* and *EGFR-SEPT-14*) were identified by others with similar frequencies (34, 38, 39, 55). A recent analysis identified the genomic landscape of fusion genes in 13 tumor types, including GBMs (40). Two identical fusion genes (*LANCL2-SEPT14* and *ZZEF1-ANKFY1*) can be detected when overlaying the identified fusions in that study with those reported here. Based on the amplification status of *MDM2* and *EGFR* and the fact that they are present as double minutes when amplified, we hypothesize fusions involving *NUP017*, *PSPH* or *VOPP1* occur secondary to high copy gene amplification. If so, this implies that GBMs harbor few functional fusion genes.

Apart from the recurrent fusions, many of the 5′ and 3′ fusion partners were also identified by others (e.g. *GRB10*, *LANCL2*, *MLLT3*, *ASCC3*, *VOPP1*, *TERT*, *VSTM2A*, *PSPH*, *NUP107* and *LEMD3*), some of which are found at significant frequency (*GRB10*, *NUP107 VOPP1*, *TERT*, *PSPH*) (38-40, 55). One of the potentially functional fusions partner is *TERT*: *TERT* fusions can represent a method to increase telomerase activity, as alternative to the frequent *TERT* promoter mutations in GBMs (56). A total of 7 samples (of which 2 GBMs) were recently identified to contain *TERT* fusion genes. In all cases identified, *TERT* acted as the 3′ fusion partner, and all contained the telomerase transcriptase domain (transcripts from exon 2 or 3 onwards) which argues against random occurrence the fusion.

Many of the reads identified by RNA-sequencing of FFPE isolated material mapped to intronic regions and represent pre-mRNA species. Similar to previously reported, our data shows that the 5′ end of an intron has a higher read-depth than the 3′ end, at least in large introns (41). The 5′-3′ decline in intronic reads is linear and is explained by a mechanism where introns are first entirely transcribed before being spliced out (41). However, in some genes have introns that are apparently spliced out before transcription of the entire intron (i.e. intra-intronic splicing). Apart from a basic insight into the mechanism of RNA maturation, we here we show that intronic reads can be used to map genomic breakpoints of fusion genes.

In summary, our results show that tumors assigned to IGS-18 or 'classical' GBMs showed a significant benefit in PFS and a trend towards benefit in OS from beva+CCNU treatment; other subtypes did not show such benefit. Expression of *FMO4* and *OSBPL3*, genes involved in drug metabolism and cell signalling, regulation of the actin cytoskeleton and cellular adhesion were specifically associated with treatment response. When validated in an independent dataset, our data will allow selection of recurrent GBM patients that benefit from beva+CCNU treatment.
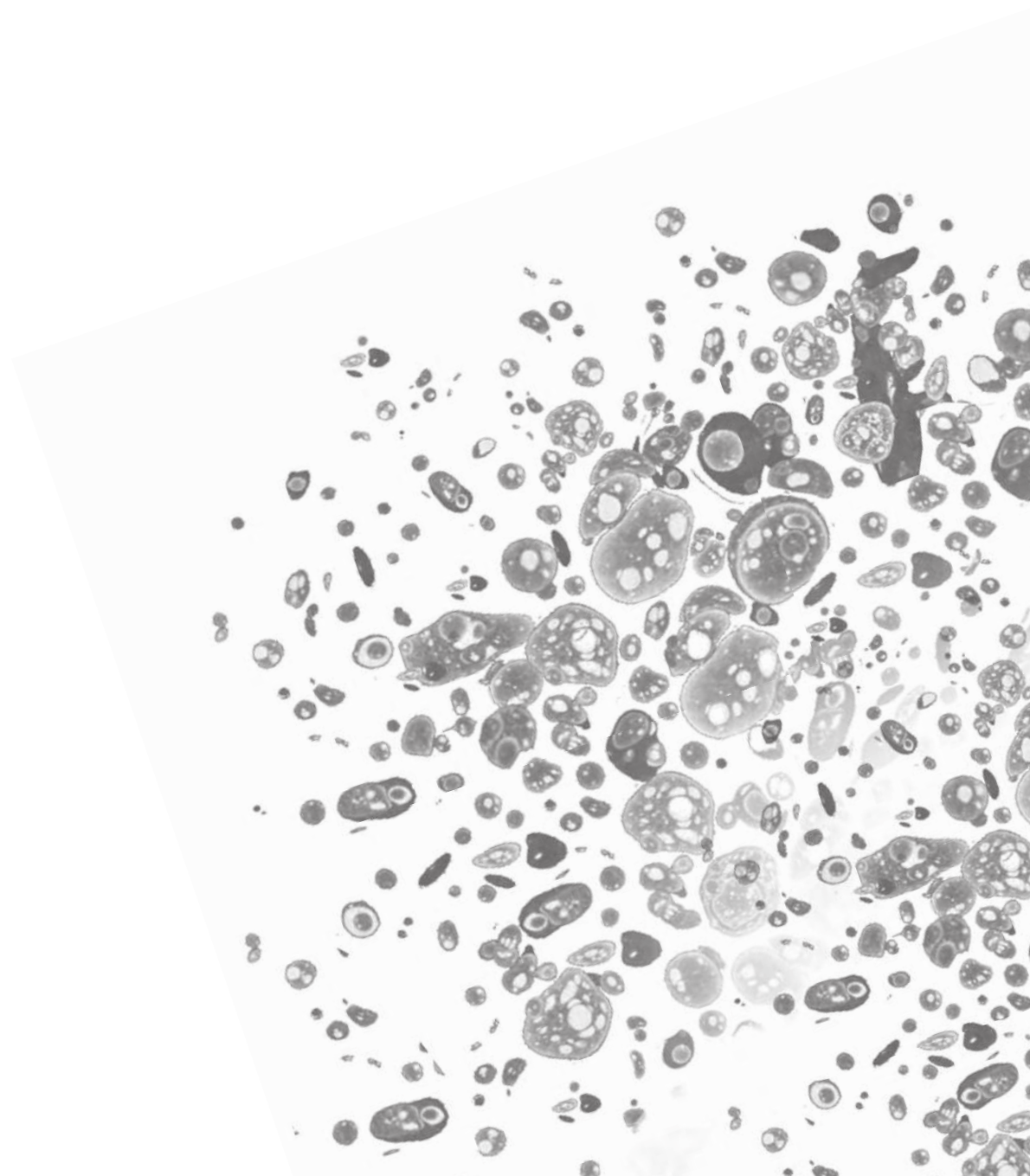
REFERENCES

1. Louis DN, Ohgaki H, Wiestler OD, Cavenee WK. WHO Classification of Tumours of the Central Nervous System, 4th edition. Lyon: World Health Organization, 2007.
2. Stupp R, Mason WP, van den Bent MJ, Weller M, Fisher B, Taphoorn MJ, et al. Radiotherapy plus concomitant and adjuvant temozolomide for glioblastoma. N Engl J Med 2005;352:987-96.
3. Weller M, Cloughesy T, Perry JR, Wick W. Standards of care for treatment of recurrent glioblastoma--are we there yet? Neuro Oncol 2013;15:4-27.
4. Gorlia T, Stupp R, Brandes AA, Rampling RR, Fumoleau P, Dittrich C, et al. New prognostic factors and calculators for outcome prediction in patients with recurrent glioblastoma: a pooled analysis of EORTC Brain Tumour Group phase I and II clinical trials. Eur J Cancer 2012;48:1176-84.
5. Fischer I, Gagner JP, Law M, Newcomb EW, Zagzag D. Angiogenesis in gliomas: biology and molecular pathophysiology. Brain Pathol 2005;15:297-310.
6. Friedman HS, Prados MD, Wen PY, Mikkelsen T, Schiff D, Abrey LE, et al. Bevacizumab alone and in combination with irinotecan in recurrent glioblastoma. J Clin Oncol 2009;27:4733-40.
7. Vredenburgh JJ, Desjardins A, Herndon JE, 2nd, Dowell JM, Reardon DA, Quinn JA, et al. Phase II trial of bevacizumab and irinotecan in recurrent malignant glioma. Clin Cancer Res 2007;13:1253-9.
8. Vredenburgh JJ, Desjardins A, Herndon JE, 2nd, Marcello J, Reardon DA, Quinn JA, et al. Bevacizumab plus irinotecan in recurrent glioblastoma multiforme. J Clin Oncol 2007;25:4722-9.
9. Khasraw M, Ameratunga MS, Grant R, Wheeler H, Pavlakis N. Antiangiogenic therapy for high-grade glioma. Cochrane Database Syst Rev 2014;9:CD008218.
10. Chinot OL, Wick W, Mason W, Henriksson R, Saran F, Nishikawa R, et al. Bevacizumab plus radiotherapy-temozolomide for newly diagnosed glioblastoma. N Engl J Med 2014;370:709-22.
11. Gilbert MR, Dignam JJ, Armstrong TS, Wefel JS, Blumenthal DT, Vogelbaum MA, et al. A randomized trial of bevacizumab for newly diagnosed glioblastoma. N Engl J Med 2014;370:699-708.
12. Batchelor TT, Mulholland P, Neyns B, Nabors LB, Campone M, Wick A, et al. Phase III randomized trial comparing the efficacy of cediranib as monotherapy, and in combination with lomustine, versus lomustine alone in patients with recurrent glioblastoma. J Clin Oncol 2013;31:3212-8.
13. Hegi ME, Diserens AC, Gorlia T, Hamou MF, de Tribolet N, Weller M, et al. *MGMT* gene silencing and benefit from temozolomide in glioblastoma. N Engl J Med 2005;352:997-1003.
14. van den Bent MJ, Brandes AA, Taphoorn MJ, Kros JM, Kouwenhoven MC, Delattre JY, et al. Adjuvant procarbazine, lomustine, and vincristine chemotherapy in newly diagnosed anaplastic oligodendroglioma: long-term follow-up of EORTC brain tumor group study 26951. J Clin Oncol 2013;31:344-50.
15. Erdem-Eraslan L, Gravendeel LA, de Rooi J, Eilers PH, Idbaih A, Spliet WG, et al. Intrinsic molecular subtypes of glioma are prognostic and predict benefit from adjuvant procarbazine, lomustine, and vincristine chemotherapy in combination with other prognostic factors in anaplastic oligodendroglial brain tumors: a report from EORTC study 26951. J Clin Oncol 2013;31:328-36.
16. Cairncross JG, Wang M, Jenkins RB, Shaw EG, Giannini C, Brachman DG, et al. Benefit from procarbazine, lomustine, and vincristine in oligodendroglial tumors is associated with mutation of IDH. J Clin Oncol 2014;32:783-90.
17. Phillips H, Sandmann T, Li C, Cloughesy TF, Chinot OL, Wick W, et al. Correlation of molecular subtypes with survival in AVAglio (bevacizumab [Bv] and radiotherapy [RT] and temozolomide [T] for newly diagnosed glioblastoma [GB]). J Clin Oncol 2014;32: 5S:suppl abstract 2001.

18. Sulman EP, Won M, Blumenthal DT, Vogelbaum MA, Colman H, Jenkins RB, et al. Molecular predictors of outcome and response to bevacizumab (BEV) based on analysis of RTOG 0825, a phase III trial comparing chemoradiation (CRT) with and without BEV in patients with newly diagnosed glioblastoma (GBM). J Clin Oncol 2013;31:suppl; abstr LBA2010.

19. Taal W, Oosterkamp HM, Walenkamp AM, Dubbink HJ, Beerepoot LV, Hanse MC, et al. Single-agent bevacizumab or lomustine versus a combination of bevacizumab plus lomustine in patients with recurrent glioblastoma (BELOB trial): a randomised controlled phase 2 trial. Lancet Oncol 2014;15:943-53.

20. Gravendeel LA, Kouwenhoven MC, Gevaert O, de Rooi JJ, Stubbs AP, Duijm JE, et al. Intrinsic gene expression profiles of gliomas are a better predictor of survival than histology. Cancer Res 2009;69:9065-72.

21. Verhaak RG, Hoadley KA, Purdom E, Wang V, Qi Y, Wilkerson MD, et al. Integrated genomic analysis identifies clinically relevant subtypes of glioblastoma characterized by abnormalities in PDGFRA, *IDH1*, *EGFR*, and NF1. Cancer Cell 2010;17:98-110.

22. Gravendeel LA, de Rooi JJ, Eilers PH, van den Bent MJ, Sillevis Smitt PA, French PJ. Gene expression profiles of gliomas in formalin-fixed paraffin-embedded material. Br J Cancer 2012;106:538-45.

23. Kapp AV, Tibshirani R. Are clusters found in one dataset present in another dataset? Biostatistics 2007;8:9-31.

24. Liao Y, Smyth GK, Shi W. featureCounts: an efficient general purpose program for assigning sequence reads to genomic features. Bioinformatics 2014;30:923-30.

25. Trapnell C, Pachter L, Salzberg SL. TopHat: discovering splice junctions with RNA-Seq. Bioinformatics 2009;25:1105-11.

26. Koboldt DC, Zhang Q, Larson DE, Shen D, McLellan MD, Lin L, et al. VarScan 2: somatic mutation and copy number alteration discovery in cancer by exome sequencing. Genome Res 2012;22:568-76.

27. Koboldt DC, Chen K, Wylie T, Larson DE, McLellan MD, Mardis ER, et al. VarScan: variant detection in massively parallel sequencing of individual and pooled samples. Bioinformatics 2009;25:2283-5.

28. Carrara M, Beccuti M, Lazzarato F, Cavallo F, Cordero F, Donatelli S, et al. State-of-the-art fusion-finder algorithms sensitivity and specificity. Biomed Res Int 2013;2013:340620.

29. Wang K, Li M, Hakonarson H. ANNOVAR: functional annotation of genetic variants from high-throughput sequencing data. Nucleic Acids Res 2010;38:e164.

30. Genomes Project C, Abecasis GR, Altshuler D, Auton A, Brooks LD, Durbin RM, et al. A map of human genome variation from population-scale sequencing. Nature 2010;467:1061-73.

31. Forbes SA, Bindal N, Bamford S, Cole C, Kok CY, Beare D, et al. COSMIC: mining complete cancer genomes in the Catalogue of Somatic Mutations in Cancer. Nucleic Acids Res 2011;39:D945-50.

32. Iyer MK, Chinnaiyan AM, Maher CA. ChimeraScan: a tool for identifying chimeric transcription in sequencing data. Bioinformatics 2011;27:2903-4.

33. van den Bent MJ, Gravendeel LA, Gorlia T, Kros JM, Lapre L, Wesseling P, et al. A hypermethylated phenotype is a better predictor of survival than *MGMT* methylation in anaplastic oligodendroglial brain tumors: a report from EORTC study 26951. Clin Cancer Res 2011;17:7148-55.

34. Brennan CW, Verhaak RG, McKenna A, Campos B, Noushmehr H, Salama SR, et al. The somatic genomic landscape of glioblastoma. Cell 2013;155:462-77.

35. Parsons DW, Jones S, Zhang X, Lin JC, Leary RJ, Angenendt P, et al. An integrated genomic analysis of human glioblastoma multiforme. Science 2008;321:1807-12.

36. Zhang K, Li JB, Gao Y, Egli D, Xie B, Deng J, et al. Digital RNA allelotyping reveals tissue-specific and allele-specific gene expression in human. Nat Methods 2009;6:613-8.

37. Bralten LB, Kloosterhof NK, Gravendeel LA, Sacchetti A, Duijm EJ, Kros JM, et al. Integrated genomic profiling identifies candidate genes implicated in glioma-genesis and a novel LEO1-SLC12A1 fusion gene. Genes Chromosomes Cancer 2010;49:509-17.

38. Singh D, Chan JM, Zoppoli P, Niola F, Sullivan R, Castano A, et al. Transforming fusions of FGFR and TACC genes in human glioblastoma. Science 2012;337:1231-5.

39. Frattini V, Trifonov V, Chan JM, Castano A, Lia M, Abate F, et al. The integrated landscape of driver genomic alterations in glioblastoma. Nat Genet 2013;45:1141-9.

40. Yoshihara K, Wang Q, Torres-Garcia W, Zheng S, Vegesna R, Kim H, et al. The landscape and therapeutic relevance of cancer-associated transcript fusions. Oncogene 2014.

41. Ameur A, Zaghlool A, Halvardson J, Wetterbom A, Gyllensten U, Cavelier L, et al. Total RNA sequencing reveals nascent transcription and widespread co-transcriptional splicing in the human brain. Nat Struct Mol Biol 2011;18:1435-40.

42. O'Connor V, Genin A, Davis S, Karishma KK, Doyere V, De Zeeuw CI, et al. Differential amplification of intron-containing transcripts reveals long term potentiation-associated up-regulation of specific Pde10A phosphodiesterase splice variants. J Biol Chem 2004;279:15841-9.

43. Singh J, Padgett RA. Rates of in situ transcription and splicing in large human genes. Nat Struct Mol Biol 2009;16:1128-33.

44. Brody Y, Neufeld N, Bieberstein N, Causse SZ, Bohnlein EM, Neugebauer KM, et al. The in vivo kinetics of RNA polymerase II elongation during co-transcriptional splicing. PLoS Biol 2011;9:e1000573.

45. Laffaire J, Di Stefano AL, Chinot O, Idbaih A, Gallego Perez-Larraya J, Marie Y, et al. An ANOCEF genomic and transcriptomic microarray study of the response to irinotecan and bevacizumab in recurrent glioblastomas. Biomed Res Int 2014;2014:282815.

46. Krueger SK, Williams DE. Mammalian flavin-containing monooxygenases: structure/function, genetic polymorphisms and role in drug metabolism. Pharmacol Ther 2005;106:357-87.

47. Lehto M, Olkkonen VM. The OSBP-related proteins: a novel protein family involved in vesicle transport, cellular lipid metabolism, and cell signalling. Biochim Biophys Acta 2003;1631:1-11.

48. Goldfinger LE, Ptak C, Jeffery ED, Shabanowitz J, Han J, Haling JR, et al. An experimentally derived database of candidate Ras-interacting proteins. J Proteome Res 2007;6:1806-11.

49. Lehto M, Mayranpaa MI, Pellinen T, Ihalmo P, Lehtonen S, Kovanen PT, et al. The R-Ras interaction partner ORP3 regulates cell adhesion. J Cell Sci 2008;121:695-705.

50. de Groot JF, Fuller G, Kumar AJ, Piao Y, Eterovic K, Ji Y, et al. Tumor invasion after treatment of glioblastoma with bevacizumab: radiographic and pathologic correlation in humans and mice. Neuro Oncol 2010;12:233-42.

51. Rubenstein JL, Kim J, Ozawa T, Zhang M, Westphal M, Deen DF, et al. Anti-VEGF antibody treatment of glioblastoma prolongs survival but results in increased vascular cooption. Neoplasia 2000;2:306-14.

52. Lu KV, Chang JP, Parachoniak CA, Pandika MM, Aghi MK, Meyronet D, et al. VEGF inhibits tumor cell invasion and mesenchymal transition through a MET/*VEGFR*2 complex. Cancer Cell 2012;22:21-35.

53. Li A, Walling J, Ahn S, Kotliarov Y, Su Q, Quezado M, et al. Unsupervised analysis of transcriptomic profiles reveals six glioma subtypes. Cancer Res 2009;69:2091-9.

54. Phillips HS, Kharbanda S, Chen R, Forrest WF, Soriano RH, Wu TD, et al. Molecular subclasses of high-grade glioma predict prognosis, delineate a pattern of disease progression, and resemble stages in neurogenesis. Cancer Cell 2006;9:157-73.

55. Shah N, Lankerovich M, Lee H, Yoon JG, Schroeder B, Foltz G. Exploration of the gene fusion land-scape of glioblastoma using transcriptome sequencing and copy number data. BMC Genomics 2013;14:818.

56. Killela PJ, Reitman ZJ, Jiao Y, Bettegowda C, Agrawal N, Diaz LA, Jr., et al. TERT promoter mutations occur frequently in gliomas and a subset of tumors derived from cells with low rates of self-renewal. Proc Natl Acad Sci U S A 2013;110:6021-6.

CHAPTER 4

Mutation specific functions of *EGFR* result in a mutation-specific downstream pathway activation

Lale Erdem-Eraslan[1], Ya Gao[1],
Nanne K. Kloosterhof, Yassar Atlasi,
Jeroen Demmers, Andrea Sacchetti,
Johan M. Kros, Peter Sillevis Smitt, Joachim Aerts,
Pim J. French

[1] These authors contributed equally to this manuscript.

ABSTRACT

Background

Epidermal growth factor receptor (*EGFR*) is frequently mutated in various types of can-cer. Although all oncogenic mutations are considered activating, different tumour types have different mutation spectra. It is possible that functional differences underlie this tumour-type specific mutation spectrum.

Methods

We have determined whether specific mutations in *EGFR* (*EGFR*, *EGFR*vIII and *EGFR*-L858R) have differences in binding partners, differences in downstream pathway activation (gene expression and phosphoproteins), and have functional consequences on cellular growth and migration.

Results

Using biotin pulldown and subsequent mass spectrometry we were able to detect mutation specific binding partners for *EGFR*. Differential binding was confirmed using a proximity ligation assay and/or Western Blot for the dedicator of cytokinesis 4 (*DOCK4*), UDP-glucose glycoprotein glucosyltransferase 1 (*UGGT1*), MYC binding protein 2 (*MYCBP2*) and Smoothelin (*SMTN*). We also demonstrate that each mutation induces the expression of a specific set of genes, and that each mutation is associated with specific phosphorylation patterns. Finally, we demonstrate using stably expressing cell lines that *EGFR*vIII and *EGFR*L858R display reduced growth and migration compared to *EGFR* wildtype expressing cells.

Conclusion

Our results indicate that there are distinct functional differences between different *EGFR* mutations. The functional differences between different mutations argue for the development of mutation specific targeted therapies.

INTRODUCTION

The epidermal growth factor receptor (*EGFR*) is a receptor tyrosine kinase that is a member of the *ERBB* protein family and is localised on the cell membrane. The receptor is activated by members of the epidermal growth factor (EGF) family (a.o. EGF, amphiregulin, TGF-a, HB-EGF and epiregulin) and binding of one such ligand results in receptor dimerisation which induces receptor phosphorylation, recruitment of adaptor proteins and subsequent activation of signal transduction cascades (1,2).

Somatic mutations in the *EGFR* gene are found in several types of cancer and the mutation spectrum includes gene amplifications, gene-fusions, deletions in the extracellular domain (e.g. *EGFR*vIII; a deletion of exons 2–7), deletions in the intracellular domain (e.g. *EGFR*vV; a deletion of exons 25–28) and mutations affecting the tyrosine kinase domain (mainly exon 19 and codon L858) (3–5). These mutations result in a constitutively activated isoform of the protein and contribute to oncogenic transformation (5–8).

Although *EGFR* mutations are activating, there are marked differences in the spectrum of mutations between tumour types. For example, the c.2573T>G missense mutation, resulting in the L858R substitution, is found in ~10–15% of all pulmonary adenocarcinomas (4). This mutation is the most frequent of all mutations in *EGFR* but has thus far never been identified in glioblastomas (GBMs) (3). The most common mutations in GBMs affect the extracellular domain of *EGFR*, including *EGFR*vIII (~30% of all GBMs) and the A289V and V598V missense mutations (3). These extracellular domain mutations are not found in pulmonary adenocarcinomas (4). One of the explanations for these tumour-type specific mutations is that each mutation invokes a unique signal transduction cascade. Indeed, *EGFR*vIII and *EGFR*wt have differential activation of the *JNK*, *STAT* and *MAPK* signalling pathways and induce the expression of a unique set of genes (9–13). Because different tumour types may be dependent on the unique pathways that are activated by different *EGFR* mutations, studying these functional differences between mutations may identify novel, tumour type specific treatment targets. Here, we have further evaluated differential activation of signal transduction pathways by *EGFR*-wt, *EGFR*-L858R and *EGFR*vIII.

METHODS

*EGFR*vIII and *EGFR*-L858R cDNAs were obtained from Addgene (Cambridge, MA), *EGFR* wildtype was a gift from Ton van Agthoven and cloned into pcDNA3.1/CT-GFP- TOPO (Invitrogen, Bleiswijk, the Netherlands). A biotin tag and eGFP were inserted C- terminal to the transmembrane domain of *EGFR* to retain the integrity of the C-terminal (intracellular) domain of *EGFR*. To demonstrate functionality, we transfected *EGFR*bio- GFP into ZR-75-1 cells. Normally, ZR-75-1 cells do not proliferate in the presence of tamoxifen (43).

However, ZR-75-1 cells expressing *EGFR*-bioGFP, cultured in the presence of tamoxifen, responded to EGF stimulation by an increase in cell proliferation, demonstrating the construct remained functional (not shown). Stably transfected HOG (human oligodendroglioma cells (44)) cell lines were created by transfection, geneticin selection and FACS sorting. Stable cell lines were derived from bulk culture and not form a single sorted cell followed by clonal propagation.

Migration and proliferation assays were performed using an Incucyte (Essen Bioscience, Ann Arbor, MI). For proliferation experiments, 50,000 cells/well were plated in a 24-well Greiner plate (Greiner Bio-One, Alphen a/d Rijn, the Netherlands). Growth curves were constructed using the Confluence v1.5 metric of the Incucyte software. For migration experiments, cells were grown to confluence in a 24-well Essen ImageLockplate after which a cell-free zone (scratch) was created using a WoundMaker. Wells were then cultured in serum-free media.

Constructs containing $EGFR^{wt-BG}$, $EGFR^{vIII-BG}$ and $EGFR^{L858R-BG}$ were transfected into HEK cell lines using Polyethylenimine 'Max' (Polysciences, Eppelheim, Germany). The $EGFR^{wt-BG}$, $EGFR^{vIII-BG}$ and $EGFR^{L858R-BG}$ proteins were then isolated using Dynabeads (Life Technologies, Carlsbad, CA, United States of America (USA)) as described previously (39). Purified proteins were washed and loaded on a SDS page gel. Nanoflow LC-MS/MS analysis was performed essentially as described by van den Berg et al. (45). Candidate binding proteins that were present in a GFP control pulldown or identified in >10% of CRAPome experiments were omitted from the analysis (14). We focused on candidate binding proteins that were identified with MASCOT scores >300. Western blots were performed as described (39). Antibodies used were *DOCK4* (1:100), *UGGT1* (1:100), *DDX21* (1:500) all from Sigma–Aldrich (Zwijndrecht, the Netherlands), *EGFR* (1:1000, Cell Signaling, Boston, MA) and GFP (1:5000, Abcam, Cambridge, United Kingdom (UK)).

Cells (HOG, U87MG, HEK) were cultured on glass slides for immunocytochemistry. Glioma samples were obtained from the Erasmus MC glioma tissue bank. Use of patient material for current study was approved by the Institutional Review Board. Antibodies used for immunocytochemistry and/or proximity ligation assays were *EGFR* (1:200, DAKO, Heverlee, Belgium) and *DOCK4* (1:100), *MYCBP2* (1:200) and *SMTN1* (1:100) all from Abcam. Proximity ligation assays were performed using a Duolink (Sigma–Aldrich) kit according to the manufacturer's instructions.

HEK cells were transiently transfected with *EGFR*bioGFP, $EGFR^{L858R}$-bioGFP and $EGFR^{vIII}$-bioGFP or BIO-eGFP constructs. Twenty hours after transfection, cells were FACS sorted to select for eGFP expressing cells. Cells were then snap frozen in liquid nitrogen and stored at -80°C. RNA extraction was performed using TriZol (Invitrogen) and checked for RNA quality on a Bioanalyzer (Agilent, Amstelveen, the Netherlands). Gene expression was performed using HU133 plus2 arrays (Affymetrix, High Wycombe, UK) run by AROS

Applied Biotechnology (Aarhus, Denmark). All experiments were performed in triplicate with each replicate experiment performed on separate days.

For reversed phase protein array (RPPA) analysis, stably transfected HOG cells were plated in six well plates and incubated in serum supplemented medium, or serum depleted medium (24 h depletion) ± 200 ng EGF for 5 min. RPPA arrays were performed by the MD Anderson RPPA core facility. Luciferase activity was measured by Dual–Luciferase Reporter Assay System (Promega). Pathway analysis was performed using Ingenuity (Redwood City, CA) and David (46).

RESULTS

We first generated constructs of wildtype *EGFR* and of two common mutations, *EGFR*vIII and L858R, and inserted a biotinylation tag and eGFP in-frame and Cterminal to the transmembrane domain. Constructs are referred to as *EGFR*^wt-BG, *EGFR*^vIII-BG and *EGFR*^L858R-BG respectively. Mass spectrometry following pulldown of biotinylated constructs identified over 3000 candidate binding partners for at least one of these constructs. When filtering for duplicate hits, and removal of proteins identified by a bio-eGFP control pulldown or present in >10% of crapome pulldown experiments (14), our list of candidate *EGFR* binding proteins included 87 unique proteins (Supplementary Table 1). Almost half (37/87) of these binding partners are known interactors of *EGFR* and include *CBL*, *PIK3CA*, *PIK3R3*, *SHC1* and *SOS1* (15–17).

Ingenuity pathway analysis indicated that the candidate *EGFR* associated proteins are involved in EGF signaling and Clathrin mediated endocytosis signalling. Candidate *EGFR* interacting proteins are enriched for proteins that are somatically mutated in GBMs. For example, 7/87 (8.0%) genes are mutated at a population frequency >1.5% (i.e. mutations found in at least 5/290 tumours) in the TCGA, a 3–4- fold enrichment compared to all genes mutated at this frequency in GBMs (485/~20.000 genes, 2.4%, P = 0.007, Fishers' exact test).

Of the 87 candidate binding proteins, 22 showed selective association to one of the *EGFR* constructs (Table 1). Selective association was defined as a relative difference in mascot scores >3, and an absolute difference in mascot scores >500 between any of the three constructs. The strongest candidate proteins included *DOCK4* (dedicator of cytokinesis 4) *UGGT1* (UDPglucose glycoprotein glucosyltransferase 1), *MYCBP2* (MYC binding protein 2, E3 ubiquitin protein ligase) and *SMTN* (Smoothelin).

Western blots on independent biotin pulldowns confirmed that *DOCK4* binds preferentially to *EGFR*^vIII-BG and *EGFR*^wt-BG but not to *EGFR*^L858R-BG (Figure 1b, Western blot experiments in two independent experiments). The association was further confirmed using a proximity ligation assay (PLA, Figure 1c). *DOCK4* also associates with *EGFR* also

under native conditions as demonstrated by a co- immunoprecipitation using anti-*EGFR* antibodies in non-transfected HEK cells (Figure 1d).

Furthermore, PLA confirmed that *DOCK4* and *EGFR* are also colocalised in *EGFR* amplified GBMs (Figure 1e). *DOCK4* remains associated with *EGFR*-wt in cells that were serum starved overnight followed by EGF stimulation (Supplementary Figure 1). These data demonstrate that *DOCK4* associates with *EGFR*$^{\text{wt-BG}}$ and *EGFR*$^{\text{vIII-BG}}$ and not (or to a lesser extent) with *EGFR*$^{\text{L858R-BG}}$.

Because *DOCK4* has been implicated in wnt pathway activation (18) we screened for differential activation of this pathway activation by the different *EGFR* constructs. However, both under basal and under wnt activated conditions, no differences in wnt pathway activation were identified (n = 3 independent experiments, data not shown).

Mass spectrometry also highlighted that *UGGT1* and *MYCBP2* preferentially associate with *EGFR*$^{\text{vIIIBG}}$ and that *SMTN* preferentially associates with *EGFR*$^{\text{L858R-BG}}$. PLA assays confirmed the association for all three proteins (Figure 2), Western blot (WB) further confirmed the associa-

Table 1. Proteins showing selective binding to one or more specific Epidermal growth factor receptor (*EGFR*) mutations.

| symbol	*EGFR* wt	*EGFR* V111	*EGFR*-p.L858R
AP1B1		961	
CRKL	561	740	229
DNM2	462	798	211
DOCK4	2725	2136	536
EXOC7	533	213	
IFI16	772	1079	
IPO5	1403	411	217
LAD1	106	669	1056
LMO7		340	1362
MYCBP2		1606	
MYO1E		156	503
NGLY1	353	1310	887
PIK3CA	147	902	86
PIK3CB	474	828	72
RTCB		558	341
SEL1L		604	174
SMTN			546
SPECC1L		69	909
SVIL		160	741
TNPO2	410	515	
UBE3C	157	828	280
UGGT1		1573	

Figure 1.
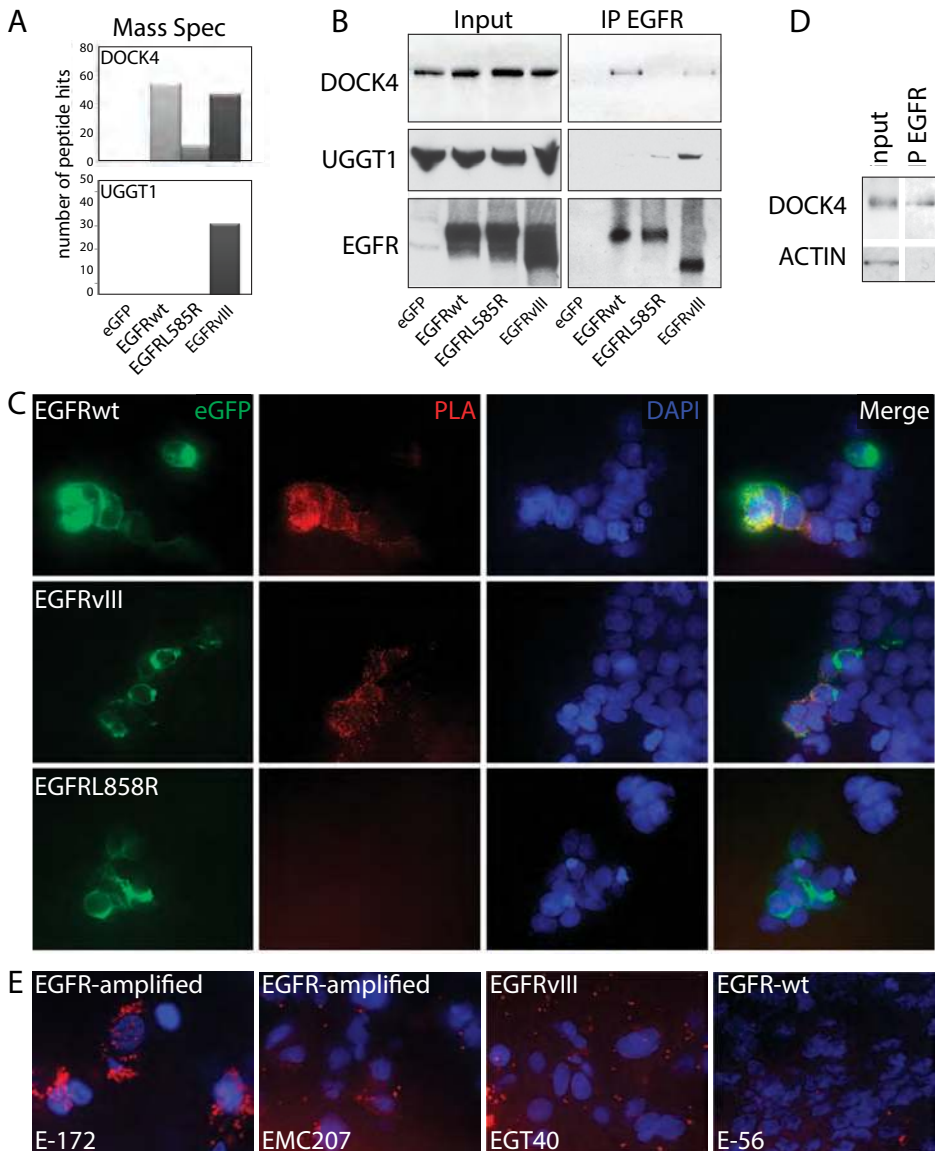
*EGFR*wt-BG, *EGFR*vIII-BG or *EGFR*L858R-BG associate with specific proteins. (A) Mass spectrometry results for *DOCK4* and *UGGT1* showing differential binding to *EGFR* mutations. (B) Confirmation of the mass spectrometry results by Western Blot on an independent pulldown. (C) A proximity ligation assay confirms that *DOCK4* colocalises with *EGFR*wt-BG and *EGFR*vIII-BG but not with *EGFR*L858R-BG or Bio-GFP control (not shown). All images taken at 63x magnification. (D) Native *EGFR* also associates with *DOCK4* as determined by immunoprecipitation of *EGFR*. (E) A proximity ligation assay shows that *DOCK4* and *EGFR* also colocalise in tumours.

UGGT1
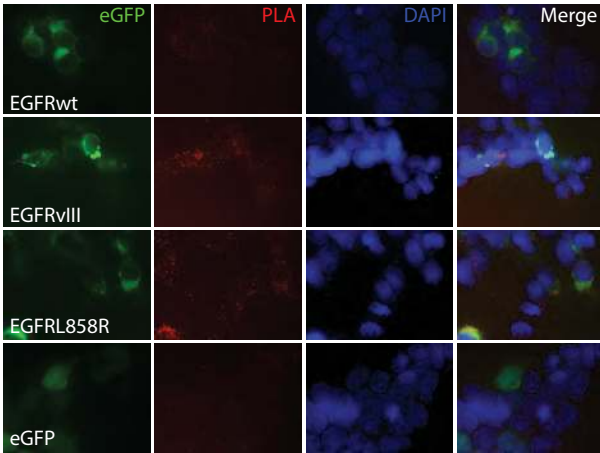
MYCBP2
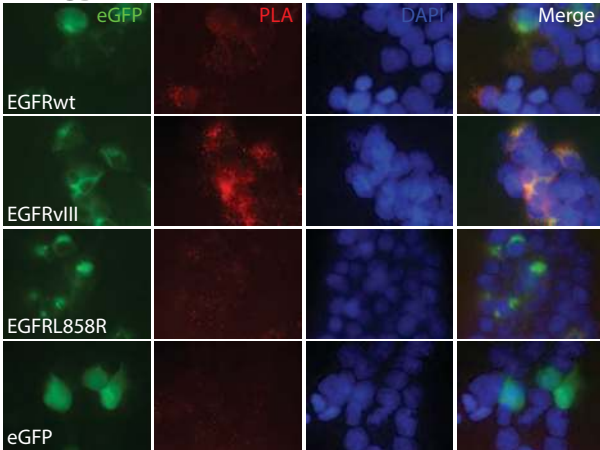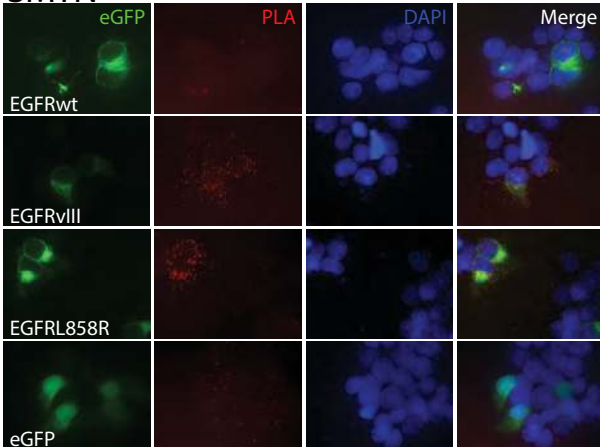
Figure 2.

*EGFR*wt-BG, *EGFR*vIII-BG or *EG-FR*L858R-BG associate with specific proteins. A proximity ligation assay shows that *UGGT1* colocalises with *EGFR*wt-BG and *EGFR*vIII-BG but not with *EGFR*L858R-BG or Bio-GFP control (see also Figure 1B). Similarly, *MYCBP2* colocalises predominantly with *EGFR*vIII-BG whereas *SMTN* predominantly colocalises with *EGFR*L858R-BG. All images taken at 63x magnification.

SMTN

tion of *UGGT1* with *EGFR*^vIII-BG (Figure 1 b). It should be noted that some (minor) association of *UGGT1*, *MYCBP1* and *SMTN* to other *EGFR* constructs were found by PLA and/or WB.

We hypothesised that the selective association of different *EGFR* mutations ultimately would result in the induction of a unique set of genes. We have therefore performed gene expression profiling of cells expressing *EGFR*^wt-BG, *EGFR*^vIII-BG, *EGFR*^L858R-BG or BIOeGFP constructs (n = 3 per construct). Statistical analysis of microarrays (SAM) identified 74, 109 and 187 probesets that were differentially expressed in *EGFR*^wt-BG, *EGFR*^vIII-BG and *EGFR*^L858R-BG expressing cell lines compared to BIO-eGFP control (with differential expression >2 and at a false discovery rate (fdr) <0.05, Supplementary Table 2). These probesets correspond to 61, 89 and 156 genes respectively. Many of these genes are found in all three comparisons and are involved in the transcription of DNA and are significantly enriched for the gene-ontology (GO) terms 'sequence-specific DNA binding', 'transcription factor activity', 'transcription regulator activity', 'DNA binding' and 'protein dimerization activity' (all P < 0.001). Top networks identified by Ingenuity pathway analysis include 'Cellular compromise, cellular function and maintenance, gene expression', 'developmental disorder, hereditary disorder, neurological disease' and 'neurological disease, cell-mediated immune response, cellular development'.

To determine whether specific mutations have specific gene-expression signatures, we performed SAM analysis comparing gene expression between the different *EGFR* mutations. A total of 17, 12 and 35 probesets were identified that were differentially expressed between *EGFR*^wt-BG versus *EGFR*^vIII-BG, *EGFR*^wt-BG versus *EGFR*^L858R-BG and *EGFR*^vIII-BG versus *EGFR*^L858RBG respectively (with differential expression >2 and fdr <0.2, Table 2, Figure 3). These probesets correspond to 15, 11 and 26 different genes respectively. Genes specifically induced by *EGFR*^vIII-BG expression include *SOCS3*, *C10ORF10* and *DTX3L* (~10, 4, and 2-fold induction respectively). *EGFR*^L858R-BG specifically induces the expression of *ARC*, *TFPI2*, *SGMS2*, *ARLB5* and *CCNA1* (~8, 8, 3, 2 and 4-fold respectively). Gene expression analysis therefore indicates that different mutations in *EGFR* induce the expression of a unique set of genes.

We next analysed phosphoprotein levels by RPPA arrays on HOG cells stably expressing *EGFR*^wt-BG, *EGFR*^vIII-BG, *EGFR*^L858R-BG or Bio-eGFP control. Three conditions were examined: normal (serum supplemented cell culture), serum free and serum free, EGF stimulated. All data are listed in Supplementary Table 3. Analysis of *EGFR* on these arrays demonstrates that all stably transfected cell lines, apart from the Bio-eGFP control, have increased levels of *EGFR* and show increased *EGFR* phosphorylation on pY1068 and pY1173. Serum deprivation does not result in a loss of *EGFR* phosphorylation (pY1068 and pY1173) which suggests that *EGFR* signalling remains active under these conditions. Finally, EGF stimulation results in a strong increase in *EGFR*_pY1068 (and to a lesser extent in pY1173), predominantly in *EGFR*^wt-BG and *EGFR*^L858R-BG expressing cells but also in BIOeGFP and expressing cells. EGF stimulation does not activate *EGFR*^vIII-BG which is in-line with the fact that this mutation affects the EGF binding domain.
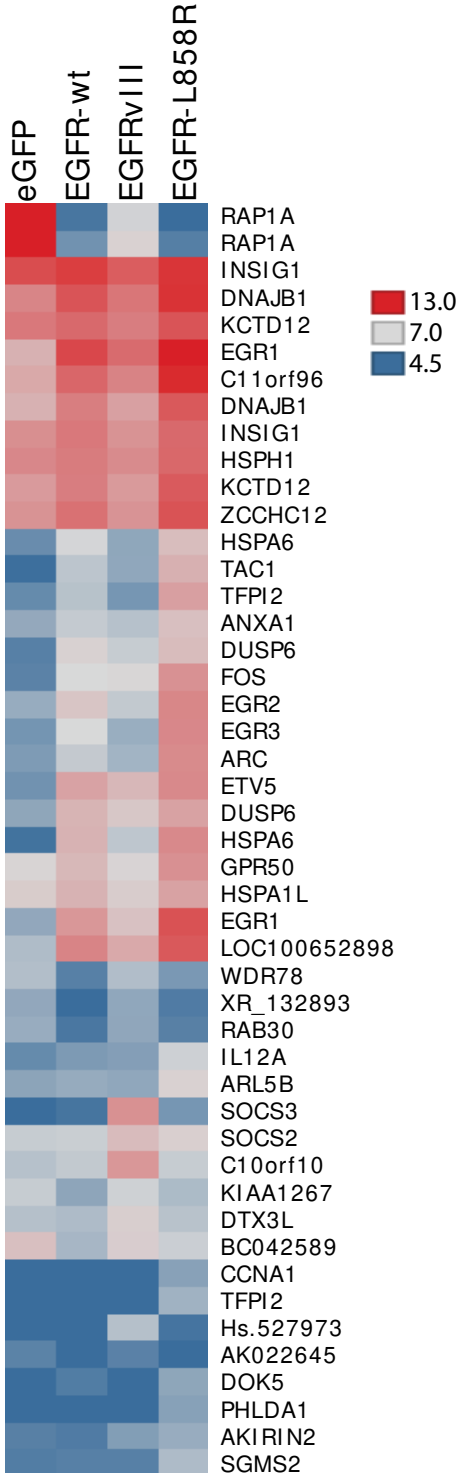
Figure 3.

Genes that are differentially expressed between *EGFR*wt-BG versus *EGFR*vIII-BG, *EGFR*[wt-BG] versus *EGFR*L858R-BG, and *EGFR*vIII-BG versus *EGFR*L858R-BG as identified by SAM analysis. Bio-eGFP control is included for reference. Scales are colour coded from 13.0 (red), 7.0 (grey) to 4.5 (blue) as RMA expression values. (For interpretation of the references to colour in this figure legend, the reader is referred to the web version of this article.)

Table 2. Probesets that are differentially expressed between EGFRwt-BG v. EGFRvIII-BG, EGFRwt-BG v. EG-*FR*L858R-BG, and *EGFR*vIII-BG *v. EGFR*L858R-BG as identified by SAM analysis

Gene_Symbol	Probeset_ID	eGFP	*EGFR*wt	*EGFR*vIII	*EGFR*-p.L858R	wt v vIII	wt v L858R	vIII v L858R
SOCS3	227697_at	4.5	4.9	9.1	5.6	X		X
RAP1A	1555339_at	13.4	4.9	7.0	4.7	X		X
C10orf10	209183_s_at	6.6	6.8	8.9	6.8	X		X
Hs.527973	206359_at	4.3	4.6	6.6	4.9	X		X
RAP1A	1555340_x_at	14.3	5.5	7.3	5.1	X		X
XR_132893	1565830_at	6.0	4.6	6.0	5.0	X		
SOCS2	203372_s_at	6.8	6.9	7.9	7.4	X		
WDR78	1554140_at	6.5	5.1	6.5	5.7	X		
DTX3L	225415_at	6.6	6.5	7.4	6.6	X		
BC042589	235456_at	7.8	6.4	7.4	6.9	X		
KIAA1267	224489_at	6.8	6.0	6.9	6.4	X		
RAB30	229072_at	6.1	4.9	6.0	5.1	X		
AK022645	232257_s_at	5.2	4.1	5.2	4.5	X		
HSPA6	213418_at	4.8	8.2	6.7	9.3	X		X
EGR1	201693_s_at	6.0	8.9	7.7	10.9	X		X
EGR1	201694_s_at	8.2	11.2	10.2	12.6	X		X
EGFR	210984_x_at	5.6	10.0	9.0	10.8	X		
AKIRIN2	223143_s_at	5.1	5.0	5.8	6.1		X	
ARC	210090_at	5.8	6.8	6.3	9.3		X	
ARL5B	242727_at	5.9	6.1	6.0	7.3		X	X
CCNA1	205899_at	3.9	4.5	3.9	5.9		X	X
EGR3	206115_at	5.6	7.1	6.1	9.3		X	X
FOS	209189_at	5.2	7.1	7.2	9.1		X	
IL12A	207160_at	5.4	5.7	5.8	6.9		X	
PHLDA1	217997_at	4.6	4.6	4.6	5.9		X	
SGMS2	242963_at	5.1	5.1	5.1	6.5		X	
TAC1	206552_s_at	4.8	6.7	6.0	8.2		X	X
TFPI2	209277_at	3.6	4.1	3.6	6.3		X	X
TFPI2	209278_s_at	5.4	6.6	5.6	8.7		X	X
HSPA1L	210189_at	7.5	8.2	7.4	8.7			X
HSPH1	208744_x_at	9.4	9.7	9.2	10.3			X
DNAJB1	200666_s_at	9.4	10.8	9.9	11.8			X
LOC100652898	227404_s_at	6.5	9.5	8.4	10.7			X
INSIG1	201627_s_at	11.0	11.5	10.6	11.7			X
DUSP6	208891_at	6.0	8.1	7.6	8.6			X
DNAJB1	200664_s_at	8.2	9.6	8.7	10.7			X
ANXA1	201012_at	6.1	6.8	6.6	7.8			X
KCTD12	212188_at	8.9	9.7	8.9	10.7			X

Table 2. Probesets that are differentially expressed between *EGFR*wt-BG *v. EGFR*vIII-BG, *EGFR*wt-BG *v. EG-FR*L858R-BG, and *EGFR*vIII-BG *v. EGFR*L858R-BG as identified by SAM analysis (continued)

Gene_Symbol	Probeset_ID	eGFP	*EGFR*wt	*EGFR*vIII	*EGFR*-p.L858R	wt v vIII	wt v L858R	vIII v L858R
HSPA6	117_at	5.4	7.0	6.0	7.9			X
DUSP6	208892_s_at	5.1	7.3	6.8	7.9			X
KCTD12	212192_at	9.8	10.2	9.7	10.8			X
ZCCHC12	228715_at	9.0	10.0	9.0	10.9			X
ETV5	203349_s_at	5.5	8.6	8.0	9.3			X
EGR2	205249_at	6.1	7.6	6.8	9.4			X
C11orf96	227099_s_at	8.5	10.3	9.5	12.0			X
GPR50	208311_at	7.2	8.0	7.2	9.1			X
DOK5	214844_s_at	4.4	5.1	4.5	6.0			X
INSIG1	201625_s_at	9.2	9.8	9.0	10.2			X

Differentially expressed genes (>2 fold change in expression level, fdr <0.2) between mutations are marked with X in one of the last three columns.

To determine whether specific mutations induce differences in their downstream pathway activation, we screened all proteins that showed a >2-fold change in levels between different constructs (Figure 4). Examples of differences identified include, under serum conditions (i) lower levels of *AKT*-pT308 (and *AKT*_pS473) in *EGFR*[L858R-BG] expressing HOG cells compared to *EGFR*[wt-BG], *EGFR*[vIII-BG] or BIO-eGFP expressing cells; (ii) lower levels of *MAPK*_pT202 phosphorylation in *EGFR*[vIII-BG] expressing cells compared to those expressing *EGFR*[wt-BG] and *EGFR*[L858R-BG].

Virtually identical data were obtained in an independent RPPA experiment (Figure 4, and Supplementary Figure 2). Western blot experiments (independently performed) further confirmed the differences in *AKT*-pT308 and *MAPK*_pT202 phosphorylation (Figure 4). These data therefore indicate that different mutations in *EGFR* can induce a differential downstream pathway phosphorylation.

Because our results indicate that each mutation has unique molecular properties, we determined whether the various forms of *EGFR* also differentially affect cell physiology. HOG cells stably expressing *EGFR*[vIII-BG] and *EGFR*[L858R-BG] showed a decreased proliferation compared to bio-eGFP or *EGFR*[wt-BG] expressing cells (Figure 5). The differences between constructs were consistently observed over multiple experiments (n = 4 experiments, six wells/experiment and four locations/well). In a wound healing assay, the *EGFR*[vIII-BG] and *EGFR*[L858R-BG] expressing HOG cells also had a significantly slower migration compared to bio-eGFP or *EGFR*[wt-BG] expressing cells (P< 0.001, for all comparisons Figure 5). The difference between constructs was consistently observed in two independent experiments (n = 2 experiments, six wells/experiment and three locations/ well). These data therefore indicate that different mutations differentially affect cell physiology.

Figure 4.
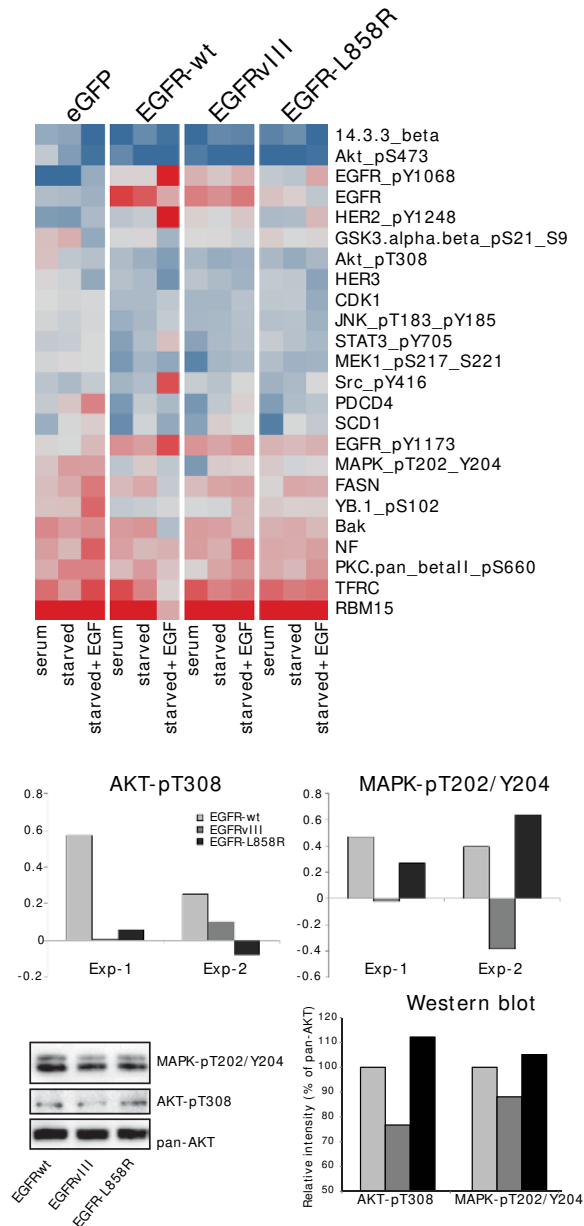
Proteins with >2-fold change in levels between different constructs as determined by RPPA analysis. Shown are RPPA results of these proteins in cells expressing *EGFRwt*- BG, *EGFR*vIII-BG, *EGFR*L858R-BG or Bio-eGFP control under normal cell culture conditions (serum supplemented) and serum free cultures ±EGF. Colours are scaled from the minimum value (blue, -1.26), average (grey, 0.41) to max RPPA value (red, 3.42). B) Confirmation by an independent RPPA experiment of *AKT*-pT308 (left) and *MAPK*_pT202 (right). Results of the original (exp-1) and confirmation (exp-2) are shown. (For interpretation of the references to colour in this figure legend, the reader is referred to the web version of this article.)
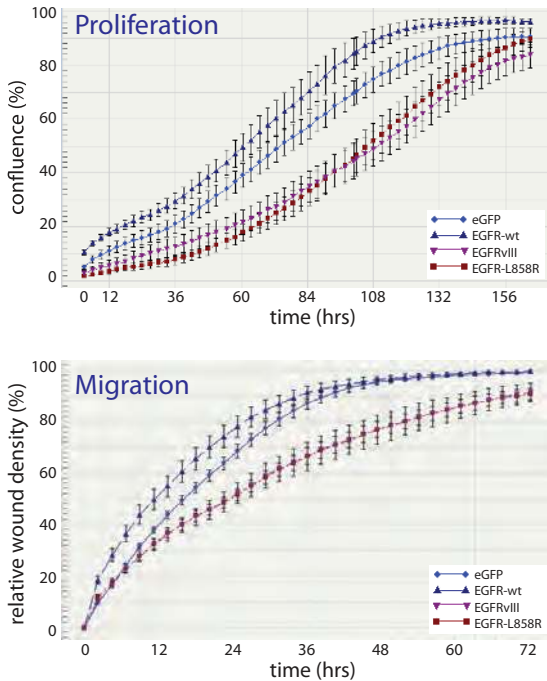
Figure 5.

Mutations in *EGFR* differentially affect proliferation (top) and migration (bottom) in HOG cells stably transfected with *EGFR*wt-BG, *EGFR*vIII-BG, *EGFR*L858R-BG or Bio-eGFP control. *EGFR*vIII-BG and *EGFR*L858R-BG have virtually identical migration.

DISCUSSION

In this study, we demonstrate different mutations in *EGFR* associate with different proteins, activate unique downstream signalling pathways (as shown by the induction of a unique set of genes and protein phosphorylation) and that cell lines expressing different *EGFR* mutation constructs display differences in physiology (proliferation and migration). Our data therefore demonstrate that different mutations have different functional consequences, which may provide an explanation for a tumour type specific mutation spectrum. Our data are in line with other studies that highlighted differences between wildtype *EGFR*, *EGFR*vIII and/ or *EGFR* p.L858R. For example, wildtype *EGFR* and *EGFR*vIII induce phosphorylation of different substrates, have differential activation of the *JNK*, *STAT* and *MAPK* signalling pathways, induce the expression of a unique set of genes and have differences in nuclear localisation (9–13,19). Our data are also in line with a study showing that both wt *EGFR* and *EGFR*vIII interact with DNA–Protein Kinase (*PRKDC*) whereas *EGFR* p.L858R does not (19): our biotin pulldown showed a ~two fold reduction in association with *PRKDC* of *EGFR*[L858R-BG] compared to both *EGFR*[wt- BG] and *EGFR*[vIII-BG] (Supplementary Table 1). We did not observe differential association of *EGFR*[wt-BG], *EGFR*[vIII-BG] and *EGFR*[L858R-BG] with *CBL* proteins, see (20) . However, binding to *Cbl* proteins occurs only after stimulation with EGF, whereas our cells were not EGF stimulated.

Apart from *EGFR*, a few proteins also show mutation specific binding partners and differential activation of downstream signalling pathways. Examples include *TP53* (R273H and R267P) and *PIK3CA* (21–24).

Because tumours often remain dependent on their acquired genetic changes for growth, these changes are direct targets for treatment. However, when each mutation activates a unique set of downstream pathways, it is possible each mutation will require specific inhibition. Indeed, different mutations in *EGFR* show differential sensitivity towards inhibitors: activating mutation in the kinase domain are associated with response to erlotinib and gefitinib whereas the *EGFR* p.A289D mutation is more sensitive to inhibition by lapatinib (7,25,26) . Moreover, kinase domain mutations do not occur in GBMs and inhibitors that act on these mutations (erlotinib and gefitinib) do not show clinical benefit in GBM patients eventhough *EGFR* is a driver in GBMs (27,28).

Our experiments demonstrate that a number of proteins differentially associate with *EGFR* constructs. It is interesting to note that mutations in *DOCK4*, *UGGT1*, *MYCBP2* and *SMTN* have been found both in GBMs (2/283, 4/283, 1/283 and 1/283 respectively) and pulmonary adenocarcinomas (16/220, 7/220, 17/ 220 and 4/220). The first of these proteins that was further examined, *DOCK4*, associates with *EGFR*[vIII-BG] and, to a lesser extent, with *EGFR*[wt-BG] (but not with *EGFR*[L858R-BG]). *DOCK4* is mutated in various tumours including bladder (~10%), colorectal (~10%) and lung (~7%). Two mutations in *DOCK4* have thus far been identified in GBMs. *DOCK4* is involved in cell migration through the activation of *RAC1* (29,30). Whether the difference in cell migration between *EGFR*[wt-BG] and *EGFR*[vIII-BG] is due to differential association with *DOCK4* remains to be determined. *DOCK4* also functions as a scaffold protein within the *Wnt* signaling pathway and is essential for activation of this pathway *in vivo* (18). However, we did not find a mutation specific activation of the *WNT* pathway.

A second differential binding protein, *UGGT1*, was found to predominantly associate with *EGFR*[vIII-BG]. *UGGT1* plays a central role in the quality control of protein folding in the endoplasmic reticulum (glycosylated proteins) where it promotes substrate solubility (31) . It was recently demonstrated that the L858R mutation in *EGFR* reduces the disorganised conformation of the protein (32) . Because *UGGT1* is involved in the quality control of protein folding, it is possible that the lack of association between *UGGT1* and *EGFR*[L858R-BG] identified in our study may be a result of an altered (i.e. less disorganised) conformation.

Similar to *UGGT1*, *MYCBP2* also showed preferential association with *EGFR*[L858R-BG]. *MYCBP2* encodes an E3 ubiquitin ligase which mediates the ubiquitinylation and subsequent degradation of target proteins. The protein is involved in the regulation of the *mTOR* pathway: knockdown of *MYCBP2* inhibits the *mTOR* pathway (33). Finally, *SMTN* showed preferential association with *EGFR*[L858R-BG]. *SMTN* co-localised with α-actin and is involved in the contraction of smooth muscle cells (34). Whether the differential as-

sociation with specific *EGFR* mutations affects the mTOR pathway or actin dynamics in tumour cells remains to be determined.

EGFR is a member of the *ERBB* protein family, a family of proteins that plays a role in several cancer types (35). The various *ERBB* family members can heterodimerise with each other, and each heterodimer can activate different signal transduction pathways (35,36). Although we demonstrate in this manuscript that different *EGFR* mutations activate unique molecular pathways, it remains to be determined whether the different mutations in *EGFR* also result in different heterodimerisation induced pathway activation. Of note, the various *ERBB* family members do not overtly show a tumour type specific mutation pattern (4,37).

Our results show that expression of *EGFR*[vIII-BG] or *EGFR*[L858R-BG] in HOG cells results in a decreased proliferation and migration, which may be counterintuitive for an oncogene. However, such reduced proliferation has been observed before in mutant melanoma cells where expression of *EGFR* confers a growth disadvantage that is further strengthened by the addition of EGF (38). Perhaps this is caused when an oncogene (such as *EGFR*) is expressed in cells that have never been dependent on the oncogene (or the various mutations therein). A similar growth disadvantage (and altered migration pattern) was observed when expressing mutant (R132H) *IDH1* into cell lines (39,40). Interestingly, *IDH1* also has a tumour-type specific mutation pattern (41,42).
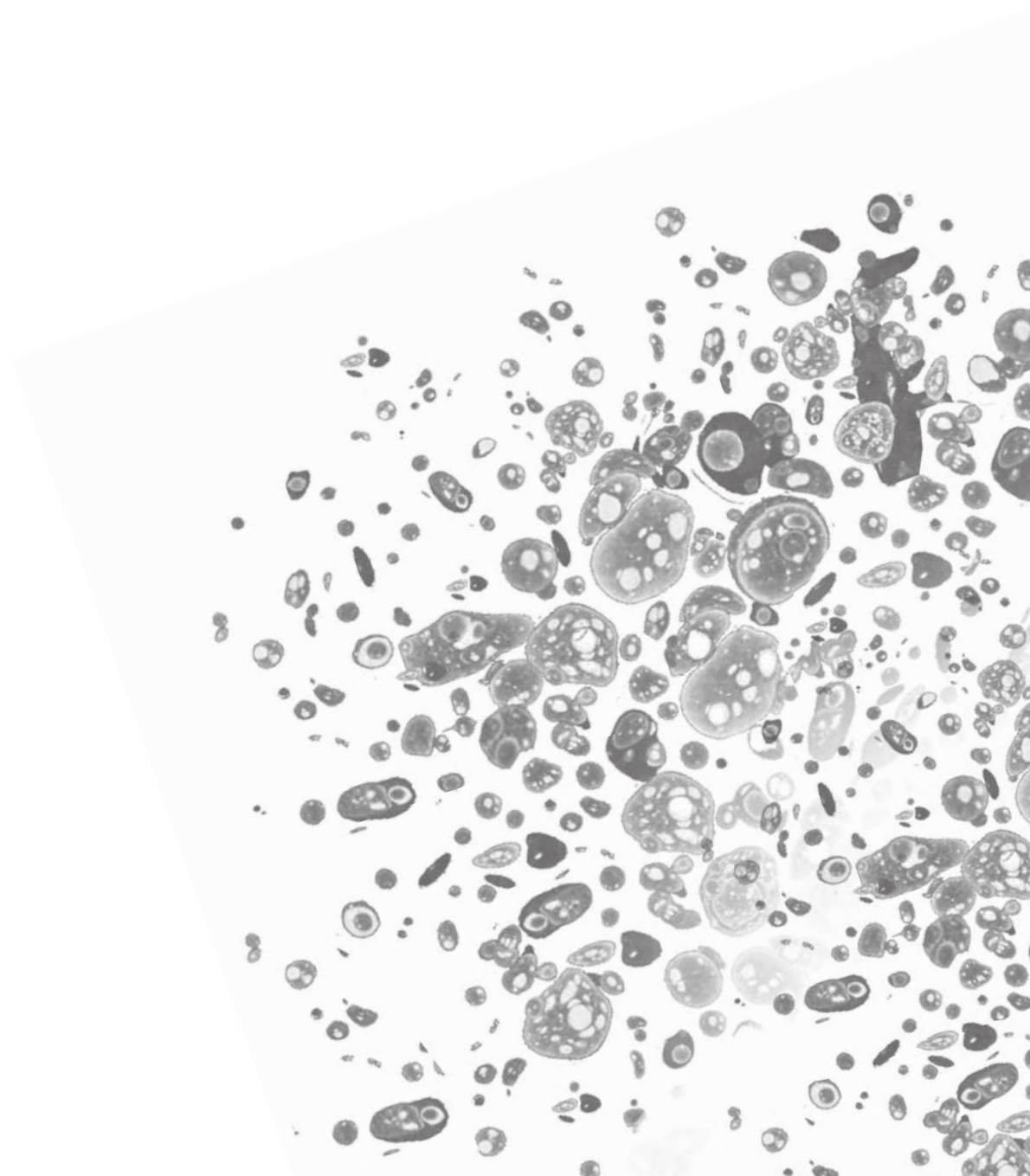
In summary, our results indicate that there are distinct differences between different mutations in *EGFR*. Whether these different mutations also have different oncogenic properties remains to be determined. However, these functional differences can lead to the identification of mutation-specific *EGFR* inhibitors.

REFERENCES

1. Weinberg RA. The Biology of Cancer: Garland Science; 2007.
2. Citri A, Yarden Y. EGF-ERBB signalling: towards the systems level. Nat Rev Mol Cell Biol 2006;7(7):505–16.
3. Brennan CW, Verhaak RG, McKenna A, Campos B, Noushmehr H, Salama SR, et al. The somatic genomic landscape of glioblastoma. Cell 2013;155(2):462–77.
4. Forbes SA, Bindal N, Bamford S, Cole C, Kok CY, Beare D, et al. COSMIC: mining complete cancer genomes in the Catalogue of Somatic Mutations in Cancer. Nucleic Acids Res 2011;39(Database issue):D945–50.
5. Zandi R, Larsen AB, Andersen P, Stockhausen MT, Poulsen HS. Mechanisms for oncogenic activation of the epidermal growth factor receptor. Cell Signal 2007;19(10):2013–23.
6. Fan QW, Cheng CK, Gustafson WC, Charron E, Zipper P, Wong RA, et al. *EGFR* phosphorylates tumor-derived *EGFR*vIII driving STAT3/5 and progression in glioblastoma. Cancer Cell 2013;24(4):438–49.
7. Vivanco I, Robins HI, Rohle D, Campos C, Grommes C, Nghiemphu PL, et al. Differential sensitivity of glioma- versus lung cancer-specific *EGFR* mutations to *EGFR* kinase inhibitors. Cancer Discov 2012;2(5):458–71.
8. Holland EC, Hively WP, DePinho RA, Varmus HE. A constitutively active epidermal growth factor receptor cooperates with disruption of G1 cell-cycle arrest pathways to induce glioma-like lesions in mice. Genes Dev 1998;12(23):3675–85.
9. Chu CT, Everiss KD, Wikstrand CJ, Batra SK, Kung HJ, Bigner DD. Receptor dimerization is not a factor in the signaling activity of a transforming variant epidermal growth factor receptor (*EGFR*vIII). Biochem J 1997;324(Pt. 3):855–61.
10. Antonyak MA, Moscatello DK, Wong AJ. Constitutive activation of c-Jun N- terminal kinase by a mutant epidermal growth factor receptor. J Biol Chem 1998;273(5):2817–22.
11. Pedersen MW, Pedersen N, Damstrup L, Villingshoj M, Sonder SU, Rieneck K, et al. Analysis of the epidermal growth factor receptor specific transcriptome: effect of receptor expression level and an activating mutation. J Cell Biochem 2005;96(2):412–27.
12. Chumbalkar V, Latha K, Hwang Y, Maywald R, Hawley L, Sawaya R, et al. Analysis of phospho-tyrosine signaling in glioblastoma identifies STAT5 as a novel downstream target of D*EGFR*. J Proteome Res 2011;10(3):1343–52.
13. Latha K, Li M, Chumbalkar V, Gururaj A, Hwang Y, Dakeng S, et al. Nuclear *EGFR*vIII-STAT5b complex contributes to glioblastoma cell survival by direct activation of the Bcl-XL promoter. Int J Cancer 2012;132:509–20.
14. Mellacheruvu D, Wright Z, Couzens AL, Lambert JP, St-Denis NA, Li T, et al. The CRAPome: a contaminant repository for affinity purification-mass spectrometry data. Nat Methods 2013;10(8):730–6.
15. Chatr-Aryamontri A, Breitkreutz BJ, Heinicke S, Boucher L, Winter A, Stark C, et al. The BioGRID interaction database: 2013 update. Nucleic Acids Res 2013;41(Database issue):D816–23.
16. Foerster S, Kacprowski T, Dhople VM, Hammer E, Herzog S, Saafan H, et al. Characterization of the *EGFR* interactome reveals associated protein complex networks and intracellular receptor dynamics. Proteomics 2013;13(21):3131–44.
17. Kandasamy K, Mohan SS, Raju R, Keerthikumar S, Kumar GS, Venugopal AK, et al. NetPath: a public resource of curated signal transduction pathways. Genome Biol 2010;11(1):R3.
18. Upadhyay G, Goessling W, North TE, Xavier R, Zon LI, Yajnik V. Molecular association between beta-catenin degradation complex and Rac guanine exchange factor DOCK4 is essential for Wnt/beta-catenin signaling. Oncogene 2008;27(44):5845–55.

19. Liccardi G, Hartley JA, Hochhauser D. *EGFR* nuclear translocation modulates DNA repair following cisplatin and ionizing radiation treatment. Cancer Res 2011;71(3):1103–14.

20. Schmidt MH, Furnari FB, Cavenee WK, Bogler O. Epidermal growth factor receptor signaling intensity determines intracellular protein interactions, ubiquitination, and internalization. Proc Natl Acad Sci U S A 2003;100(11):6505–10.

21. Coffill CR, Muller PA, Oh HK, Neo SP, Hogue KA, Cheok CF, et al. Mutant p53 interactome identifies nardilysin as a p53R273H-specific binding partner that promotes invasion. EMBO Rep 2012;13(7):638–44.

22. Vaughan CA, Frum R, Pearsall I, Singh S, Windle B, Yeudall A, et al. Allele specific gain-of-function activity of p53 mutants in lung cancer cells. Biochem Biophys Res Commun 2012;428(1):6–10.

23. Ross RL, Askham JM, Knowles MA. PIK3CA mutation spectrum in urothelial carcinoma reflects cell context-dependent signaling and phenotypic outputs. Oncogene 2013;32(6):768–76.

24. Pang H, Flinn R, Patsialou A, Wyckoff J, Roussos ET, Wu H, et al. Differential enhancement of breast cancer cell motility and metastasis by helical and kinase domain mutations of class IA phosphoinositide 3-kinase. Cancer Res 2009;69(23):8868–76. [25] Lynch TJ, Bell DW, Sordella R, Gurubhagavatula S, Okimoto RA, Brannigan BW, et al. Activating mutations in the epidermal growth factor receptor underlying responsiveness of nonsmall- cell lung cancer to gefitinib. N Engl J Med 2004;350(21): 2129–39.

26. Paez JG, Janne PA, Lee JC, Tracy S, Greulich H, Gabriel S, et al. *EGFR* mutations in lung cancer: correlation with clinical response to gefitinib therapy. Science 2004;304(5676):1497–500.

27. Rich JN, Reardon DA, Peery T, Dowell JM, Quinn JA, Penne KL, et al. Phase II trial of gefitinib in recurrent glioblastoma. J Clin Oncol 2004;22(1):133–42.

28. van den Bent MJ, Brandes AA, Rampling R, Kouwenhoven MC, Kros JM, Carpentier AF, et al. Randomized phase II trial of erlotinib versus temozolomide or carmustine in recurrent glioblastoma: EORTC brain tumor group study 26034. J Clin Oncol 2009;27(8):1268–74.

29. Hiramoto K, Negishi M, Katoh H. Dock4 is regulated by RhoG and promotes Rac-dependent cell migration. Exp Cell Res 2006;312(20):4205–16.

30. Kobayashi M, Harada K, Negishi M, Katoh H. Dock4 forms a complex with SH3YL1 and regulates cancer cell migration. Cell Signal 2014;26(5):1082–8.

31. Ferris SP, Jaber NS, Molinari M, Arvan P, Kaufman RJ. UDPglucose: glycoprotein glucosyltransferase (UGGT1) promotes substrate solubility in the endoplasmic reticulum. Mol Biol Cell 2013;24(17):2597–608.

32. Shan Y, Eastwood MP, Zhang X, Kim ET, Arkhipov A, Dror RO, et al. Oncogenic mutations counteract intrinsic disorder in the *EGFR* kinase and promote receptor dimerization. Cell 2012;149(4):860–70.

33. Han S, Witt RM, Santos TM, Polizzano C, Sabatini BL, Ramesh V. Pam (Protein associated with Myc) functions as an E3 ubiquitin ligase and regulates TSC/mTOR signaling. Cell Signal 2008;20(6):1084–91.

34. Niessen P, Rensen S, van Deursen J, De Man J, De Laet A, Vanderwinden JM, et al. Smoothelin-a is essential for functional intestinal smooth muscle contractility in mice. Gastroenterology 2005;129(5):1592–601.

35. Karamouzis MV, Badra FA, Papavassiliou AG. Breast cancer: the upgraded role of HER-3 and HER-4. Int J Biochem Cell Biol 2007;39(5):851–6.

36. Lemmon MA, Schlessinger J, Ferguson KM. The *EGFR* family: not so prototypical receptor tyrosine kinases. Cold Spring Harb Perspect Biol 2014;6(4):a020768.

37. Cerami E, Gao J, Dogrusoz U, Gross BE, Sumer SO, Aksoy BA, et al. The cBio cancer genomics portal: an open platform for exploring multidimensional cancer genomics data. Cancer Discov 2012;2(5):401–4.

38. Sun C, Wang L, Huang S, Heynen GJ, Prahallad A, Robert C, et al. Reversible and adaptive resistance to BRAF(V600E) inhibition in melanoma. Nature 2014;508(7494):118–22.

39. Bralten LB, Kloosterhof NK, Balvers R, Sacchetti A, Lapre L, Lamfers M, et al. *IDH1* R132H decreases proliferation of glioma cell lines in vitro and in vivo. Ann Neurol 2011;69(3):455–63.

40. Wang JB, Dong DF, Wang MD, Gao K. *IDH1* overexpression induced chemotherapy resistance and *IDH1* mutation enhanced chemotherapy sensitivity in Glioma cells in vitro and in vivo. Asian Pac J Cancer Prev 2014;15(1):427–32.

41. Gravendeel LA, Kloosterhof NK, Bralten LB, van Marion R, Dubbink HJ, Dinjens W, et al. Segregation of non-p.R132H mutations in *IDH1* in distinct molecular subtypes of glioma. Hum Mutat 2010;31(3):E1186–99.

42. Schaap FG, French PJ, Bovee JV. Mutations in the isocitrate dehydrogenase genes *IDH1* and *IDH2* in tumors. Adv Anat Pathol 2013;20(1):32–8.

43. van Agthoven T, Veldscholte J, Smid M, van Agthoven TL, Vreede L, Broertjes M, et al. Functional identification of genes causing estrogen independence of human breast cancer cells. Breast Cancer Res Treat 2009;114(1):23–30.

44. Buntinx M, Vanderlocht J, Hellings N, Vandenabeele F, Lambrichts I, Raus J, et al. Characterization of three human oligodendroglial cell lines as a model to study oligodendrocyte injury: morphology and oligodendrocyte-specific gene expression. J Neurocytol 2003;32(1):25–38.

45. van den Berg DL, Snoek T, Mullin NP, Yates A, Bezstarosti K, Demmers J, et al. An Oct4-centered protein interaction network in embryonic stem cells. Cell Stem Cell 2010;6(4):369–81.

46. Huang da W, Sherman BT, Lempicki RA. Systematic and integrative analysis of large gene lists using DAVID bioinformatics resources. Nat Protoc 2009;4(1):44–57.

CHAPTER 5

Tumor-specific mutations in low-frequency genes affect their functional properties

Lale Erdem-Eraslan, Daphne Heijsman,
Maurice de Wit, Andreas Kremer,
Andrea Sacchetti, Peter J Van der Spek,
Peter AE Sillevis Smitt, Pim J French

ABSTRACT

Causal genetic changes in oligodendrogliomas (OD) with 1p/19q co-deletion include mutations in *IDH1*, *IDH2*, *CIC*, *FUBP1*, *TERT* promoter and *NOTCH1*. However, it is generally assumed that more somatic mutations are required for tumorigenesis. This study aimed to establish whether genes mutated at low frequency can be involved in OD initiation and/or progression. We performed whole-genome sequencing on three anaplastic ODs with 1p/19q co-deletion. To estimate mutation frequency, we performed targeted resequencing on an additional 39 ODs. Whole- genome sequencing identified a total of 55 coding mutations (range 8–32 mutations per tumor), including known abnormalities in *IDH1*, *IDH2*, *CIC* and *FUBP1*. We also identified mutations in genes, most of which were previously not implicated in ODs. Targeted resequencing on 39 additional ODs confirmed that these genes are mutated at low frequency. Most of the mutations identified were predicted to have a deleterious functional effect. Functional analysis on a subset of these genes (e.g. *NTN4* and *MAGEH1*) showed that the mutation affects the subcellular localization of the protein (n = 2/12). In addition, HOG cells stably expressing mutant *GDI1* or *XPO7* showed altered cell proliferation compared to those expressing wildtype constructs. Similarly, HOG cells expressing mutant *SASH3* or *GDI1* showed altered migration. The significantly higher rate of predicted deleterious mutations, the changes in subcellular localization and the effects on proliferation and/or migration indicate that many of these genes functionally may contribute to gliomagenesis and/or progression. These low-frequency genes and their affected pathways may provide new treatment targets for this tumor type.

INTRODUCTION

Oligodendrogliomas (ODs) account for 20 % of all glial tumors and are thought to arise from oligodendroglial precursor cells (OPCs). They are classified as either grade II or grade III and have a more favorable clinical and prognostic outcome with respect to other gliomas (1).

Frequently occurring driver mutations in oligodendrogliomas include mutations in *IDH1*, *CIC*, *FUBP1*, *TERT* promoter and *NOTCH* (2–6). However, tumor formation is assumed to require more somatic mutations (7). Interestingly, many other somatic mutations within proteincoding genes have also been identified in oligodendrogliomas, albeit at a low frequency (8). The role of most of these infrequent mutations in tumorigenesis and/ or progression is unclear. To date, only few studies have suggested a functional impact of genes mutated at low frequency in gliomas (9–13). Therefore, low-frequency genes that play a role in the initiation and/or progression of ODs need to be identified to better understand OD pathogenesis and for development of targeted therapies.

Here, we have performed whole-genome sequencing on three ODs to identify all genetic changes in these tumors. We then performed targeted resequencing on an additional 39 tumors to demonstrate that many of these mutations occur at low frequency. Functional analysis of a subset of these low-frequency genes (*NTN4*, *GDI1*, *MAGEH1*, *SASH3*, *ZNF238*, *OR5D14*, *ZNF57*, *DCUN1D2*, *ARSE*, *XPO7*, *GABRE* and *PGLYRP4*) suggest that they can contribute to tumor pathogenesis and therefore are unlikely to be passengers. These genes and their affected pathways open up entirely novel treatment targets for this tumor type.

MATERIALS AND METHODS

Patient material

OD samples were collected from the Erasmus MC tumor archive. Use of patient material was approved by the Institutional Review Board and patients provided written informed consent according to national and local regulations for the clinical study and correlative tissue studies. After surgical resection, all samples were snap-frozen and stored at - 80°C. Non-neoplastic DNA was isolated from blood and stored at - 80. Assessment of 1p19q LOH was performed previously (14, 15). Patient characteristics are listed in supplementary Table 1.

DNA extraction and sequencing

Tumor DNA was extracted from fresh frozen (FF) tumor samples using the AllPrep DNA/ RNA mini kit (Qiagen, Venlo, the Netherlands). Matched normal DNA was isolated from

1 ml blood as part of routine diagnostic procedures. Whole-genome sequencing was performed by Complete Genomics (Mountain View, US) using 5 l g DNA. Whole-genome sequencing data analysis was performed using cgatools version 1.4.0 and described in supplementary methods. All mutations were validated by Sanger sequencing. Targeted resequencing on an additional 39 ODs was performed by Baseclear (Leiden, the Netherlands). Library construction and resequencing data analysis were described in supplementary methods.

Cell lines and sorting

Constructs of wildtype and mutated genes were generated by site directed mutagenesis (n = 12), and C-terminally fused to GFP for visualization. Subsequently, Human oligodendroglial (HOG) cells (16) and HEK 293 cells were transiently transfected with wildtype or mutant constructs using lipofectamine according to the manufacturer's instructions. Stably transfected HOG cells were created as described in supplementary methods.

Functional analysis

For proliferation experiments, cells (50.000 cells/well) were plated in a 24-well Greiner plate (Greiner Bio-One, Alphen a/d Rijn, the Netherlands) and followed using an Incucyte (Essenbioscience, Hertfordshire, United Kingdom). Growth curves were constructed using the Confluence v1.5 metric of the Incucyte software.

For migration experiments, cells were grown to confluence in a 24-well Essen ImageLockplate after which a cell-free zone (scratch) was created using a WoundMaker. Wells were then washed in PBS after which serum-free media was added to the plates. All plates were followed for 5 days and images were automatically captured at 3-h intervals from 3 to 4 separate regions within a well. Relative wound density, wound width and wound confluency curves were constructed using data points of every capture. All proliferation and migration experiments were performed at least in triplicate. Flow cytometric cell cycle analysis using propidium iodide was performed as described in supplementary methods.

RESULTS

Whole-genome sequencing

To identify somatic alterations in oligodendrogliomas, we performed whole-genome sequencing on DNA of three ODs and their matched germline DNA. All tumors were WHO grade III and had 1p19q co-deletion. The mapped sequence of the six samples varied between 237 and 249 Gb, resulting in a coverage between respectively 83 and 90-fold per genome. Confident diploid calls could be made for 94–95 % of the reference

genome. On average 3,5 million genetic variants were identified per sample. Of these, 55 (range of 8–32 variants per sample), were localized to coding exons, were neither synonymous nor present in dbSNP130 and had a somatic score [- 20 (see supplementary methods) (Figure 1). Identified variants consisted of missense (84 %), nonsense (9 %) and frameshifts (7 %). All 55 mutations were validated by Sanger sequencing (supplementary Table 2).

We performed an in silico analysis on all 55 genes to estimate the effect of mutation on protein. Polyphen-2 predictions were available for 43 genes of which 22 were probably damaging, 9 possible damaging, and 12 were benign. In randomly picked mutations identified with a lower confidence score (i.e. somatic scores B- 20) the rate of damaging mutations was significantly lower: 10 probably damaging, 8 possible damaging and 21 benign changes, (p = 0.033, Chi square test). The identified mutations also had a slight tendency towards a higher conservation compared to mutations with somatic scores B- 20: GERPscore 2.71 ± 2.96 v 1.75 ± 3.61 p = 0.156). The 55 mutations identified by whole-genome sequencing therefore were often predicted to have deleterious effects on the protein.

Targeted resequencing

Because we aimed to determine functional effects of genes mutated at low frequency in gliomas, we performed targeted resequencing of 44 (of the 55 identified by wholegenome sequencing) genes that were thusfar not implicated in gliomagenesis (supplementary Table 2). Resequencing was performed on the entire coding region of the 44 genes on 39 grade II/III ODs of which 28/39 had 1p/19q LOH, 5/39 had loss of 1p or 19q and 6/39 had no 1p19q loss. We chose this dataset because it represents a typical cohort of histologically diagnosed oligodendrogliomas where most will have 1p19q co-deletion, but some have other, more aggressive genetic changes.

No mutations were found in 39 of the 44 genes in any of the additional 39 tumors. Of the remaining five genes, mutations were identified in only one additional sample (Figure 2, supplementary Table 4). In our samples, the mutations were all present at a high allele frequency (range 39–84 %) suggesting that the mutation is present in a large proportion of the resected tumor, at least within the tissue investigated. Among the 28 tumors with 1p19q co-deletion, mutations in only three of the 44 genes were identified (supplementary Table 5). Although in individual tumors the allele frequency was high, the overall mutation frequency of all 44 genes was low. The mutations in the 44 genes identified by our screen therefore are 'low-frequency genes': genes mutated at low frequency in oligodendrogliomas.

Apart from these low-frequency genes, we included a set of known cancer genes (*IDH1*, *IDH2*, *PTEN*, *TP53*, *NOTCH1*, *EGFR*, *CDKN2A*, *CDKN2B*, *NF1* and *PIK3R1*) for reference on our targeted resequencing effort. Analysis of these known cancer-relevant genes

Figure 1.
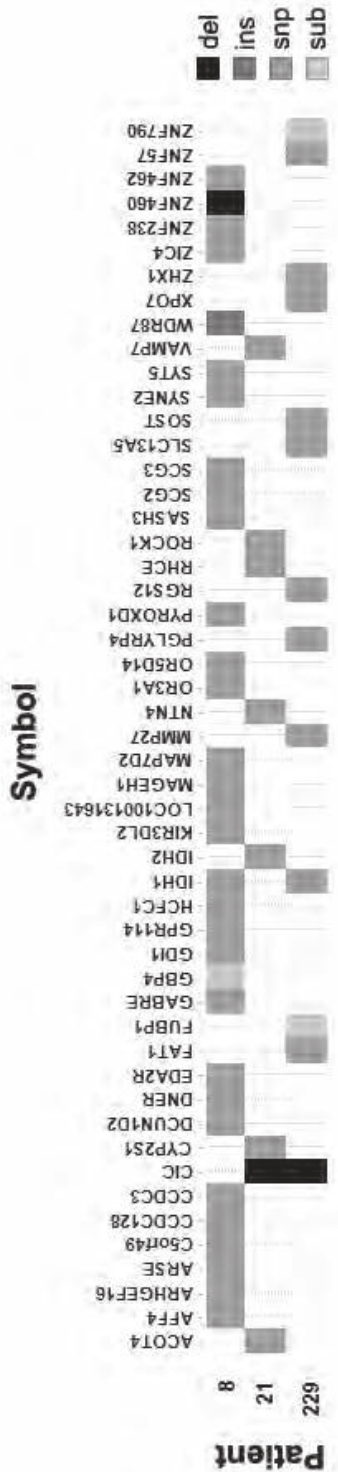
Somatic genetic alterations in three oligodendrogliomas identified by whole- genome sequencing. Shown are all mutations identified in three tumors that (i) were localized to the coding regions of exons,(ii) were nonsynonymous, (iii) were absent from dbSNP130 and (iv) had a somatic score[-20]. Alterations are coded in greyscale by the type of mutation (deletion, insertion, snp, substitution). The number of alterations range from 8 to 32 variants per sample. All 55 mutations were validated by Sanger sequencing.
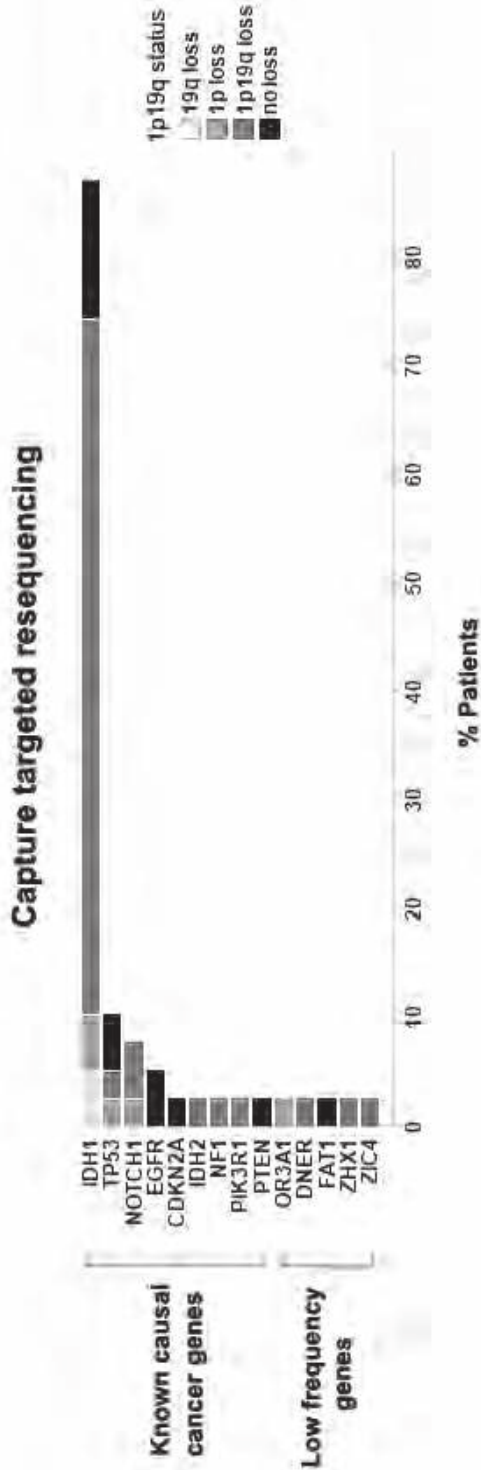
Figure 2.

Targeted resequencing on 39 ODs confirms that many genes are mutated at low frequency. Of the known cancer genes (*IDH1/2, TP53, NOTCH1, EGFR, CDKN2A, NF1, PIK3R1* and *PTEN*), a total of 48 mutations (range 1–4 mutations per tumor) were identified in 39 tumors (known causal cancer genes). Of the genes identified by whole-genome sequencing that thus far are not implicated in oligodendrogliomas, no mutations were found in 39 of the 44 genes in any of the additional 39 tumors (not shown). In the remaining five genes, we identified mutations in only one additional sample (indicated in the figure as low-frequency genes). Distribution of 1p19q status is reported for each identified mutation. Mutations in *EGFR, CDKN2A* and *PTEN* were only found in patients with intact 1p19q status.

revealed a total of 48 mutations (range of 1–4 mutations per tumor), which consisted of missense (44) and nonsense (4) variants. These include mutations in *IDH1* (34 mutations in 39 tumors), *TP53* (4/39), *NOTCH1* (3/39), *EGFR* (2/39), *IDH2* (1/39), *CDKN2A* (1/39), *NF1* (1/39), *PIK3R1* (1/39) and *PTEN* (1/39) (Figure 2, supplementary Table 4). Mutations in *EGFR*, *CDKN2A* and *PTEN* were only found in patients with intact 1p19q chromosomes. Targeted resequencing therefore confirmed a high frequency of mutations in genes that drive oligodendrogliomas.

To better determine the incidence of the identified mutations, we analyzed exome sequencing data of 7 oligodendrogliomas from Bettegowda et al. (2), 16 oligodendrogliomas from Yip et al. (5) and 170 low-grade gliomas (LGG) and 290 glioblastomas (GBM) (8) from the TCGA dataset. In this large dataset, most (36/44) mutations identified by wholegenome sequencing that thus far are not implicated in oligodendrogliomas, were also identified in one of these datasets; eight were uniquely identified by us. The frequency was however low: often only one sample was identified in the external datasets with a mutation in that gene (supplementary Figure1).

Mutations in low-frequency genes can affect the proteins' subcellular localization In order to determine whether these low-frequency genes may be involved in glioma pathogenesis, we performed a more detailed molecular analysis on 12/44 of those genes (Figs. 3, 4, 5). These 12 genes were randomly picked from the 44 low-frequency genes. Transient transfection revealed that in 2/12 constructs, the mutation affects the proteins' subcellular localization. In the gene *NTN4*, the mutation resulted in a strong nuclear localization, which was absent in the wildtype (Figure 3). For *MAGEH1*, the mutation resulted in a reduced or even absent nuclear localization. No differences in the subcellular localization between wildtype and mutant constructs were found in cells expressing *GDI1*, *ZNF238*, *SASH3*, *XPO7*, *ZNF57*, *GABRE*, *OR5D14*, *PGLYRP4*, *ARSE* and *DCUN1D2* (not shown).
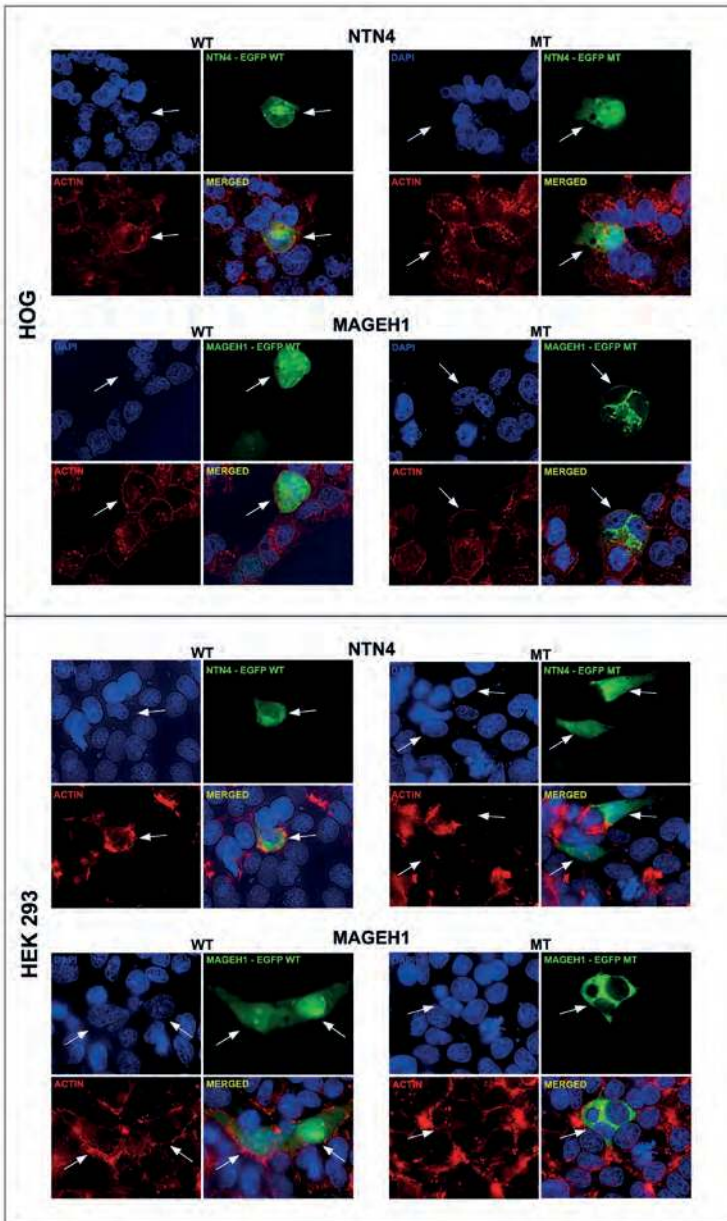
Low-frequency genes can affect proliferation and/or migration

To further examine the functional properties of low-frequency genes, we generated cell lines stably expressing the mutant or wildtype variant of four genes and performed functional analysis on proliferation and migration (Figs. 4, 5).

The first gene examined was *GDI1*, in which the mutation was located in the geranyl–geranyl transferase domain (c.577C>T, p.R193C). HOG cells stably expressing wildtype *GDI1* have increased proliferation compared to those expressing *GDI1*[R193C] or eGFP (p =0.003, p = 0.04, respectively, n = 2). This is also confirmed by flow cytometry, showing that in cells expressing wildtype *GDI1*, 7.5 % more cells are found in the S-G2-M phase and 8.5 % less in the G1 compared to those expressing *GDI1*[R193C] (supplementary Figure 2). No differences in proliferation were observed between *GDI1*[R193C] and eGFP cells (p = 0.7). Similarly, HOG cells stably expressing *GDI1* wildtype showed increased migration

Figure 3.

Mutations in low-frequency genes can affect the subcellular localization of proteins. HOG and HEK 293 cells were transiently transfected with either the wildtype or mutant construct and stained or GFP (green), DAPI (blue) and Alexa fluor phalloidin (red). A total of twelve wildtype and mutant construct pairs were made. In both cell lines, the mutated *NTN4* construct showed a stronger nuclear staining pattern compared to the wild-type construct. For *MAGEH1*, the mutation resulted in a reduced or even absent nuclear staining. No differences in the subcellular localization between wildtype and mutant constructs were found in HOG and HEK 293 cells expressing *GDI1*, *ZNF238*, *SASH3*, *XPO7*, *ZNF57*, *GABRE*, *OR5D14*, *PGLYRP4*, *ARSE* and *DCUN1D2* (not shown).

compared to $GDI1^{R193C}$ or eGFP (p = 0.003, p = 0.0005 respectively, n = 2). No differences in migration were observed between $GDI1^{R193C}$ and eGFP cells (p = 0.3). The differences in both proliferation and migration between wildtype and mutant constructs indicate that the mutation in $GDI1$ affects the functional property of the protein.

Our second gene examined was $XPO7$, in which a mutation was identified in the ARM-type fold domain (c.709G>A, p.D237N). An increase in proliferation was observed during the first 24 h in cells stably expressing $XPO7^{D237N}$ compared to wildtype and eGFP cells (p = 0.02, p=0.001 (n = 2), respectively). After 24 h, the proliferation rate was similar in cells stably expressing wildtype, $XPO7^{D237N}$ and eGFP. Because of the differences in proliferation at the start of the experiment, $XPO7^{D237N}$ cells reach confluency more rapid than wildtype or eGFP cells. The initial difference was consistently observed in multiple experiments with 3–6 wells per experiment and 4 positions per well. Because cells were plated at 2 different densities (50.000 and 100.000 cells per well) the observed difference in initial proliferation rates appeared independent of plating density. A possible explanation for this difference is that $XPO7^{D237N}$ cells recover more rapidly after plating.
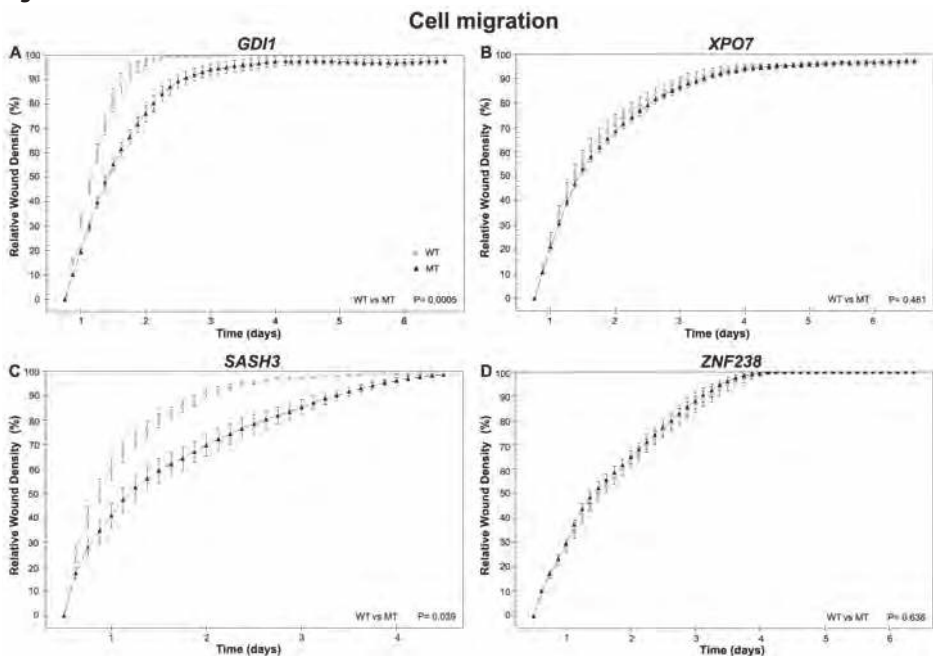
Figure 4.
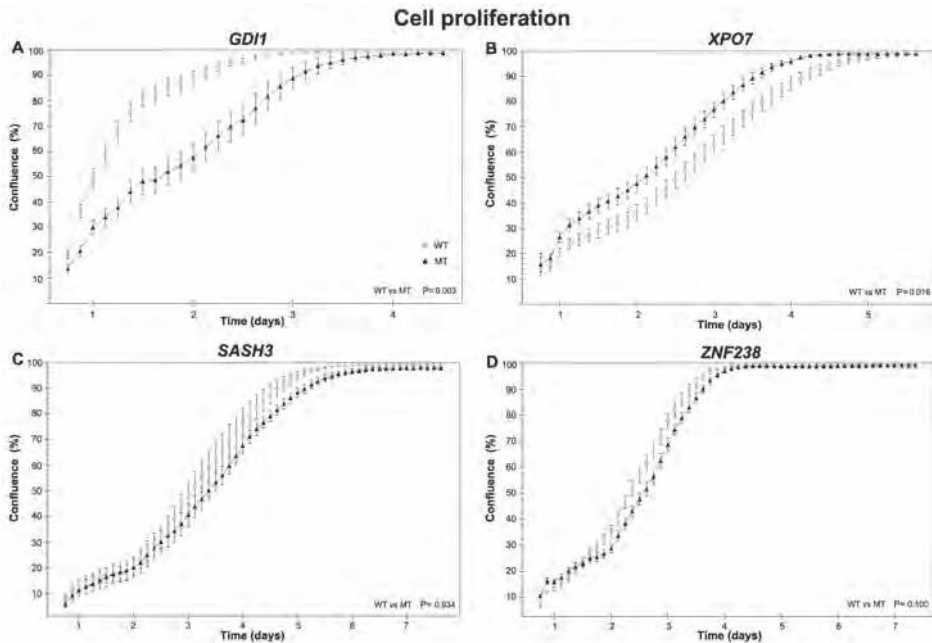
Mutations in low-frequency genes can affect cell growth. a HOG cells stably expressing wildtype $GDI1$ show increased proliferation compared to $GDI1^{R193C}$ expressing cells (p = 0.003, n = 2 independent experiments). b Cells stably expressing $XPO7^{D237N}$ show a higher rate of proliferation during the first 24 h, compared to wildtype expressing cells (p = 0.02, (n = 2)). After 24 h, similar proliferation rates were observed in wildtype and $XPO7^{D237N}$. c HOG cells stably expressing $SASH3$ wildtype or $SASH3^{R288*}$ and d wildtype or $ZNF238^{V121I}$ show similar proliferation rates (n = 3)

Migration of cells expressing $XPO7^{D237N}$ or wildtype was higher than those expressing eGFP (p = 0.05, p = 0.03, respectively (n = 2)). No differences in migration were observed between cells expressing $XPO7^{D237N}$ and wildtype (p = 0.5). The effect of the identified point mutation in *XPO7* on proliferation highlights its importance for protein function in these cells.

The third gene examined was *SASH3*, in which the mutation was located in the SAM domain (c.862C> T), partially disrupting this domain in the C-terminal region (p.R288*). HOG cells stably expressing *SASH3* wildtype, $SASH3^{R288*}$ or eGFP have a similar proliferation rate (n = 3). However, cells expressing wildtype *SASH3*, show increased migration compared to $SASH3^{R288*}$ or eGFP. The difference in migration between wildtype and $SASH3^{R288*}$ indicates that the mutation affects the function of the wildtype protein (p = 0.001, n = 2).

Our last gene examined was *ZNF238*, in which the mutation was located in a BTB/POZ fold domain (c.361G>A,p.V121I). In HOG cells stably expressing *ZNF238* wildtype or $ZNF238^{V121I}$ constructs, we observed a slight decrease in proliferation compared to eGFP

Figure 5.

Mutations in low-frequency genes can affect cell migration. a HOG cells stably expressing *GDI1* wildtype have a higher migration rate compared to $GDI1^{R193C}$ expressing cells (p = 0.003, n = 2 independent experiments). b No differences in migration were observed between cells expressing wildtype and $XPO7^{D237N}$ or between cells expressing *ZNF238* wildtype and mutant (d) (p = 0.5). c Cells expressing wildtype *SASH3*, show increased migration compared to $SASH3^{R288*}$ (p = 0.039)

expressing cells (p<0.001, n = 4).Amore pronounced effect was observed in migration: HOG cells stably expressing *ZNF238* wildtype and *ZNF238*[V121I] show a strong decrease compared to eGFP. These results were consistently observed in multiple experiments (p< 0.001, n = 4). Although no differences were observed between wildtype and mutant constructs, the results do indicate that wildtype or *ZNF238*[V121I] constructs affect cellular proliferation and migration.

DISCUSSION

In this study, we have performed whole-genome and targeted resequencing on 3 and 39 oligodendrogliomas to identify somatic mutations. Apart from the known frequently mutated genes such as *IDH1*, *CIC* and *FUBP1*, our study also identified genes that were infrequently mutated (i.e. in one or two samples only). Most low-frequency genes are predicted to affect the protein's function by in silico analysis. A significantly higher proportion of genes had a potential deleterious effect compared to mutations in genes identified with a lower confidence score (i.e. somatic scores B- 20). Functional analysis of these low-frequency genes indicated that the identified mutation can affect protein subcellular localization and/or cell physiology. Our results therefore suggest that (at least some of) these genes may be relevant for gliomagenesis and/or contribute to progression.

The frequency of mutations identified at a higher frequency in our study (*IDH1*, *CIC* and *FUBP1*) are similar to those reported by others for this tumor type. Mutations in the *ATRX* gene were not identified; this gene is frequently mutated in other glioma subtypes including WHO grade IIIII astrocytomas (71 %), oligoastrocytomas (68 %) and secondary glioblastomas (57 %) (2, 5). Also similar to reported by others, mutations in *EGFR*, *CDKN2A* and *PTEN* were mutually exclusive with 1p19q co-deletion (2–5, 8).

To our knowledge, our study is the first to functionally study low-frequency genes on a larger scale. Several other studies have demonstrated a functional impact of genes mutated at a low frequency (9–13, 17). Our data therefore are in line with the hypothesis that genes mutated at low frequency in gliomas can functionally contribute to gliomagenesis.

Of the genes examined, the mutations identified in *NTN4* and *MAGEH1* were predicted as "probably damaging" by Polyphen-2 analysis and affected the protein subcellular localization. Both mutations in *NTN4* and *MAGEH1* are not located in any of the known signal peptides for protein localization. These mutations may affect protein folding and sorting, however this would be accompanied by an accumulation of proteins in the ER, and we did not observe such accumulation in our transfected cells.

Of the genes examined in more detail, the mutation identified in *GDI1* was predicted as "probably damaging" by Polyphen-2 analysis and did not affect the protein subcellular localization. Our data show that HOG cells stably expressing wildtype *GDI1* have increased proliferation and migration compared to those expressing *GDI1*^{R193C} or eGFP. The proliferation experiments were validated by flow cytometry, showing that wildtype *GDI1* expressing cells are more present in the S-G2-M phase and less in the G1 compared to mutant *GDI1* expressing cells. *GDI1* encodes for GDP dissociation inhibitor 1, which is involved in recycling of Rab proteins and contains a GTPase activation GDI1-β2/GDI1-β and geranyl–geranyl transferase domain (supplementary Figure 3) (18–20). The GTPase activating domain of *GDI1* interacts with the GDP-bound Rab proteins, while the geranyl–geranyl domain interacts with the prenylated binding motif of Rab protein (21).

The altered migration may be caused by a differential activation of Rab proteins by *GDI*. Rab proteins belong to the Ras superfamily and are involved in vesicle trafficking between cellular compartments along actin or microtubules (22). Binding of *GDI* to prenylated GDP-bound Rab protein in the cytosol mediates the delivery of Rab proteins to membranes during vesicle formation and their return into the cytosol after vesicle fusion (23, 24). Importantly, Rab proteins seem to direct migration of cancer cells by regulating integrin recycling (25). This mutation is functionally important as mutated *GDI1* does not stimulate cell proliferation and migration whereas wildtype *GDI1* does.

The second gene examined was *XPO7*, in which the mutation was also predicted to be probably damaging by Polyphen-2 analysis. The mutation did not affect the protein subcellular localization. Our data indicate that both wildtype and *XPO7*^{D237N} increase the proliferation rate of HOG cells. *XPO7* encodes for exportin 7, which is a nuclear transport receptor that exports cargos from the nucleus into the cytoplasm (26). This protein contains a N-terminal Importin-beta domain that binds to RAN and an ARM-type fold domain (26). Its C-terminal region is thought to be involved in the recognition of substrates with broad specificity (27). The fact that both wildtype and *XPO7*^{D237N} stimulate cell proliferation and migration, highlights the importance of this gene.

The third gene examined was *SASH3*, in which the mutation was predicted as probably damaging by Polyphen-2 analysis and did not affect the protein subcellular localization. The current study found that cells expressing wildtype *SASH3*, but not *SASH3*^{R288*}, show increased migration, indicating that the mutation affects the function of the wildtype protein. *SASH3* encodes a signaling adapter protein, containing a SLY motif in the N-terminal region, a SH3 motif and a SAM motif in the C-terminal region (28). SAM families of receptors are known to play a role in many developmental processes including cell migration, neuronal formation and angiogenesis (28). They seem to mediate signal transduction by connecting downstream effector proteins to cell surface receptors (29, 30). The altered migration pattern in *SASH3*^{R288*} expressing cells may therefore be caused by disturbed signal transduction pathways that lead to cell migration. This mutation is

functionally important as *SASH3*[R288*] does not stimulate cell migration where wildtype *SASH3* does.

The last gene examined was *ZNF238*, in which the mutation was predicted as "probably damaging" by Polyphen-2 analysis and did not affect the protein subcellular localization. Our data indicate that cells stably expressing wildtype or *ZNF238*[V121I] decrease proliferation and migration compared to control. The present finding is consistent with other studies in which *ZNF238* was found to decrease proliferation (31, 32) and that *ZNF238* is essential for neuronal migration in experimental mouse models (32 –34). *ZNF238* encodes a transcriptional repressor that contains a BTB/POZ fold domain in the N-terminal region and four zinc fingers in the C-terminal region (35, 36). This protein family plays a role in many processes, including DNA damage response, cell cycle and developmental processes (31–34, 37). Our observation that wildtype and mutant constructs affect cellular proliferation and migration, highlights the important role of this gene.

Although our data argue that many genes are functionally relevant for gliomas, there are some limitations to our study. For all functional experiments, we have only utilized the HOG cell line, as these cells have been well characterized and resemble immature oligodendrocytes (16). Whether these effects are retained in other cell lines remains to be determined. For example, to determine whether these genes indeed contribute to gliomagenesis, similar experiments need to be performed in stem cells, patient derived xenografts and various in vivo experiments. However because mutations occur at such low frequency, patient-derived primary cultured tumor cell lines containing these mutations are hard to obtain. Moreover, oligodendrogliomas with 1p19qLOH and/or *IDH1* mutated tumors virtually cannot be propagated *in vitro*. Nevertheless, our data shows that even in a single cell line, a substantial proportion of low-frequency genes functionally affects cell physiology.

Another limitation of this study is that we have only performed functional analysis of a few genes. However, in a substantial proportion of the examined genes, the mutation affected the function of the wildtype protein. Our data therefore suggest that a substantial proportion of low-frequency genes are functionally relevant for glioma initiation and/or progression.

In contrast to may be expected for oncogenic mutations, we found that the proliferation and/or migration rate was reduced in cells expressing *GDI1*[R1193C], *ZNF238*[V121I] and *SASH3*[R288*]. It is not uncommon for ectopic expression of oncogenes in various cell lines to result in reduced proliferation and altered migration. In fact, Sun et al. have shown that expression of *EGFR* in mutant melanoma cells confers a growth disadvantage that is further strengthened by the addition of *EGFR* ligand (38). A similar growth disadvantage (and altered migration pattern) was observed when expressing *IDH1*[R132H] (10, 39). Perhaps, this is a relatively common physiological response of cells that have never been dependent on a specific oncogene. It is however also possible that the mutation does

not contribute to tumor formation/progression but simply has deleterious effects on the functioning of the wildtype protein.

In conclusion, we have demonstrated that low-frequency genes can affect the proteins' subcellular localization and/ or physiology in HOG cells. These findings indicate that low-frequency genes functionally can contribute to gliomagenesis and/or progression and suggest these genes as new therapeutic targets for treatment for this tumor type.
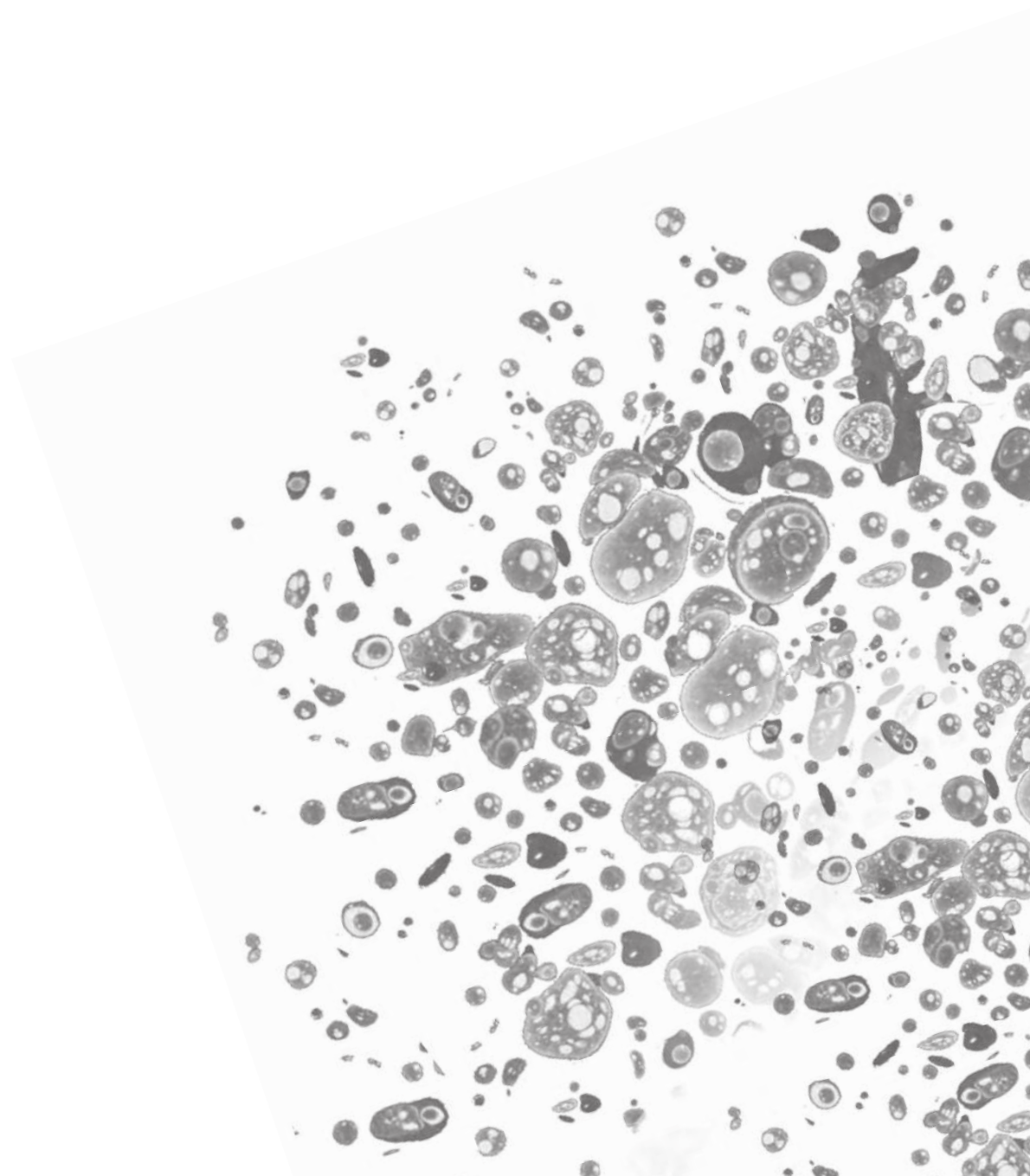
REFERENCES

1. Bromberg JE, van den Bent MJ (2009) Oligodendrogliomas: molecular biology and treatment. Oncologist 14:155–163. doi:10. 1634/theoncologist.2008-0248

2. Bettegowda C, Agrawal N, Jiao Y, Sausen M, Wood LD, Hruban RH, Rodriguez FJ, Cahill DP, McLendon R, Riggins G, Velculescu VE, Oba-Shinjo SM, Marie SK, Vogelstein B, Bigner D, Yan H, Papadopoulos N, Kinzler KW (2011) Mutations in CIC and FUBP1 contribute to human oligoden-droglioma. Science 333:1453–1455. doi:10.1126/science.1210557

3. Jiao Y, Killela PJ, Reitman ZJ, Rasheed AB, Heaphy CM, de Wilde RF, Rodriguez FJ, Rosemberg S, Oba-Shinjo SM, Nagahashi Marie SK, Bettegowda C, Agrawal N, Lipp E, Pirozzi C, Lopez G, He Y, Friedman H, Friedman AH, Riggins GJ, Holdhoff M, Burger P, McLendon R, Bigner DD, Vogelstein B, Meeker AK, Kinzler KW, Papadopoulos N, Diaz LA, Yan H (2012) Frequent ATRX, CIC, FUBP1 and *IDH1* mutations refine the classification of malignant gliomas. Oncotarget 3:709–722

4. Sahm F, Koelsche C, Meyer J, Pusch S, Lindenberg K, Mueller W, Herold-Mende C, von Deimling A, Hartmann C (2012) CIC and FUBP1 mutations in oligodendrogliomas, oligoastrocytomas and astrocytomas. Acta Neuropathol 123:853–860. doi:10.1007/ s00401-012-0993-5

5. Yip S, Butterfield YS, Morozova O, Chittaranjan S, Blough MD, An J, Birol I, Chesnelong C, Chiu R, Chuah E, Corbett R, Docking R, Firme M, Hirst M, Jackman S, Karsan A, Li H, Louis DN, Maslova A, Moore R, Moradian A, Mungall KL, Perizzolo M, Qian J, Roldan G, Smith EE, Tamura-Wells J, Thiessen N, Varhol R, Weiss S, Wu W, Young S, Zhao Y, Mungall AJ, Jones SJ, Morin GB, Chan JA, Cairncross JG, Marra MA (2012) Concurrent CIC mutations, *IDH* mutations, and 1p/19q loss distin-guish oligodendrogliomas from other cancers. J Pathol 226:7–16. doi:10.1002/path.2995

6. Killela PJ, Reitman ZJ, Jiao Y, Bettegowda C, Agrawal N, Diaz LA Jr, Friedman AH, Friedman H, Gallia GL, Giovanella BC, Grollman AP, He TC, He Y, Hruban RH, Jallo GI, Mandahl N, Meeker AK, Mertens F, Netto GJ, Rasheed BA, Riggins GJ, Rosenquist TA, Schiffman M, Shih IM, Theodorescu D, Torbenson MS, Velculescu VE, Wang TL, Wentzensen N, Wood LD, Zhang M, McLendon RE, Bigner DD, Kinzler KW, Vogelstein B, Papadopoulos N, Yan H (2013) TERT promoter mutations occur frequently in gliomas and a subset of tumors derived from cells with low rates of self-renewal. Proc Natl Acad Sci USA 110:6021–6026. doi:10.1073/pnas.1303607110

7. Hanahan D, Weinberg RA (2011) Hallmarks of cancer: the next generation. Cell 144:646–674. doi:10.1016/j.cell.2011.02.013

8. Brennan CW, Verhaak RG, McKenna A, Campos B, Noushmehr H, Salama SR, Zheng S, Chakravarty D, Sanborn JZ, Berman SH, Beroukhim R, Bernard B, Wu CJ, Genovese G, Shmulevich I, Barnholtz-Sloan J, Zou L, Vegesna R, Shukla SA, Ciriello G, Yung WK, Zhang W, Sougnez C, Mikkelsen T, Aldape K, Bigner DD, Van Meir EG, Prados M, Sloan A, Black KL, Eschbacher J, Finocchiaro G, Friedman W, Andrews DW, Guha A, Iacocca M, O'Neill BP, Foltz G, Myers J, Weisenberger DJ, Penny R, Kucher-lapati R, Perou CM, Hayes DN, Gibbs R, Marra M, Mills GB, Lander E, Spellman P, Wilson R, Sander C, Weinstein J, Meyerson M, Gabriel S, Laird PW, Haussler D, Getz G, Chin L, Network TR (2013) The somatic genomic landscape of glioblastoma. Cell 155:462–477. doi:10.1016/j.cell.2013.09.034

9. Bralten LB, Gravendeel AM, Kloosterhof NK, Sacchetti A, Vrijenhoek T, Veltman JA, van den Bent MJ, Kros JM, Hoogenraad CC, Sillevis Smitt PA, French PJ (2010) The CASPR2 cell adhesion mol-ecule functions as a tumor suppressor gene in glioma. Oncogene 29:6138–6148. doi:10.1038/ onc.2010.342

10. Wang K, Pan L, Che X, Cui D, Li C (2010) Gli1 inhibition induces cell-cycle arrest and enhanced apoptosis in brain glioma cell lines. J Neurooncol 98:319–327. doi:10.1007/s11060-009-0082-3

11. Basto D, Trovisco V, Lopes JM, Martins A, Pardal F, Soares P, Reis RM (2005) Mutation analysis of B-RAF gene in human gliomas. Acta Neuropathol 109:207–210. doi:10.1007/s00401-004-0936-x

12. Davies H, Bignell GR, Cox C, Stephens P, Edkins S, Clegg S, Teague J, Woffendin H, Garnett MJ, Bottomley W, Davis N, Dicks E, Ewing R, Floyd Y, Gray K, Hall S, Hawes R, Hughes J, Kosmidou V, Menzies A, Mould C, Parker A, Stevens C, Watt S, Hooper S, Wilson R, Jayatilake H, Gusterson BA, Cooper C, Shipley J, Hargrave D, Pritchard- Jones K, Maitland N, Chenevix- Trench G, Riggins GJ, Bigner DD, Palmieri G, Cossu A, Flanagan A, Nicholson A, Ho JW, Leung SY, Yuen ST, Weber BL, Seigler HF, Darrow TL, Paterson H, Marais R, Marshall CJ, Wooster R, Stratton MR, Futreal PA (2002) Mutations of the BRAF gene in human cancer. Nature 417:949–954. doi:10.1038/nature00766

13. Singh D, Chan JM, Zoppoli P, Niola F, Sullivan R, Castano A, Liu EM, Reichel J, Porrati P, Pellegatta S, Qiu K, Gao Z, Ceccarelli M, Riccardi R, Brat DJ, Guha A, Aldape K, Golfinos JG, Zagzag D, Mik-kelsen T, Finocchiaro G, Lasorella A, Rabadan R, Iavarone A (2012) Transforming fusions of FGFR and TACC genes in human glioblastoma. Science 337:1231–1235. doi:10.1126/science.1220834 J Neurooncol (2015) 122:461–470 469

14. Bralten LB, Kloosterhof NK, Gravendeel LA, Sacchetti A, Duijm EJ, Kros JM, van den Bent MJ, Hoogenraad CC, Sillevis Smitt PA, French PJ (2010) Integrated genomic profiling identifies candidate genes implicated in glioma-genesis and a novel LEO1- SLC12A1 fusion gene. Genes Chromosom Cancer 49:509–517.doi:10.1002/gcc.20760

15. French PJ, Swagemakers SM, Nagel JH, Kouwenhoven MC, Brouwer E, van der Spek P, Luider TM, Kros JM, van den Bent MJ, Sillevis Smitt PA (2005) Gene expression profiles associated with treatment response in oligodendrogliomas. Cancer Res 65:11335–11344. doi:10.1158/0008-5472.CAN-05-1886

16. Buntinx M, Vanderlocht J, Hellings N, Vandenabeele F, Lambrichts I, Raus J, Ameloot M, Stinissen P, Steels P (2003) Characterization of three human oligodendroglial cell lines as a model to study oligodendrocyte injury: morphology and oligodendrocyte- specific gene expression. J Neurocy-tol 32:25–38

17. Charest A, Lane K, McMahon K, Park J, Preisinger E, Conroy H, Housman D (2003) Fusion of FIG to the receptor tyrosine kinase ROS in a glioblastoma with an interstitial del(6)(q21q21). Genes Chromosom Cancer 37:58–71. doi:10.1002/gcc.10207

18. D'Adamo P, Menegon A, Lo Nigro C, Grasso M, Gulisano M, Tamanini F, Bienvenu T, Gedeon AK, Oostra B, Wu SK, Tandon A, Valtorta F, Balch WE, Chelly J, Toniolo D (1998) Mutations in GDI1 are responsible for X-linked non-specific mental retardation. Nat Genet 19:134–139. doi:10.1038/487

19. Garrett MD, Zahner JE, Cheney CM, Novick PJ (1994) GDI1 encodes a GDP dissociation inhibitor that plays an essential role in the yeast secretory pathway. EMBO J 13:1718–1728

20. Luan P, Balch WE, Emr SD, Burd CG (1999) Molecular dissection of guanine nucleotide dissociation inhibitor function in vivo. Rab-independent binding to membranes and role of Rab recycling factors. J Biol Chem 274:14806–14817

21. Gavriljuk K, Itzen A, Goody RS, Gerwert K, Kotting C (2013) Membrane extraction of Rab proteins by GDP dissociation inhibitor characterized using attenuated total reflection infrared spectros-copy. Proc Natl Acad Sci USA 110:13380–13385. doi:10.1073/pnas.1307655110

22. Stenmark H (2009) Rab GTPases as coordinators of vesicle traffic. Nat Rev Mol Cell Biol 10:513–525. doi:10.1038/nrm2728

23. Sivars U, Aivazian D, Pfeffer SR (2003) Yip3 catalyses the dissociation of endosomal Rab-GDI complexes. Nature 425:856–859. doi:10.1038/nature02057

24. Ullrich O, Stenmark H, Alexandrov K, Huber LA, Kaibuchi K, Sasaki T, Takai Y, Zerial M (1993) Rab GDP dissociation inhibitor as a general regulator for the membrane association of rab proteins. J Biol Chem 268:18143–18150

25. Recchi C, Seabra MC (2012) Novel functions for Rab GTPases in multiple aspects of tumour progression. Biochem Soc Trans 40:1398–1403. doi:10.1042/BST20120199

26. Koch P, Bohlmann I, Schafer M, Hansen-Hagge TE, Kiyoi H, Wilda M, Hameister H, Bartram CR, Janssen JW (2000) Identification of a novel putative Ran-binding protein and its close homologue. Biochem Biophys Res Commun 278:241–249. doi:10.1006/bbrc.2000.3788

27. Kutay U, Hartmann E, Treichel N, Calado A, Carmo-Fonseca M, Prehn S, Kraft R, Gorlich D, Bischoff FR (2000) Identification of two novel RanGTP-binding proteins belonging to the importin beta superfamily. J Biol Chem 275:40163–40168. doi:10.1074/jbc.M006242200

28. Beer S, Simins AB, Schuster A, Holzmann B (2001) Molecular cloning and characterization of a novel SH3 protein (SLY) preferentially expressed in lymphoid cells. Biochim Biophys Acta 1520:89–93

29. Nakamoto M (2000) Eph receptors and ephrins. Int J Biochem Cell Biol 32:7–12

30. Pasquale EB (1997) The Eph family of receptors. Curr Opin Cell Biol 9:608–615

31. Okado H, Ohtaka-Maruyama C, Sugitani Y, Fukuda Y, Ishida R, Hirai S, Miwa A, Takahashi A, Aoki K, Mochida K, Suzuki O, Honda T, Nakajima K, Ogawa M, Terashima T, Matsuda J, Kawano H, Kasai M (2009) The transcriptional repressor RP58 is crucial for cell-division patterning and neuronal survival in the developing cortex. Dev Biol 331:140–151. doi:10.1016/j.ydbio.2009.04.030

32. Tatard VM, Xiang C, Biegel JA, Dahmane N (2010) ZNF238 is expressed in postmitotic brain cells and inhibits brain tumor growth. Cancer Res 70:1236–1246. doi:10.1158/0008-5472.CAN-09-2249

33. Ohtaka-Maruyama C, Hirai S, Miwa A, Heng JI, Shitara H, Ishii R, Taya C, Kawano H, Kasai M, Nakajima K, Okado H (2013) RP58 regulates the multipolar-bipolar transition of newborn neurons in the developing cerebral cortex. Cell Rep 3:458–471. doi:10.1016/j.celrep.2013.01.012

34. Xiang C, Baubet V, Pal S, Holderbaum L, Tatard V, Jiang P, Davuluri RV, Dahmane N (2012) RP58/ZNF238 directly modulates proneurogenic gene levels and is required for neuronal differentiation and brain expansion. Cell Death Differ 19:692–702. doi:10.1038/cdd.2011.144

35. Aoki K, Meng G, Suzuki K, Takashi T, Kameoka Y, Nakahara K, Ishida R, Kasai M (1998) RP58 associates with condensed chromatin and mediates a sequence-specific transcriptional repression. J Biol Chem 273:26698–26704

36. Meng G, Inazawa J, Ishida R, Tokura K, Nakahara K, Aoki K, Kasai M (2000) Structural analysis of the gene encoding RP58, a sequence-specific transrepressor associated with heterochromatin. Gene 242:59–64

37. Heng JI, Qu Z, Ohtaka-Maruyama C, Okado H, Kasai M, Castro D, Guillemot F, Tan SS (2013) The zinc finger transcription factor RP58 negatively regulates Rnd2 for the control of neuronal migration during cerebral cortical development. Cereb Cortex. doi:10.1093/cercor/bht277

38. Sun C, Wang L, Huang S, Heynen GJ, Prahallad A, Robert C, Haanen J, Blank C, Wesseling J, Willems SM, Zecchin D, Hobor S, Bajpe PK, Lieftink C, Mateus C, Vagner S, Grernrum W, Hofland I, Schlicker A, Wessels LF, Beijersbergen RL, Bardelli A, Di Nicolantonio F, Eggermont AM, Bernards R (2014) Reversible and adaptive resistance to BRAF(V600E) inhibition in melanoma. Nature 508:118–122. doi:10.1038/nature13121

39. Bralten LB, Kloosterhof NK, Balvers R, Sacchetti A, Lapre L, Lamfers M, Leenstra S, de Jonge H, Kros JM, Jansen EE, Struys EA, Jakobs C, Salomons GS, Diks SH, Peppelenbosch M, Kremer A, Hoogenraad CC, Smitt PA, French PJ (2011) *IDH1* R132H decreases proliferation of glioma cell lines in vitro and in vivo. Ann Neurol 69:455–463. doi:10.1002/ana.22390

DISCUSSION

In this thesis, we have described several methods to identify prognostic and predictive markers in gliomas using high-throughput profiling technologies and have shown their clinical relevance in two randomized clinical trials (chapters 1-3). We have also evaluated the functional consequences of different mutations in *EGFR* and infrequent gene mutations in ODs. We found that different mutations in *EGFR* can have different functional effects (chapter 4). Functional analyses of infrequently mutated genes in oligodendrogliomas have shown that the identified mutations may affect their functional properties (chapter 5).

Molecular markers

The diagnosis of gliomas has been primarily dependent on the histological examination of the tumor. However, due to histological heterogeneity of gliomas and interobserver variability, classification is often difficult and a more integrated diagnosis is required. With recent findings in molecular biology, use of molecular markers has increased in gliomas to assist diagnosis, prognosis and predict response to therapy.

1p19qLOH, and *IDH1* mutations are molecular markers that occur early in glioma development and enable molecular separation of gliomas into oligodendroglial (1p19q codel, *IDH1/2, CIC, FUBP1, TERT* mutations) and astrocytic lineage *(IDH1*, *ATRX*, *TP53* mutations) in combination with other molecular markers. These markers are very powerful to aid classification of gliomas. Besides these markers, *EGFR* status and *MGMT* promoter methylation are also often being assessed, the latter also having predictive value in response to TMZ in GBMs. In this thesis, we have shown that expression-based intrinsic glioma subtyping has additional value by segregating tumors based on their transcriptome and integrating the single molecular markers in one assay. Therefore, intrinsic glioma subtyping represents a comprehensive and accurate method to help diagnosis, predict prognosis and treatment response.

High throughput profiling

For gene expression-based molecular subtyping, we made use of both micro-array based platform (DASL) and RNA-sequencing (RNA-seq). Both platforms showed a high correlation in gene expression profiles. However, RNA-seq does not rely on transcript-specific probes, it can therefore also detect novel transcripts, gene fusions, indels and single nucleotide variations and is deprived of probe-dependent technical issues. This technology also offers a broader dynamic range than microarrays, which makes detection of more differentially expressed genes with higher fold change possible. Despite RNA-seq has more advantages over micro-array based platforms, until recently, the latter is still more commonly used, likely because RNA-seq is new to most users, more expensive and data analysis requires knowledge and expertise. We believe that once

these limitations are solved, RNA-seq will become the predominant application for gene expression analysis.

To bring a biomarker to the clinic, it is mandatory to show a meaningful clinical benefit, supported by strong validation data. Both expression profiling and methylation profiling have shown predictive value in EORTC 26951. As a technique however, methylation profiling provides a more robust and reliable outcome as this method measures a positive versus negative signal (unmethylated v. methylated) compared to fold changes in gene expression levels. In addition methylation uses DNA, which is intrinsically more stable than RNA. Hence, methylation offers several technological advantages over expression profiling and is more applicable in the clinical setting. We therefore believe that full-scale implementation of expression profiling in the clinical setting is not yet feasible in the near future, considering the costs and complexity. However expression based single markers, such as the genes *FMO4* and *OSBPL3* identified from RNA-seq data in the BELOB study, may be more readily implemented. It should be noted however that these specific markers need independent validation.

Even if more difficult to use, we have shown that expression profiling provides useful diagnostic and prognostic information: expression based intrinsic glioma subtypes are composed of different histological subtypes and have different prognosis. The predictive value of response to PCV in anaplastic oligodendrogliomas of intrinsic subtypes however needs to be strengthened by validation in prospective clinical trials.

High throughput DNA sequencing of clinically relevant genes is easier to perform and could be integrated in an assay to quickly screen tumors for a pattern. Other parameters affecting the choice of assay are the costs and simplicity of generated data analysis. To use a marker in the clinic, it should be easy to perform, cost-effective and quickly analyzed and reported to the clinic.

EGFR

In chapter 4, we have analyzed the functional consequences of different activating mutations in *EGFR*. We used the most common mutation in GBM, *EGFR* vIII, which includes an in frame deletion of exons 2-7 and the common p.L858R mutation in pulmonary adenocarcinomas. Both mutations are constitutively activating and are not found in the other tumor type. We found differences in binding partners and activated downstream pathways between *EGFR* wt, vIII and *EGFR* p.L858R, which is in line with previous studies (1-6). As these mutations activate different downstream pathways, these patients may require mutation-specific treatment regimens.

An additional complicating factor is that even within one tumor, different mutations in *EGFR* can exist. It is possible that each activates unique pathways and they may require unique treatments. As *EGFR* inhibition in GBMs has had limited clinical benefit, novel *EGFR* inhibitors should be considered for this tumor type. However, in order to develop

mutation-specific *EGFR* inhibitors or antibodies (e.g. *EGFR* vIII antibody), pathways mediating downstream effects of these mutations need to be well addressed and specifically targeted.

Low-frequency genes

The process of tumor formation requires many somatic mutations. High throughput efforts studying 1p19q co-deleted ODs identified frequent aberrations in the genes *CIC*, *IDH1* and *FUBP1*. Surprisingly, little attention has been paid to the mutations whose frequencies in the population are low. The identification of rare mutations may provide exciting new treatment targets. To our knowledge, we are the first to study functionally low-frequency genes on a larger scale. In this thesis, we identified mutations in the genes *NTN4*, *MAGEH1*, *GDI1*, and *SASH3* that affect their functional properties and may contribute to glioma progression. Treatment aimed at targeting a single gene may be ineffective, as different driver mutations exist within one tumor. These affected genes are likely part of a molecular pathway and therefore treatment aimed at targeting pathways by inhibition or reactivation should be considered. Simultaneously targeting multiple affected pathways could give the best results.
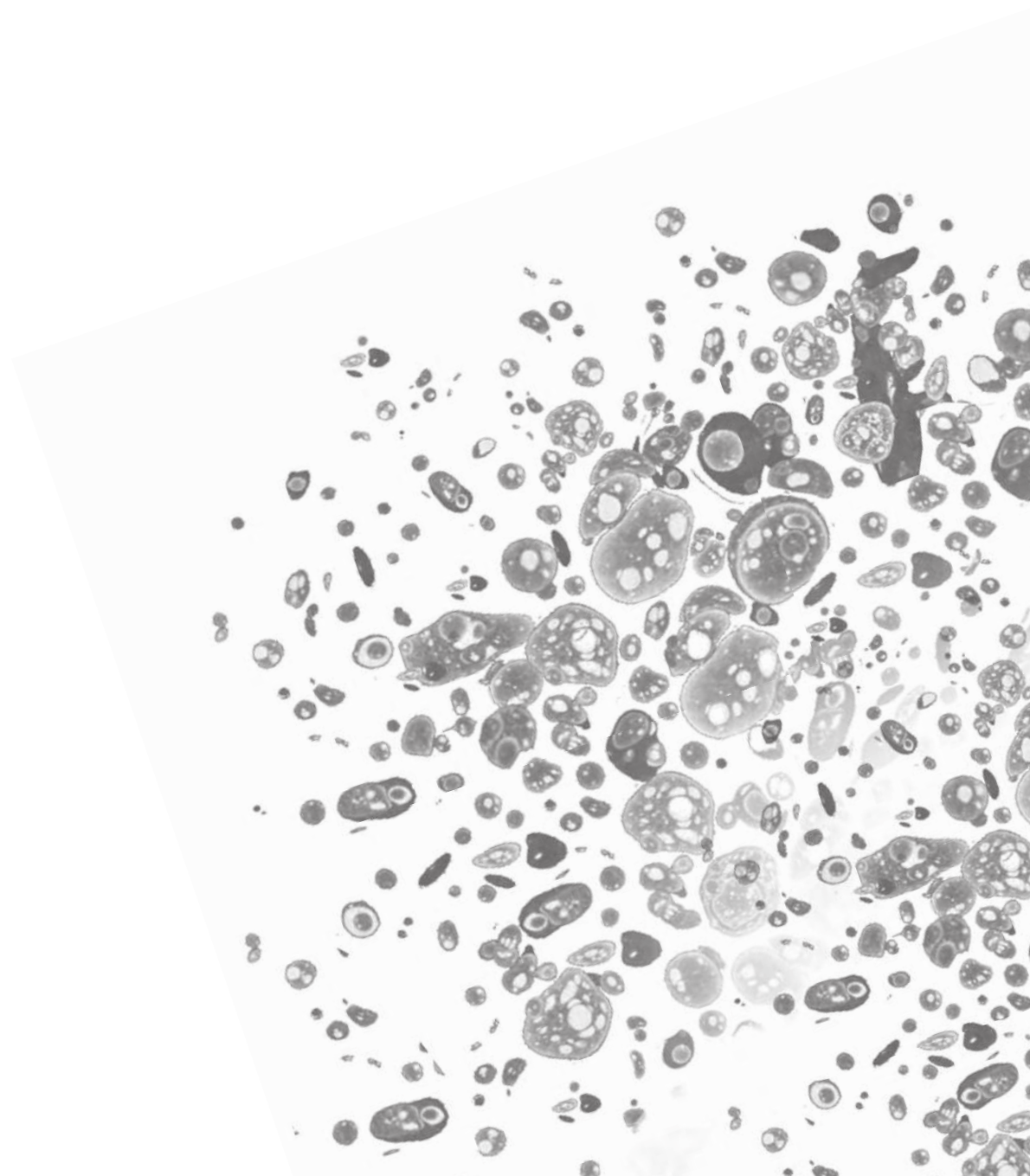
Unfortunately, *in vitro* functional testing of genetic changes and affected pathways is time consuming, and therefore, limits the number of experiments that can be done. High-throughput platforms for functional testing therefore should be developed to enable more rapidly to distinguish driver mutations from passenger mutations, determine which pathways are activated and which drug (combinations) are most effective.

High throughput technologies have enabled us to perform screening of a large amount of patients for prognostic and predictive markers. The future challenge will be to translate these findings into daily clinical practice. The identified predictive markers in this thesis need to be functionally analyzed *in vitro* and *in vivo* and validated in large prospective randomized trials. In addition, the development of novel treatments targeting these changes is required. Identification of novel targets and development of targeted treatments takes many years before implementation in the clinic, however this is the only way to improve patient outcome. In the future, we expect that high- throughput technologies will make a large contribution to a more patient specific approach with treatment aimed at patient specific molecular alterations.

REFERENCES

1. Chu CT, Everiss KD, Wikstrand CJ, Batra SK, Kung HJ, Bigner DD. Receptor dimerization is not a factor in the signalling activity of a transforming variant epidermal growth factor receptor (*EGFR*vIII). The Biochemical journal. 1997;324 (Pt 3):855-61.

2. Antonyak MA, Moscatello DK, Wong AJ. Constitutive activation of c-Jun N-terminal kinase by a mutant epidermal growth factor receptor. J Biol Chem. 1998;273(5):2817-22.

3. Pedersen MW, Pedersen N, Damstrup L, Villingshoj M, Sonder SU, Rieneck K, et al. Analysis of the epidermal growth factor receptor specific transcriptome: effect of receptor expression level and an activating mutation. J Cell Biochem. 2005;96(2):412-27.

4. Chumbalkar V, Latha K, Hwang Y, Maywald R, Hawley L, Sawaya R, et al. Analysis of phosphotyrosine signaling in glioblastoma identifies STAT5 as a novel downstream target of Delta*EGFR*. Journal of proteome research. 2011;10(3):1343-52.

5. Latha K, Li M, Chumbalkar V, Gururaj A, Hwang Y, Dakeng S, et al. Nuclear *EGFR*vIII- STAT5b complex contributes to glioblastoma cell survival by direct activation of the Bcl-XL promoter. Int J Cancer. 2013;132(3):509-20.

6. Liccardi G, Hartley JA, Hochhauser D. *EGFR* nuclear translocation modulates DNA repair following cisplatin and ionizing radiation treatment. Cancer Res. 2011;71(3):1103-14.

SUMMARY

Gliomas are the most frequent primary brain tumors in adults. Despite multimodality treatment strategies, the survival of patients with a diffuse glioma remains poor. There has been an increasing use of molecular markers to assist diagnosis and predict prognosis and response to therapy. Although several prognostic and predictive response markers have been identified, considerable research still needs to be done to improve on these. For example, there are patients with *MGMT*-methylated promoters who respond poorly. Therefore, the identification of novel predictive response markers and therapeutic targets are desperately needed for this dismal disease.

In chapters 1-3, we describe prognostic and identify novel predictive markers in randomized clinical trials. In chapter 1, we determined the gene expression profiles of samples from a large European phase III clinical trial (EORTC 26951) to evaluate the treatment responses within defined intrinsic glioma subtypes (IGSs). IGSs are molecularly similar tumors that have been previously identified by unsupervised gene expression analysis. In this study, we showed that gene expression profiling can be performed on formalin fixed-paraffin-embedded clinical trial samples. We found that all six IGSs were present in EORTC 26951, confirming that within a well-defined histological subtype, different molecular subtypes exist. In addition, we confirmed that IGS subtypes are prognostic for OS: Tumors assigned to IGS-9 (characterized by tumors with a high percentage of 1p/19q LOH and *IDH1* mutations) had the most favorable prognosis, while those assigned to IGS-23 (without 1p/19q LOH and *IDH1* mutations) had the worst prognosis. Moreover, tumors assigned to IGS-9 showed benefit from adjuvant PCV chemotherapy and when combined with other prognostic factors (such as 1p/19q LOH and *IDH1* mutations), IGSs improved outcome prediction. Intrinsic subtypes can therefore be used to assess the molecular heterogeneity within clinical trials and may be used as a prognostic and predictive marker. However, for use in a clinical setting, these data require validation in an external dataset.

In chapter 2, we describe another method to profile gliomas that is based on DNA-methylation. Methylation is a process by which methyl groups are added to cytosine residues, ultimately leading to inactivation of the gene. The CpG island hypermethylated phenotype (CIMP) is defined as elevated levels of DNA methylation with CIMP+ tumors showing better clinical response than CIMP- tumors. Besides CIMP, methylation of *MGMT* has been established as a predictive marker in gliomas. The methylation status of the *MGMT* promoter can be assessed using *MGMT*-STP27 prediction model. Here, we performed genome-wide methylation profiling on material from EORTC 26951 and assessed CIMP and *MGMT*-STP27 status. First, we have shown that methylation profiling is feasible on archival samples. Then, in a univariate analysis, we have shown that survival in patients with CIMP+ or *MGMT*-STP27 methylated tumors was improved compared to CIMP- and/or *MGMT*-STP27 unmethylated tumors. Importantly, the *MGMT*STP27 status was predictive for response to adjuvant PCV chemotherapy in these tumors. *MGMT*-

STP27 may therefore be used to identify AODs and AOAs with improved prognosis and identify patients that are likely to benefit from adjuvant PCV chemotherapy.

In chapter 3, we describe gene expression profiling on samples of a randomized phase II trial (BELOB). This trial provided evidence of benefit of the addition of bevacizumab (Beva) to CCNU chemotherapy in recurrent GBM patients. In this study, we determined the gene expression profiles of BELOB samples to identify patients who benefit most from combined Beva+CCNU treatment. We found that tumors assigned to IGS-18 (classical GBMs) showed a trend towards benefit from Beva+CCNU treatment. No such benefit was found in other glioma subtypes. Expression of *FMO4* and *OSBPL3* were particularly associated with treatment response.

In chapter 4 and 5, we perform functional analysis on different mutations on the *EGFR* gene and infrequently mutated genes in oligodendrogliomas and describe the different functional effects of each mutation.
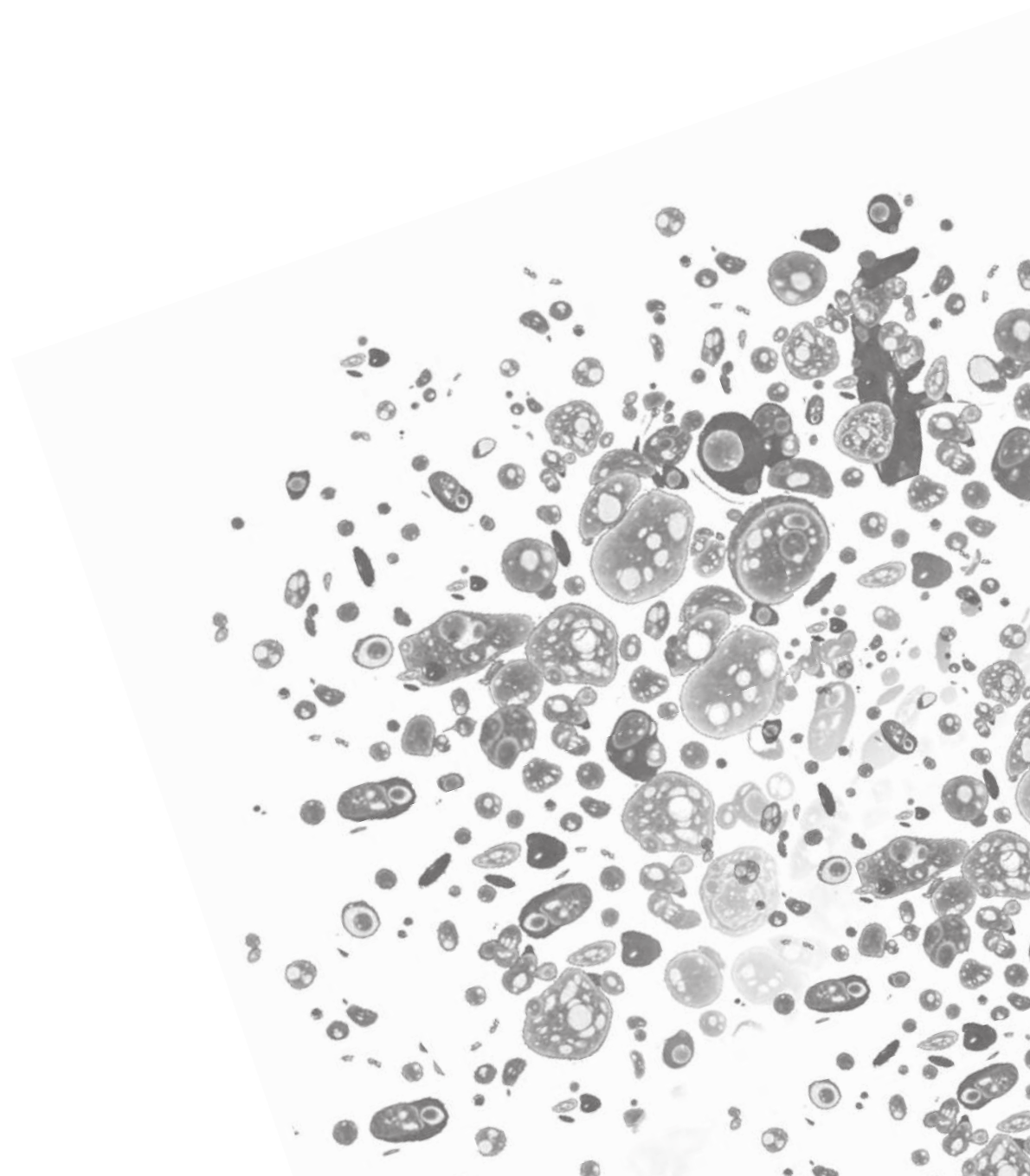
In chapter 4, we show that different mutations within a single gene (*EGFR*) can have different molecular consequences. We compared the most common mutation in GBM, *EGFR* vIII, with the most common mutation in pulmonary adenocarcinomas (p.L858R) and with *EGFR* wildtype. Using mass spectrometry, we showed that there are different binding partners for *EGFR* vIII, *EGFR* p.L858 and *EGFR* wildtype. Furthermore, we found that each mutation activates different signal transduction pathways and ultimately, results in differences in physiology (proliferation and migration). As these mutations have different functions, each mutation may need its own unique treatment.

In chapter 5, we identify infrequently mutated genes in oligodendrogliomas by whole genome and targeted resequencing and describe the functional consequences of a subset of those genes *in silico* and *in vitro*. Functional analysis showed that the function of many of 'low frequency' genes, differs from its wildtype counterpart. This differential effect suggests that these genes can contribute to the disease and therefore may offer new therapeutic targets for oligodendrogliomas.

In summary, we describe several new predictive markers (chapters 1-3) and describe the functional effects of different mutations in *EGFR* (chapter 4) and infrequently mutated genes in oligodendrogliomas (chapter 5).

SAMENVATTING

Gliomen zijn de meest voorkomende primaire hersentumoren bij volwassenen. Ondanks multimodale behandeling, is de overleving van patiënten met een glioom nog steeds slecht. Tegenwoordig is er een toenemend gebruik van moleculaire markers voor de diagnose, prognose en om de respons op therapie te voorspellen. Hoewel verschillende prognostische en predictieve respons markers zijn geïdentificeerd, moet nog veel onderzoek gedaan worden om deze te verbeteren. Zo zijn er patiënten met een gemethyleerd *MGMT* die het slecht doen. Daarom moeten nieuwe predictieve markers en therapeutische targets geïdentificeerd worden voor deze sombere ziekte.

In de hoofdstukken 1-3, beschrijven we prognostische en identificeren we nieuwe predictieve markers in gerandomiseerde klinische studies. In hoofdstuk 1, beschrijven we de genexpressie analyse van monsters uit een grote Europese fase III klinische studie (EORTC 26951). In deze studie zijn alle zes IGSs (IGSs zijn moleculair vergelijkbare tumoren die eerder zijn geïdentificeerd door een ongesuperviseerde genexpressie analyse) in EORTC 26951 aangetoond waarmee bevestigd wordt dat er verschillende moleculaire subtypen voorkomen binnen één histologische subtype. Daarnaast hebben we bevestigd dat deze subtypes prognostisch zijn voor overleving. Patienten met een IGS-9 tumor hadden de meest gunstige prognose, terwijl IGS-23 tumoren de slechtste prognose hadden. Bovendien hadden patienten met een IGS-9 tumor baat bij adjuvante PCV chemotherapie. Intrinsieke subtypen kunnen daarom worden gebruikt om de moleculaire heterogeniteit in klinische studies te bepalen en dienen als prognostische en predictieve markers.

In hoofdstuk 2 beschrijven we een andere methode om gliomen te profileren, namelijk op basis van DNA methylering. Methylering is een proces waarbij methylgroepen worden toegevoegd aan cytosine residuen, wat uiteindelijk leidt tot inactivatie van het gen. De CpG island hypermethylated fenotype (CIMP) wordt gedefinieerd als een verhoogd niveau van DNA methylatie waarbij CIMP+ tumors een klinisch betere respons vertonen dan CIMP- tumoren. Naast CIMP, heeft methylatie van *MGMT* gen ook een predictieve waarde in gliomen. De methylatie van het *MGMT* promotor kan worden beoordeeld met behulp van het *MGMT*-STP27 model. We hebben genome-wide methylatie gedaan op materiaal van EORTC 26951 en hebben de CIMP en *MGMT*-STP27 status bepaald. Daarna hebben we in een univariate analyse aangetoond dat patiënten met CIMP of *MGMT*-STP27 gemethyleerde tumoren een verbeterde overleving hebben ten opzichte van CIMP- en of *MGMT*-STP27 ongemethyleerde tumoren. In een multivariate analyse was de *MGMT*STP-27 status tevens voorspellend voor response op adjuvante PCV chemotherapie. *MGMT*-STP27 kan daarom gebruikt worden om anaplastische oligodendrogliomen en oligoastrocytomen met een verbeterde prognose te identificeren en het effect van adjuvante PCV chemotherapie te voorspellen.

In hoofdstuk 3 beschrijven we genexpressie analyse op monsters van een gerandomiseerde fase II studie (BELOB). De BELOB studie suggereerde dat toevoeging van
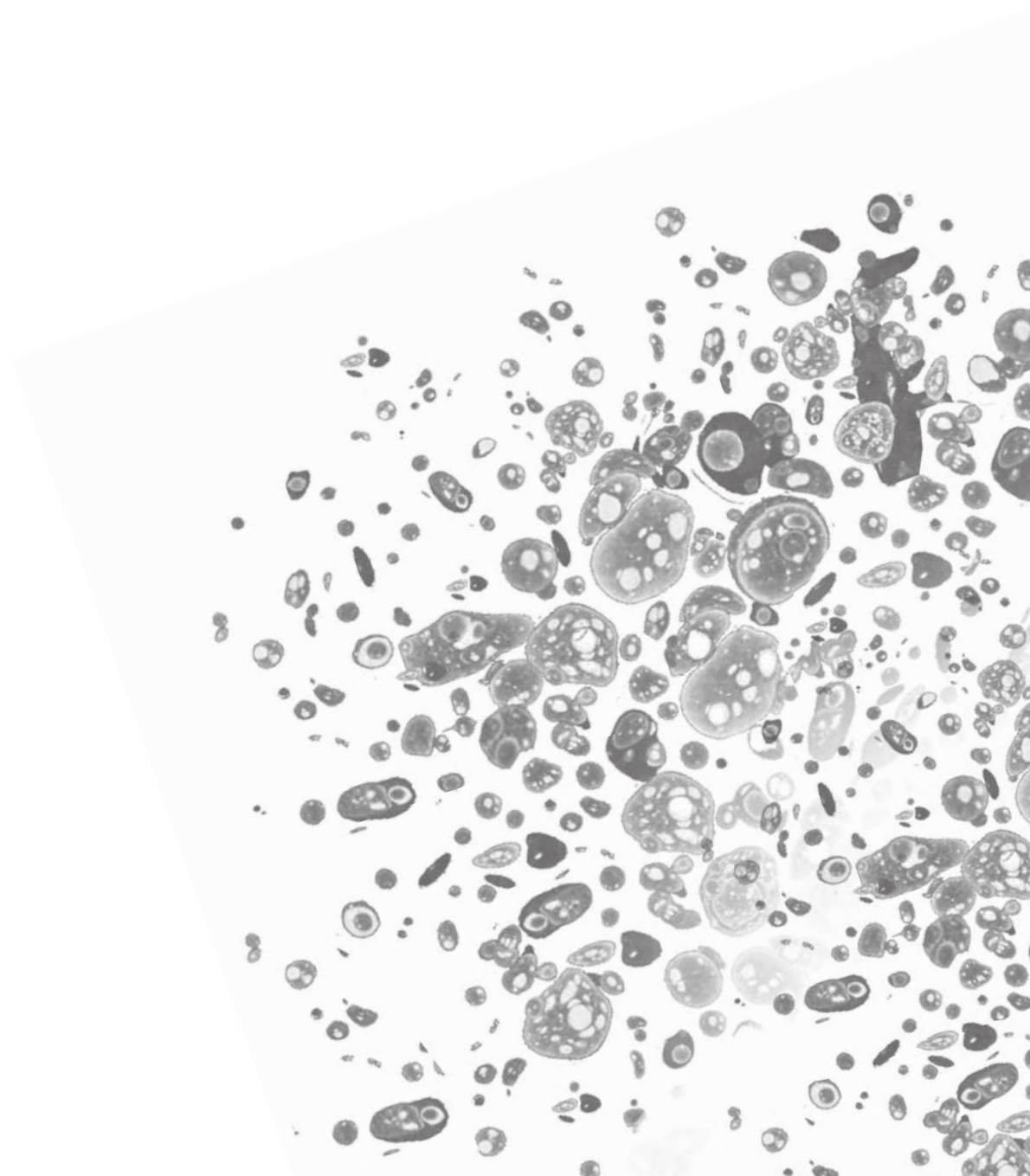
bevacizumab (Beva) aan CCNU chemotherapie de overleving verbetert bij recidiverende GBM-patiënten. In onze studie laten we zien dat IGS-18 tumoren een trend hadden om voordeel te hebben van een gecombineerde Beva + CCNU behandeling. Een dergelijk voordeel werd niet gevonden in andere glioom subtypes. Expressie van *FMO4* en *OSBPL3* waren vooral geassocieerd met respons op behandeling. Deze voorspellende markers kunnen de selectie van recidiverende GBM- patiënten die baat hebben bij Beva + CCNU behandeling mogelijk maken.

Hoofdstuk 4 en 5 beschrijven de functionele analyse van verschillende mutaties in het *EGFR* gen en in infrequent gemuteerde genen in oligodendrogliomen. In hoofdstuk 4 tonen we aan dat verschillende mutaties in één gen (*EGFR*) verschillende moleculaire gevolgen kunnen hebben. We vergeleken de meest voorkomende mutatie in GBM, *EGFR* vIII, met de meest voorkomende mutatie in pulmonaire adenocarcinomen (p.L858R) met elkaar en met wildtype *EGFR*. Met behulp van massaspectrometrie, tonen we aan dat er verschillende bindingspartners zijn voor *EGFR* vIII, *EGFR* p.L858 en normaal *EGFR*. Bovendien tonen we aan dat elke mutatie verschillende signaal transductieroutes activeert. Daarnaast tonen cellijnen die stabiel *EGFR* vIII en *EGFR* L858R tot expressie brengen verminderde proliferatie en migratie in vergelijking met cellen die normaal *EGFR* tot expressie brengen. Aangezien deze mutaties verschillende bindingspartners hebben, verschillende signaaltransductieroutes aanzetten en verschillen tonen in fysiologie, is het mogelijk dat elke mutatie een eigen unieke behandeling krijgt.

In hoofdstuk 5 identificeren we infrequent gemuteerde genen in oligodendrogliomen en beschrijven we de functionele gevolgen van een subset van die genen. Functionele analyse toonde aan dat mutaties in een aantal genen de lokalisatie van het eiwit verandert en/of fysiologie van cellen beïnvloedt. Het is daarom mogelijk dat deze genen een rol spelen in dit tumortype en zo als nieuwe therapeutische targets dienen.

Samengevat beschrijven we in dit proefschrift een aantal nieuwe voorspellende markers voor respons op therapie (hoofdstukken 1-3) en beschrijven we de functionele effecten van verschillende mutaties in *EGFR* (hoofdstuk 4) en infrequent gemuteerde genen in oligodendrogliomen (hoofdstuk 5).
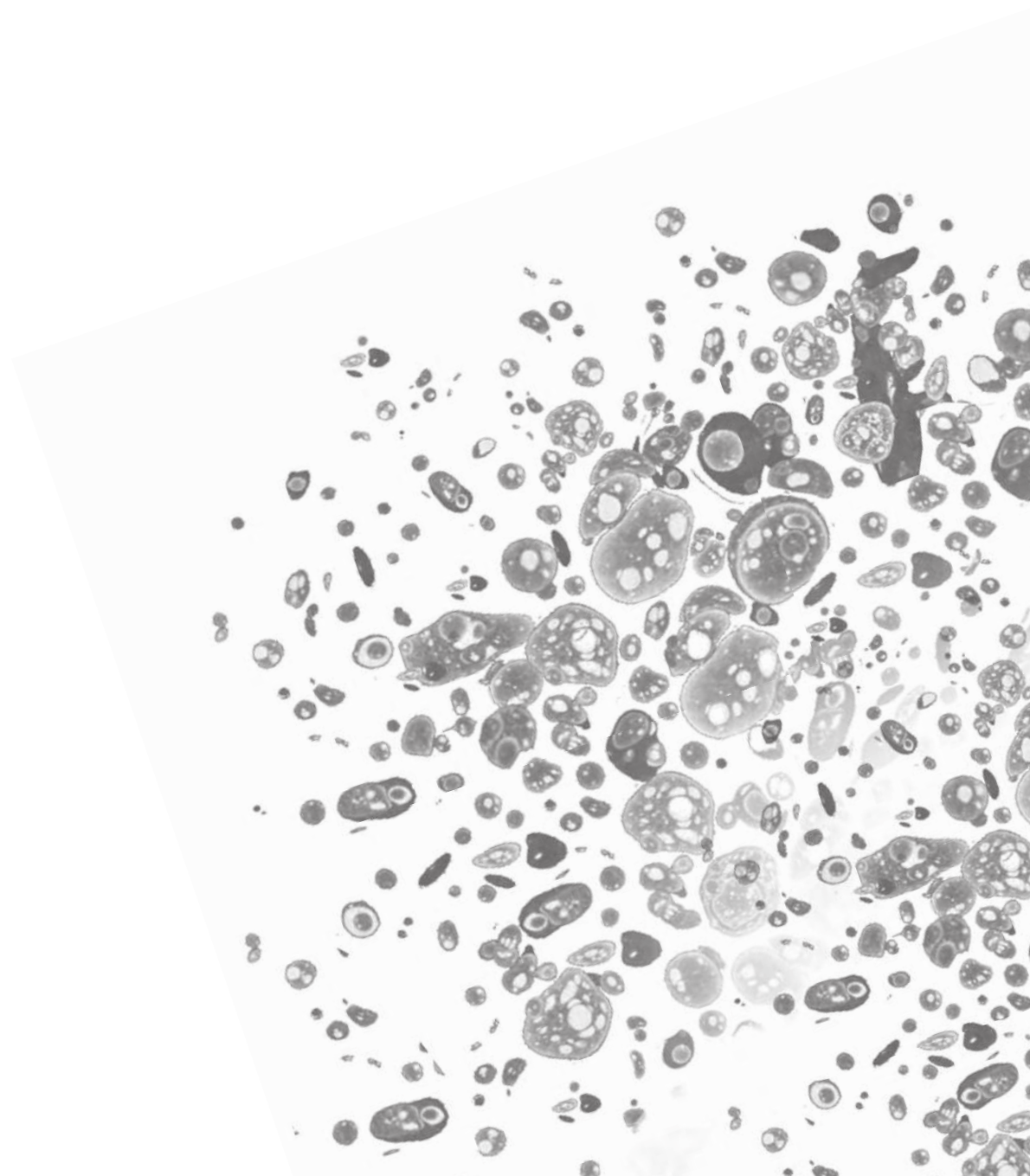
LIST OF ABBREVIATIONS

A	Astrocytoma
AA	Anaplastic astrocytoma
AOA	Anaplastic oligoastrocytoma
AOD	Anaplastic oligodendroglioma
CBTRUS	Central Brain Tumor Registry of the United States
CCNU	Lomustine
CIMP	CpG island methylator phenotype
DASL	cDNA-mediated Annealing, Selection, Extension, and Ligation
DNA	Deoxyribonucleic acid
EGFR	Epidermal growth factor receptor
EORTC	European Organisation for Research and Treatment of Cancer
FDR	False discovery rate
FF	Fresh frozen
FFPE	Formalin-fixed paraffin-embedded
FISH	Fluorescence in sity hybridization
GBM	Glioblastoma
IDH1	Isocitrate dehydrogenase 1 gene
IDH2	Isocitrate dehydrogenase 2 gene
IGSs	Intrinsic glioma subtypes
KPS	Karnofsky performance score
LOH	Loss of heterozygosity
MGMT	0-6methylguanine-DNA methyltransferase
OA	Oligoastrocytoma
OD	Oligodendroglioma
OS	Overall survival
PA	Pilocytic astrocytoma
PCR	Polymerase chain reaction
PCV	Procarbazine, Lomustine, and Vincristine chemotherapy
PFS	Progression-free survival
RNA	Ribonucleic acid
RT	Radiotherapy
SNP	Single-nucleotide polymorphism
TMZ	Temozolomide
WHO	World Health Organization
WGS	Whole-genome sequencing

DANKWOORD

Dit proefschrift zou natuurlijk niet tot stand zijn gekomen zonder de bijdrage van velen. Van alle betrokken personen, wil ik met name de volgende mensen nadrukkelijk bedanken voor hun geleverde bijdrage aan het ontstaan van dit proefschrift.

Allereerst wil ik mijn promoter professor Peter Sillevis Smitt en co-promoter dr. Pim French bedanken voor de deskundige kennis, de goede medewerking en de kansen die ze me hebben gegeven. Zonder jullie hulp, sturing en adviezen was het mij niet gelukt. Ontzettend bedankt voor alles.

De promotiecommissie wil ik graag bedanken voor het lezen en beoordelen van het manuscript en voor de ongetwijfeld uitdagende vragen die ze zullen stellen tijdens de verdediging op 15 maart aanstaande.

Professor Max Kros wil ik van harte bedanken voor het reviewen van ons patiënten materiaal en voor de tips die hij me heeft gegeven.

Ook professor Martin van den Bent wil ik bedanken voor de goede adviezen en het aangeleverde materiaal afkomstig uit de klinische studies de hij begeleidt.

Mijn directe collega's, Diya, Esther, Eric, Maurice, Jory, Kitty, Johan, Nanne, Lonneke en Linda, hartelijk dank voor de gezelligheid en het harde werken! Diya, I am very happy to have known you. Thank you so much for your friendship, positive energy and standing next to me today.

De afdeling neurochirurgie (professor Clemens Dirven, professor Sieger Leenstra, Martine, Zineb, Jenneke, Lotte en alle anderen) proteomics, bioinformatica (Daphne en Peter van der Spek), pathologie (Andrea) en de afdeling interne geneeskunde (met name Renee) wil ik bedanken voor de geleverde input, hulp en de gezelligheid. Renee bedankt voor alle gezellige kopjes koffie die we hebben gedronken. Zineb, bedankt voor de goede gesprekken die we onder het genot van vele kopjes koffie hebben gehad. Ik waardeer je vriendschap zeer en daarom ben ik blij dat jij een van mijn paranimfen bent!

Paul Eilers en Johan wil ik bedanken voor de nuttige bijeenkomsten van de methylerings data.

Naast collega's wil ik ook mijn vrienden en familie bedanken. Lieve vriendinnen van de middelbare school (Romy en Lili) en de universiteit (Melda, Zeliha, Shamni, Hilal, Emel), wat ben ik gezegend met zoveel lieve leuke mensen om me heen. Bedankt voor alle interesse die jullie altijd in mij en mijn promotiezonderzoek toonden. In het bijzonder wil

ik Emel bedanken voor de vriendschap, steun en het oprecht meeleven met de mooie en minder mooie momenten van mijn PhD traject. Dank je wel voor alles!

Dan mijn paranimfen, ook al zijn ze eerder genoemd. Diya en Zineb, ik ben ontzettend blij en vereerd dat jullie vandaag naast mij staan!
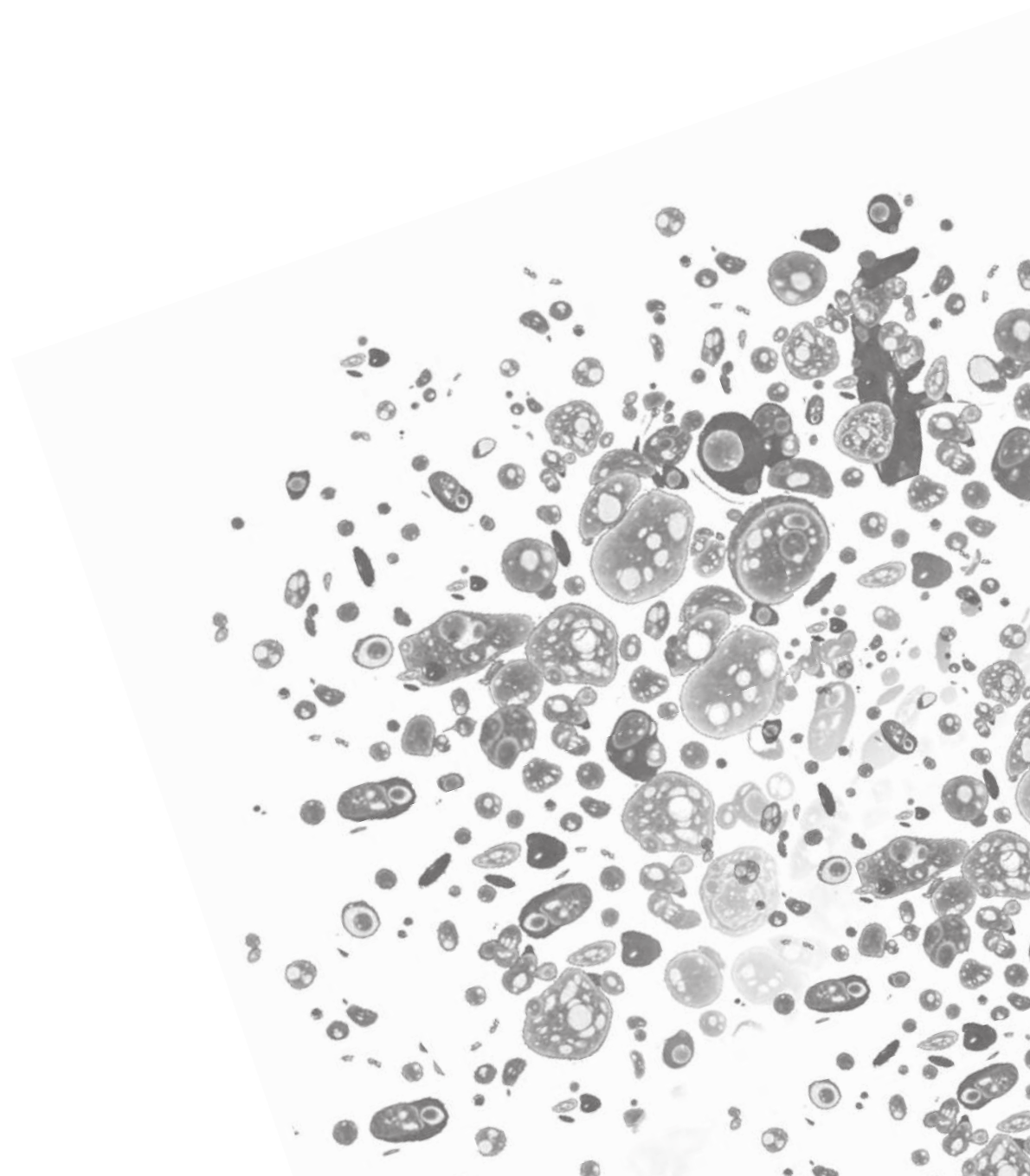
Ik wil mijn lieve familie en met name mijn ouders en m'n zusje bedanken voor alle steun, aanmoediging en geloof in mij. Ik ben enorm trots dat ik jullie dochter/zus ben. Al ruim 30 jaar staan jullie onvoorwaardelijk voor mij klaar en hebben jullie mij gemaakt tot wat ik nu ben en waar jullie konden geholpen.

Naast mijn eigen ouders wil ik ook mijn schoonouders en schoonzusje bedanken voor hun steun, vertrouwen en het meeleven in de periode dat ik dit onderzoek deed. Lieve Zehra, bedankt voor het mooie kalligrafie en Ebru ontwerp van de omslag!

Lieve Ahmet, toen ik wilde beginnen aan m'n PhD heb jij me daarin gesteund. Dankzij jouw onvoorwaardelijke steun, liefde en geduld is het allemaal gelukt. Dank je wel voor alles, ik hou ontzettend veel van je!

CURRICULUM VITAE

Lale Erdem was born in Rotterdam on May 29, 1986. In 2004, she graduated secondary school (gymnasium) at the Erasmiaans Gymnasium, Rotterdam. Thereafter, she studied Biomedical Sciences at the University of Utrecht (2005-2008). During her study she participated in several different activities. She was a coach and student-teacher in the Foundation Education center in Rotterdam. In addition, she worked as an interviewer and data entry employee on various studies at the Erasmus University Rotterdam and University of Utrecht. Because of her interest in the mechanism of cancer, she then studied Oncology at the Vrije University of Amsterdam (2008-2010). During the master, she has done research internships at the Cancer Center Amsterdam (CCA) and the Institute for Research in Biomedicine (IRB) in Barcelona. In 2010, she started her PhD research at the Department of Neurology under supervision of dr. PJ French and Professor P. A. Sillevis Smitt. Since February 2015 she became a resident at the Department of Clinical Chemistry of the Erasmus MC and Groene Hart hospital.
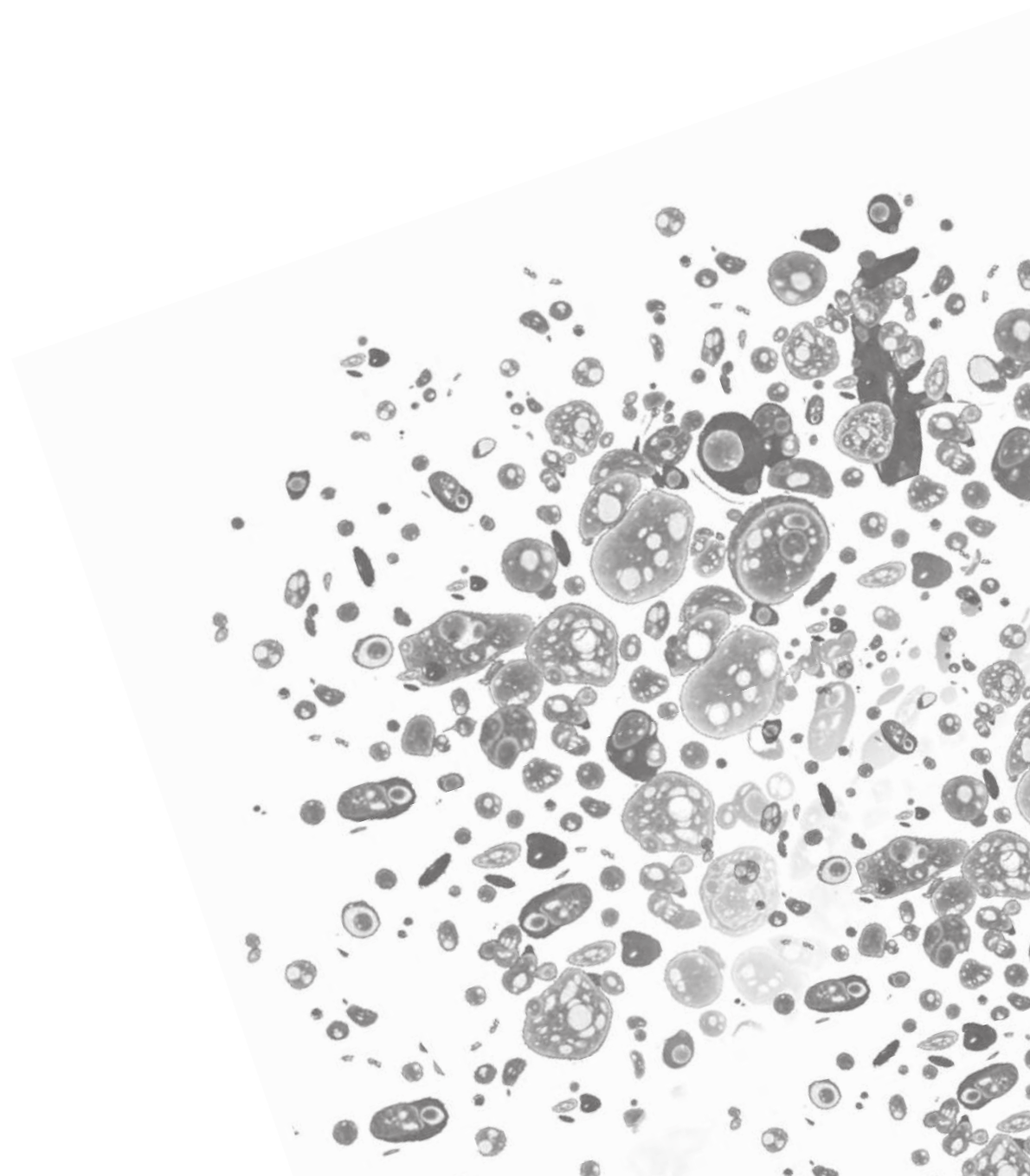
LIST OF PUBLICATIONS

Publications included in this thesis:

Erdem-Eraslan L, Hoogstrate Y, Bottcher R, Naz-Kahn H, Stubbs A, Gao Y, de Wit M, Sillevis Smitt PA, Kros JM, van den Bent MJ, French PJ. Identification of recurrent GBM patients that may benefit from Bevacizumab and CCNU. A report from the BELOB trial conducted by the Dutch Neurooncology Group.
Cancer Res. 2016 Jan 13. [Epub]

Erdem-Eraslan L, Gao Y, Kloosterhof NK, Atlasi Y, Demmers J, Sacchetti A, Kros JM, Sillevis Smitt P, Aerts J, French PJ. Mutation specific functions of *EGFR* result in a mutation-specific downstream pathway activation. Eur J Cancer. 2015 May;51(7):893-903.

Erdem-Eraslan L, Heijsman D, de Wit M, Kremer A, Sacchetti A, van der Spek PJ, Sillevis Smitt PA, French PJ. Tumor-specific mutations in low-frequency genes affect their functional properties. J Neurooncol. 2015 May;122(3):461-70.

van den Bent MJ, Erdem-Eraslan L, Idbaih A, de Rooi J, Eilers PH, Spliet WG, den Dunnen WF, Tijssen C, Wesseling P, Sillevis Smitt PA, Kros JM, Gorlia T, French PJ. *MGMT*-STP27 methylation status as predictive marker for response to PCV in anaplastic Oligodendrogliomas and Oligoastrocytomas. A report from EORTC study 26951. Clin Cancer Res. 2013 Oct 1;19(19):5513-22.
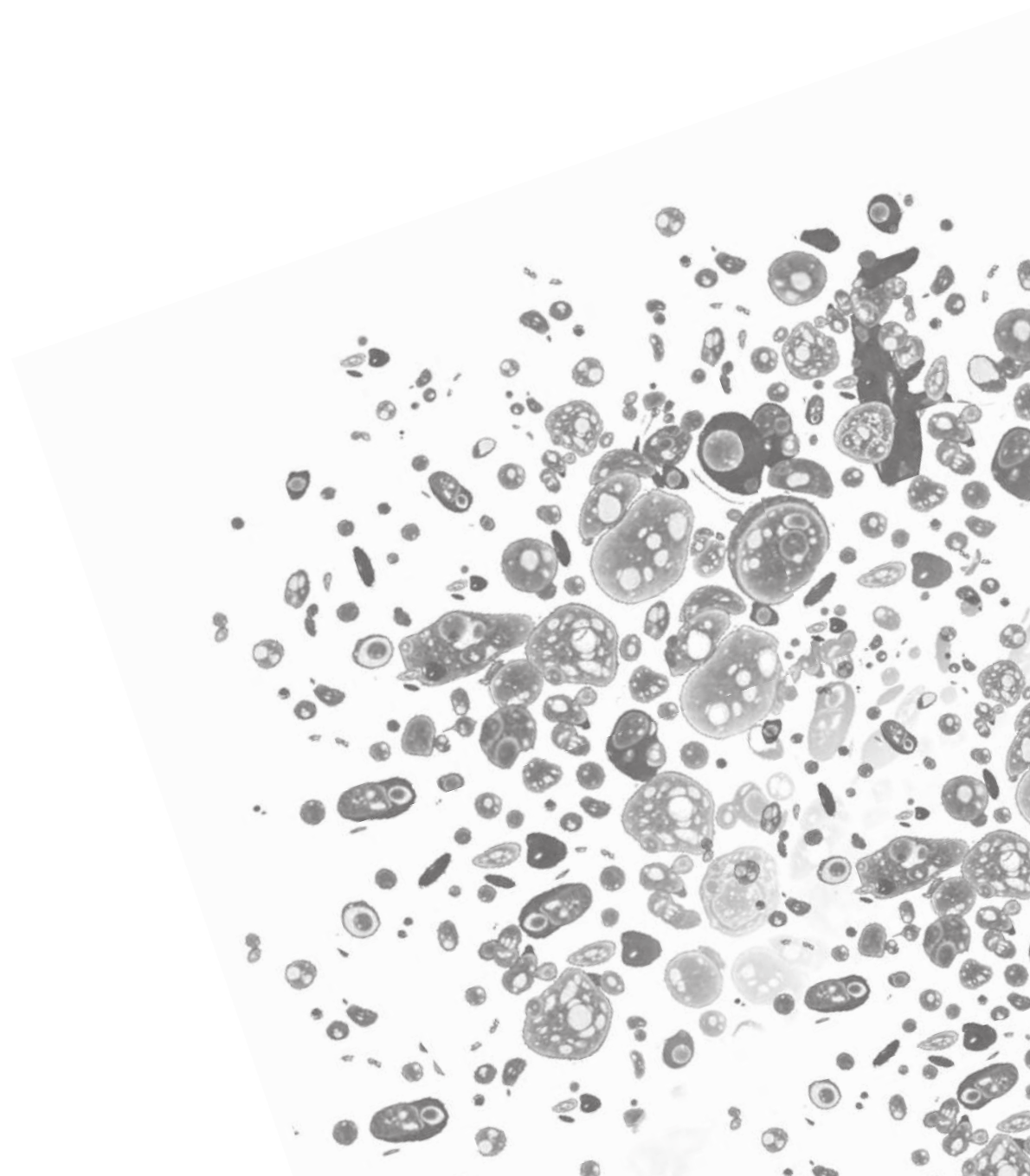
Erdem-Eraslan L, Gravendeel LA, de Rooi J, Eilers PH, Idbaih A, Spliet WG, den Dunnen WF, Teepen JL, Wesseling P, Sillevis Smitt PA, Kros JM, Gorlia T, van den Bent MJ, French PJ. Intrinsic molecular subtypes of glioma are prognostic and predict benefit from adjuvant procarbazine, lomustine, and vincristine chemotherapy in combination with other prognostic factors in anaplastic oligodendroglial brain tumors: a report from EORTC study 26951. J Clin Oncol. 2013 Jan 20;31(3):328-36.

Other publications:
Erdem L, Giovannetti E, Leon LG, Honeywell R, Peters GJ. Polymorphisms to predict outcome to the tyrosine kinase inhibitors gefitinib, erlotinib, sorafenib and sunitinib. Curr Top Med Chem. 2012;12(15):1649-59. Review.

Bralten LB, Nouwens S, Kockx C, Erdem L, Hoogenraad CC, Kros JM, Moorhouse MJ, Sillevis Smitt PA, van der Spek P, van Ijcken W, Stubbs A, French PJ. Absence of common somatic alterations in genes on 1p and 19q in oligodendrogliomas. PLoS One. 2011;6(7):e22000.

Giovannetti E, Erdem L, Olcay E, Leon LG, Peters GJ. Influence of polymorphisms on *EGFR* targeted therapy in non-small-cell lung cancer. Front Biosci (Landmark Ed). 2011 Jan 1;16:116-30. Review.

PHD PORTFOLIO

Name PhD student: Lale Erdem-Eraslan
Erasmus MC Department: Neurology Research
school: Molecular Medicine
PhD period: 2010-2014
Promotor: Prof. P.A.E. Sillevis Smitt
Supervisor: Dr. P.J. French

PhD training

Courses	Year	ECTS
Artikel 9 Proefdierkunde	2013	3 ECTS
Molecular diagnostics VIII	2013	0.6 ECTS
Research management for PhD students and postdocs	2012	0.2 ECTS
Basic and translational oncology	2012	0.6 ECTS
Workshop browsing Genes and Genomes with UCSC	2012	0.4 ECTS
Basic course on R Workshop	2012	0.2 ETCS
Course on Photoshop/Illustrator	2011	0.2 ECTS
Biomedical English writing and communication	2009	4 ECTS

(Inter)national conferences and presentations

SNO Miami,FL, *oral*	2014	0.4 ECTS
AACR, Washington DC, *poster*	2013	0.4 ECTS
Landelijk werkgroep Neuro-oncologie (LWNO), *oral*	2010-2014	0.4 ECTS
Molecular Medicine day, poster	2010-2014	0.8 ECTS
Josephine Nefkens meetings, *oral*	2010-2014	0.4 ECTS
CBG/CGC meetings	2011-2014	0.4 ECTS

OTHER MEETINGS

Weakly JNI research meetings	2010-2014	2 ECTS
Biweekly Neurooncology meetings	2010-2014	1 ECTS
Molmed Bridge meetings	2010-2014	0.5 ECTS

TEACHING

Supervising MLO technicians in training	2013-2014	2 ECTS